

**Master Thesis**

# **Dimension Prediction of Marine System Equipment Based on First Principles**

**Yuefeng Hu**



**Supervisor : Ir. Peter de Vos**

**Professor : Prof.ir. J.J Hopman**

# **DIMENSION PREDICION OF MARINE SYSTEM EQUIPMENT BASED ON FIRST PRINCIPLES**

MASTER OF SCIENCE THESIS

For the degree of Master of Science in Marine Technology at Delft University of  
Technology

Yuefeng Hu

January 12, 2016

Faculty of Mechanical, Maritime and Materials Engineering · Delft University of  
Technology



# Abstract

In this thesis, a new method of sizing marine equipment will be applied to main components of marine auxiliary systems. Contrary to the straight fit method through a database, the new method is based on the working principles of the machine, which means the developed mathematical expressions are based on the underlying physical relationships between the machine's dimensions and its specifications (power output, speed, etc). Apart from the main specifications, the selection of the technical parameters of the machine in the mathematical expressions could also influence the final overall dimension of the machines. However, due to the material characteristics, the technical parameters (shear stress, mean pressure, overall heat transfer coefficient, etc) of different marine components are in confined ranges respectively. That means there is a lower limit to the machine's overall dimensions given a certain specification. The author tries to explore a rough range of these technical parameters. The result is a 'rubber' design model that could be applied to predict dimensions of the primary marine components in the preliminary design stage. The new method has already been successfully applied to diesel engines, electric machines and gearboxes and it is thought to be generally applicable. In this thesis, the dimension prediction model based on first principles is applied to other marine system components; namely shell and tube heat exchangers, plate heat exchangers and centrifugal pumps. The results prove the applicability and universality of the sizing model.

# Table of Contents

---

Preface.....	VIII
1. Introduction .....	1
1.1. Background .....	1
1.2. Objectives.....	3
1.3. Outline of this thesis.....	4
2. Literature Review .....	6
2.1. Approaches for ship configuration design .....	8
2.2. 'Black box method' of dimension prediction of components .....	14
2.3. Methodology of the 'first principle' approach .....	19
2.4. Literature review of marine components .....	27
2.4.1. Shell and tube heat exchanger.....	27
2.4.2. Plate heat exchanger .....	29
2.4.3. Centrifugal pump.....	31
3. Generating Results of 'Black Box' Method.....	33
3.1. Introduction.....	33
3.2. The generated results by 'black box' method .....	34
3.3. Discussion .....	40
4. Shell and Tube Heat Exchanger.....	42
4.1. General information of shell and tube heat exchangers .....	42
4.2. Configuration of shell and tube heat exchanger .....	43
4.3. Sizing the primary element of shell and tube heat exchanger .....	45
4.4. Sizing secondary element and core of shell and tube heat exchanger .....	53
4.5. Sizing the whole shell and tube heat exchanger .....	57

4.6.	Model implementation and results discussion of STHE .....	59
4.7.	Summary .....	67
5.	Plate Heat Exchanger .....	69
5.1.	General information of plate heat exchanger .....	69
5.2.	Configuration of plate heat exchanger .....	72
5.3.	Sizing primary element of plate heat exchanger.....	74
5.4.	Sizing the whole plate heat exchanger.....	83
5.5.	Model implementation and results discussion of plate heat exchanger ....	86
5.6.	Summary .....	93
6.	Centrifugal Pump .....	95
6.1.	General information of centrifugal pump .....	95
6.2.	Configuration of centrifugal pump .....	100
6.3.	Sizing the primary element of a centrifugal pump.....	102
6.4.	Sizing the secondary element and core of centrifugal pump .....	107
6.5.	Sizing the whole centrifugal pump.....	110
6.6.	Model implementation and results discussion of centrifugal pump .....	111
6.7.	Summary .....	119
7.	Case Study .....	121
7.1.	Propulsion system of the 'BERNARDUS' tug vessel .....	121
7.2.	Auxiliary system of the 'PETROJARL 1' FPSO vessel .....	128
7.3.	Conclusion.....	134
8.	Conclusion and Recommendation.....	135
8.1.	Conclusions .....	135
8.2.	Recommendations for future work .....	136

References.....	138
Nomenclature.....	141
Appendix A.....	146
Appendix B.....	181
Appendix C .....	183
Appendix D .....	195

# Preface

---

In order to finish my Master of Science program in Marine Engineering at the Delft University of Technology (DUT), I started my graduation project in February 2015. The graduation project was carried out for approximate ten months at university. This graduation project actually relates to part of the PhD research of Ir. P. de Vos in DUT who is also my daily supervisor of my graduation project. The PhD project MOSES CD (Model-based Ship Energy System Conceptual Design) consists of three parts: network modeling for variation of system topology, performance prediction of marine systems and dimension prediction of the marine system components [1]. This project of course relates to the last part of P.de Vos' PhD project.

I would like to use this preface to thank some people who gave me special help and support during my graduation project. During my internship in IV Nevesbu, I got a lot of help from the staff in the office, Martin van Vliet, Rene Hereman, Arnold Wiskerke, etc. They gave me a lot of advice and offered a real case study for my graduation project. Without their help, I could not get such detailed dimension description of the shell and tube heat exchangers and applied them into my model.

I also need to give my great appreciate to Dr.ir.C.A.Infante.Ferreia who put a lot of effort to my thesis and correct mistakes I didn't notice. Furthermore, I must thank in particular professor J.J.Hopman and professor Douwe Stapersma. They gave me a clear direction of my graduation project which was extremely important for me at the beginning period. I also gain a lot from both of them.

Finally but most importantly, I would thank my daily supervisor P. de Vos. I could say it is not possible to complete this thesis without his patient help, constructive advice and cheerful encouragement.

# 1. Introduction

---

This chapter will introduce the background and objectives of the ‘first principle’ method of dimension prediction of marine system components. After that, the main structure of this thesis will also be presented to give readers an outline of the work.

## 1.1. Background

*Marine engineering is the art of integrating the components into systems in order to be able to perform a specific set of functions [2].*

For a vessel, its mission is basically achieved from well-functioning and cost-effective marine systems. It is the conviction of the author that only it is possible to achieve the certain mission completely when suitable marine components are designed and arranged properly within the marine systems. In order to design and arrange marine components in a marine system, the dimensions of these marine equipment are essential aspects that need to be considered by ship designers (everything needs to fit inside the ship). Therefore, an efficient method to evaluate the dimension of marine components (diesel engine, gearbox, electric machine, etc) within a complete marine engineering system is always of interest for ship designers. A new approach of dimension prediction of marine system components has been proposed by *D. Stapersma* and *P. de Vos* and is based on first principles. As a matter of fact, the research of first principles based dimension prediction model is also part of *P. de Vos*’ PhD research.

The PhD project MOSES CD (Model-based Ship Energy System Conceptual Design) of *P. de Vos* aims to improve the conceptual design of an onboard energy distribution systems (also known as platform systems or main and auxiliary systems). It consists of three major parts: network modeling for variation of system topology, performance

modeling for prediction of system performance and dimensions modeling for prediction of component dimension [1]. The new method of marine component dimension prediction applied in this thesis is obviously related to the last part of PhD project by P. de Vos.

The new method tries to improve on the current method of dimensions prediction which uses regression analysis. This method is only called the 'current' method as there are indications that this method is frequently applied in marine industry practice for components' dimension prediction. The current method is called here the 'black box' method. The 'black box' method applies regression analysis to build up mathematical relationships between e.g. power output and dimensions of marine equipment (description of details is given in Chapter 2). However, such mathematical relationships rarely relate to the physical working principle of the machine. The first principles based approach (a new method for dimension prediction) actually tries to improve on this black box approach by relating the dimension of a machine to its working principles, i.e. moving away from 'black box' to 'white box'. However a 'white box' is impossible to reach, thus the new method could be regarded as a 'grey box' approach.

Thus, a question may be asked by readers:

*What exactly are the differences between the 'black box' method and 'first principle' method and is the 'first principle' method an improvement?*

The detailed comparison and discussion about these two methods will be covered in the following chapters. *Stapersma* and *de Vos* in their paper [1] have already applied this first principles based approach to diesel engines, electric machines and gearbox and gained positive results. Another question could be raised:

*Is it also possible to apply this new method to other marine components?*

As the statement by *Stapersma* and *de Vos*, the sizing model based on first principles is thought to be generally applicable [1]. Therefore, the author tries to apply this new method to size other marine components (heat exchangers, centrifugal pumps) and discusses the results and performance of the models. The process of the model implementation will be presented in Chapters 4, 5, 6.

## **1.2. Objectives**

After illustrating the background and the raised questions in Section 1.1, the objectives of this thesis are raised accordingly. The first objective is checking whether the ‘first principle’ method of dimension prediction is generally applicable. Thus author tries to apply this method to other marine components.

Secondly, the comparison between the ‘first principle’ method and ‘black box’ method is also needed to be studied. The comparison will be mainly studied based on the new researched marine components.

Thirdly, in order to check the applicability of the sizing models in practice, employing them in case studies to size integrated marine systems is an efficient means of verification.

Consequently, the objectives of this thesis are set:

- Apply the ‘first principle’ sizing model to new marine components: shell and tube heat exchangers, plate heat exchangers and centrifugal pumps.
- Compare the ‘first principle’ method and ‘black box’ method.
- Case studies e.g. propulsion system and cargo oil heating system.

### 1.3. Outline of this thesis

Chapter 1 is an introduction of this thesis which describes the background of this new method of dimension prediction of marine system components. Furthermore, the objectives and the scope of the work are set as well.

Chapter 2 is a literature review which consists of four parts. The first part is investigating the literature about the existing ship conceptual design approaches to check whether there is a need for marine components dimension prediction. The second part is studying the literature about the 'black box' method of dimension prediction of marine system components and making comparisons with the 'first principle' method. The third part is a brief literature review of the 'conference paper' (*Dimension prediction models of ship system components based on first principles*) written by *Stapersma* and *de Vos*. Through the literature view, the methodology of this new sizing approach will be summarized and served as a guide for the new applications (heat exchangers and centrifugal pumps). Ultimately, in order to build up 'first principle' models for new marine system components (heat exchangers, centrifugal pumps), literature review about working principle, detailed geometry of these machines will be investigated as well.

Chapter 3 generates the results of the dimension prediction by using the 'black box' method for the components under consideration in this thesis (heat exchangers, centrifugal pump). Regression analysis is applied to find 'fit-functions' that predict the dimensions of these components based on the 'input-data', i.e. required power output or capacity, mass flows, etc.

Chapters 4, 5, 6 are the core of the whole thesis, in which the author will apply the 'first principle' methodology, explained in Chapter 2, to evaluate the dimension of shell and tube heat exchangers, plate heat exchangers and centrifugal pumps separately. The results of implementing the sizing models based on manufacturer data will be

discussed to check whether the 'first principle' method is efficient or not. Furthermore, the comparisons with the results generated based on 'black box method' in Chapter 3 will also be discussed.

Chapter 7 is a case study which needs employing the built 'first principle' sizing model in the previous chapters to real marine systems. This chapter could be regarded as a verification of the 'first principle' sizing models of the researched marine components.

Chapter 8 contains the conclusions and relevant future work.

## 2. Literature Review

---

Chapter 1 introduced a new method of marine equipment dimension prediction based on first principles. One could wonder whether this new methodology is necessary. Do we need marine equipment dimension prediction? And if so, how did we do it before? This chapter provides a literature review answering these questions.

Theoretically, the dimension prediction modeling method is often employed for supporting ship configuration approaches in early ship design stages. In modern ship preliminary design environment, several approaches for ship configuration design have been developed and can be applied in actual ship design process. Therefore, one of the aspects of this literature review in this chapter is learning the existing approaches for ship configuration design to check whether the dimension prediction modeling method could support these approaches. A ship configuration approach is an integration of several aspects, such as dimension prediction of large marine system components, finding the location of different spaces onboard the ship and the interconnections between different spaces (passageways), etc. Different methods may be available to evaluate each of these aspects, for example for component dimension prediction a 'black box' method may be used or the 'first principle' method as described in this thesis. Here an entire ship configuration approach could be regarded as an 'upper-level approach' and the methods supporting the whole approach are 'lower-level methods'. There are more than one method available for dimension prediction of marine system components. Therefore, another aspect of this literature review is an analysis of the 'black box' method for equipment dimension prediction. Likely weaknesses of the 'black box' method will be discussed. The third aspect is a literature review about the 'first principle' method proposed by *Stapersma* and *de Vos*. Based on this literature review, the process of the methodology will be illustrated to readers. Ultimately, in order to establish the dimension prediction model for new components (heat exchangers and centrifugal pumps), the working principle

and relevant configuration details of these marine components need to be studied from literature as well. This is the last aspect of this literature review. In conclusion, the objectives of the literature research consist of four sections.

- Investigate the existing ship conceptual design approaches to check whether there is a need for component dimension prediction.
- An analysis of the 'black box' method for dimension prediction of marine system components.
- Investigate the methodology of the 'first principle' sizing approach and summarize the general process of the methodology.
- Study the working principles and other relevant topics of marine auxiliary system components (shell and tube heat exchangers, plate heat exchangers and pumps) for the further model establishment.

## 2.1. Approaches for ship configuration design

The term 'configuration' is described as the relative position of the systems inside a ship by *Van Oers* [3]. It is also noteworthy that the term 'system' defined by *Van Oers* is different from the common marine engineering interpretation of systems (electric system, propulsion system, etc) described in the ship. 'System' defined by *Van Oers* is that "*A part of ship. In this dissertation, any part of the ship is considered to be a system, regardless of its purpose or size. As such, the common distinction between systems, subsystems and components is not used in this dissertation; all parts are called systems instead.*"[3] *Van Oers* also discussed the common word 'arrangement' mainly concerned the internal layout within a fixed envelope whereas 'configuration' could contain the variation of the envelope shape and size (see *Van Oers* [3]). Configuration design in early ship design stage is essential because only if each component is attributed a position can systems reveal whether they fit correctly (see in *Andrews and Dicks* [4]). In the process of literature review, several approaches are explored in ship configuration design, such as 'Knowledge-Based Conceptual Exploration Model' (*Van der Nat* [5]), 'A Packing Approach for Ship Configuration' (*Van Oers* [3]), 'Building Block Methodology' (*Andrews and Dicks* [4]), etc. In the following part of this literature review, these existing methods will be investigated to see whether these approaches relate to marine component dimension prediction and concurrently answer the question: "*Is there a need for component dimension prediction?*"

Figure 2.1 shows a 'V-diagram' proposed by *Van Oers* in his 'Packing Approach' for early stage ship design which illustrates the steps of the design process and dependencies between each other [3]. The initial step for a naval architect is to define an explicit mission of the ship he will design. A specific mission leads to functions which are fulfilled by internal marine systems which themselves consists of subsystems and components. Systems, subsystems and components need to be

arranged inside the ship's hull, which is the ship configuration problem that *Van Oers* tries to solve. The configuration of the ship serves as an input for evaluation whole of the performance of the ship. Ultimately, the outcome of each performance of each system establishes an overall measurement of the ship's ability to fulfill its mission effectively [3]. From Figure 2.1, it can be seen that the block 'Sub-systems, components' is dash-dotted. As explained by *Van Oers*, the detailed design and selection of 'subsystems and component' is not considered in his approach. Accordingly, a presumption is made by *Van Oers* that the size of subsystems and components is known. However, the size of components and subsystems will considerably influence the configuration of the ship. This is also admitted by *Van Oers*.

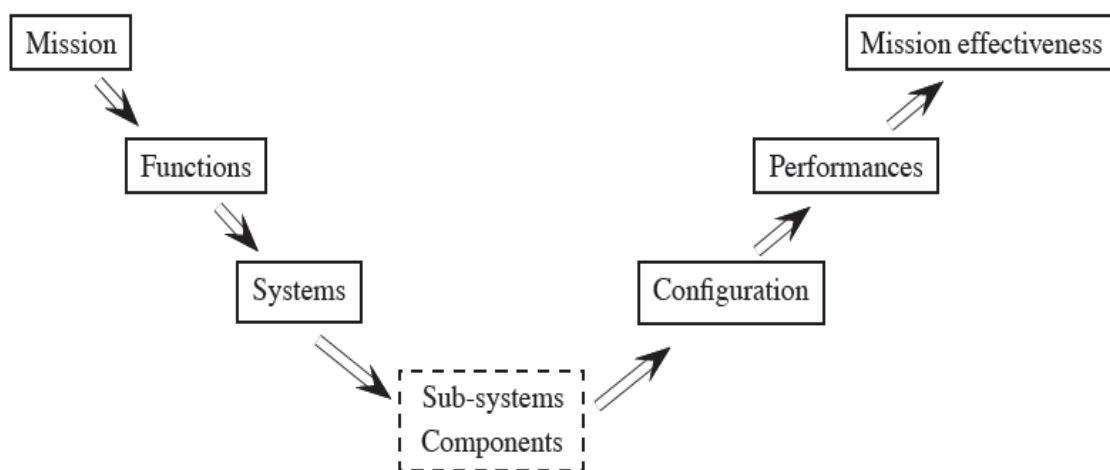


**Figure 2.1 "V-diagram" of ship design process, reference[3]**

As a matter of fact, the dimension model for sizing objects (components) is mentioned by *Van Oers* that *"These range from a simple look-up table that determines gas turbine size as a function of required propulsion power to a complex, physics-based model to determine the main electric motor size for a diesel-electric submarine"* [3]. The 'physics-based model' here is essentially similar to our 'first principle' model which uses basic physical relations to predict the dimensions of marine components. The detailed methodology about how to establish the component dimension model is not proposed by *Van Oers* in his 'Packing Approach'. Consequently, in order to apply the 'Packing Approach' in actual ship configuration design process, it is critical to

employ a method of predicting rough dimension of components within envelopes in the ship before building up packing model for the ship. In other words, our target for dimension prediction should be considered as necessary to create the required input for the process of ship configuration design.

Not only *Van Oers*' 'Packing Approach' requires component dimension prediction. It is also relevant in other preliminary ship design approaches. Actually, the 'Packing Approach' for early stage design can be regarded as a development based on *Van der Nat*'s [5] configuration design approach, 'Knowledge-Based Conceptual Exploration Model'. For instance, *Van Oers* [3] innovated the set of object types based on ship configuration proposed by *Van der Nat* [5] from three types to seven types for describing the entire design in a variable level of detail. Besides that, 'Packing Approach' still uses three types of descriptions of a ship ('numerics', 'geometry' and 'topology'), as proposed by *Van der Nat*. *Van der Nat* in his dissertation argued that creating an entire configuration, but with an appropriate level of detail is also significant [5]. Therefore, a decomposition method is applied in submarine design by *Van der Nat*, which could guarantee that no overlap or neglect happens. (see in *Van der Nat* [5]). Thus, *Van der Nat* decomposed the whole submarine into different types of objects. The method of sizing objects is clustering the same type of components into one object to size and he concluded that less than 100 objects are enough to describe a submarine. Before sizing different type of objects, geometric descriptions of components within objects need to be researched in advance. Accordingly, an accurate component dimension prediction model is critical for evaluating the size of different type of objects in *Van der Nat*'s submarine configuration approach.

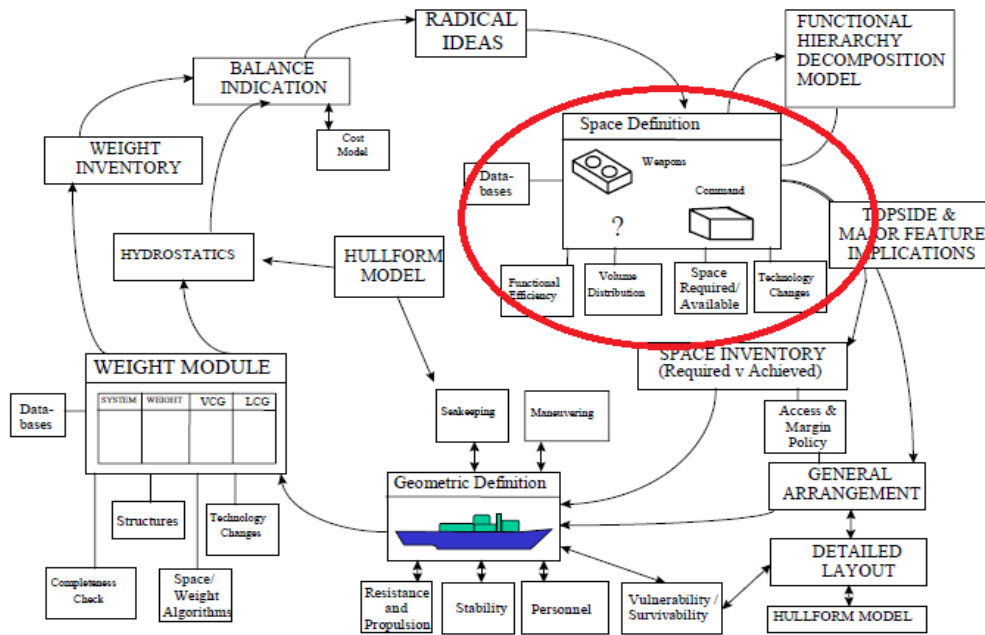


**Figure 2.2 Overview of the Design Building Block Methodology applied to surface ship, reference [4]**

Another approach relating to the ship configuration design is ‘Design Building Block (DBB) Approach’ proposed by *Andrews and Dicks* [4]. The basic idea of DBB approach is separating the functions of a ship into discrete elements and positioning them properly and then putting the architectural factors in the center of the process (see *Alexander et al.* [6]). *Andrews et al.* [7] illustrated that the ‘DDB’ approach could allow ship designers to pick up more alternatives to meet specific requirements. Figure 2.2 is an overview of the Design Building Block Methodology which is applied to surface ships. In the figure, the block ‘Space Definition’ within the red circle obviously has a relationship with ship configuration and size of marine components. In order to make ‘space definition’ within a ship, designers need to decompose the integrated block (system) into discrete space for arranging marine equipment or weapons. During the process of decomposition available space for components or subsystems, prediction of required space for various marine components is necessary. Here we notice that the input block is ‘databases’ for ‘space definition’, which implies that *Andrews* probably employs the ‘black box’ method for component dimension

prediction in this case. In the next section, the author will discuss the weaknesses of this 'black box' method for component dimension prediction.

In addition, the same situation also happens in another preliminary warship design tool called CONDES, proposed by *Hyde and Andrews* [8]. In the CONDES model, a balanced design is proposed to represent a valid solution in the preliminary stage. There are three classical balances which are:

$$\text{Ship Weight} = \text{Displacement}$$

$$\text{Space Required} \leq \text{Space available}$$

$$\text{Stability (GM}_T\text{) Required} \leq \text{Stability achieved}$$

The second balance equation relates to the configuration design problem. Here the strategy of ensuring required space is less than or equal to available space, applied by *Hyde and Andrews* [8], is the top-down method raised by *Guida and Zanella* [9] which starts with an estimated overall space form with a certain size. After sizing the overall available space, geometrical (space and size) and topological realization of marine components are made by dimension evaluation and located into a fixed space (see *Van der Nat* [5]).

Another example is the 'ship synthesis model' for naval surface ship proposed by *Michael Robert Reed* [10]. The method is used for estimating the volume, weight, the center of gravity, electric load of a naval ship. Except that, the model can also predict the performance of actual vessel using standard input specifications which generally comes from sample data [10]. The 'synthesis model' program is made up of several program subroutines and each of them determines specific features of the naval ship.

Among these different functional subroutines, subroutine 'EPLANT' and 'MBSIZE' in the 'synthesis model' are designed for determining their configuration within a naval

ship. The 'EPLANT' subroutine is employed for estimating the size of electric plants and generators through the electric load relations based on sample data. The sizing approach applied here, is essentially using 'black box' method based on limited sample data.

From a review of the models and approaches discussed above, it is concluded that parametric geometry description is mostly used in early stage ship design. The parametric geometry description is widely used by numerical concept models which can generate a large number of alternatives with the purpose of generating the valid design [3]. For example, the literature "Parametric Design and Hydrodynamic Optimization of Ship Hull Forms" by *Harries* [11] uses the parametric geometry description to generate variations of the hull shape. *Smith et al.* [12] employ the method to design the configuration of equipment aboard an offshore platform. In addition, the dimension prediction model proposed by *Stapersma and de Vos* [1] is also based on parametric geometry description. *Van Oers* argued that the development of parametric numerical and geometrical description for ship configuration design is still needed [3]. That is also one of the reasons why the 'first principle' method of component dimension prediction is carried out by *Stapersma and de Vos* [1].

Furthermore, it can be found that decomposing the entire vessel into several blocks in terms of function or configuration is widely applied in modern early stage ship design (e.g. 'Packing Approach' by *Van Oers* [3], 'DBB' approach by *Andrews and Dicks* [4], 'Integrated Approach' by *Alexander et al.* [6]). In order to estimate the dimension of these blocks, it is essential to make an initial dimension prediction of the marine components within the blocks or packages. Accordingly, an efficient and flexible prediction tool for sizing marine system components is necessary to cope with different particular requirements of the ship configuration approaches.

Based on the literature review, the author found that most early ship design approaches employ a 'black box method' for component dimension prediction.(e.g. DBB approach ,Packing Approach, Synthesis Model etc). It is however possible to define weaknesses of the 'black box' method. This warrants the development of a new dimension prediction tool. In the next section, relevant literature about the 'black box' method of dimension prediction will be reviewed. The method will later be compared with 'first principle method' of dimension prediction.

## **2.2. 'Black box method' of dimension prediction of components**

In practice, the 'black box' method, which uses regression analysis, is widely used for quantitative evaluation in many different engineering fields. Based on the purpose of this research, the scope is set on dimension prediction of marine components, i.e. applying regression analysis to predict dimensions of marine components when required performance is known. Theoretically, 'black box' method of dimension prediction is finding the mathematical relationship between performance parameters (e.g. power output, speed, heat transfer capacity) of components (diesel engine, electric machine, heat exchangers, etc) and the dimensions of them (length, width, height) based on manufacturers data of these marine components. To do this, the gathered numerical data between power output and component dimension are plotted in a graph. And then the 'fit trend-line' function is employed in the graph to determine the mathematical relationship between values in x-axis and y-axis, i.e. relationship between performance parameter (x-axis) and dimension (y-axis). The 'fit trend-line' function also gives the degree of accuracy of the fitted trend-line with the coefficient of determination, called  $R^2$  which is in the range of (-1,1) [13]. In the range of  $R^2$ , '-1' is the perfect negative correlation, '1' is the perfect positive correlation and '0' is no correlation.

Figure 2.3 is an example of applying regression analysis to find the mathematical relationship between the power output and specific height of diesel engine by *Van Es* [13]. The useful manufacturer data is usually collected from tech specs, project guides, websites, brochures and software (e.g.GES) [13]. As discussed in Section 2.1, the ‘black box’ method for dimension prediction is applied in many approaches and projects, such as All Electric Ship project in the Netherlands (*van Dijk, Frouws* [14, 15]), ‘Packing Approach’ for early ship design stage (*Van Oers* [3]) and ‘Ship Synthesis Model’ by *Reed* [10]. However, some weaknesses and expectations of this method are also mentioned in some reference. For instance, *Van Oers* in his thesis expected a more accurate predicting tool of sizing components [3]. In the following part, the weaknesses of ‘black box’ method compared with the ‘first principle’ method will be discussed.

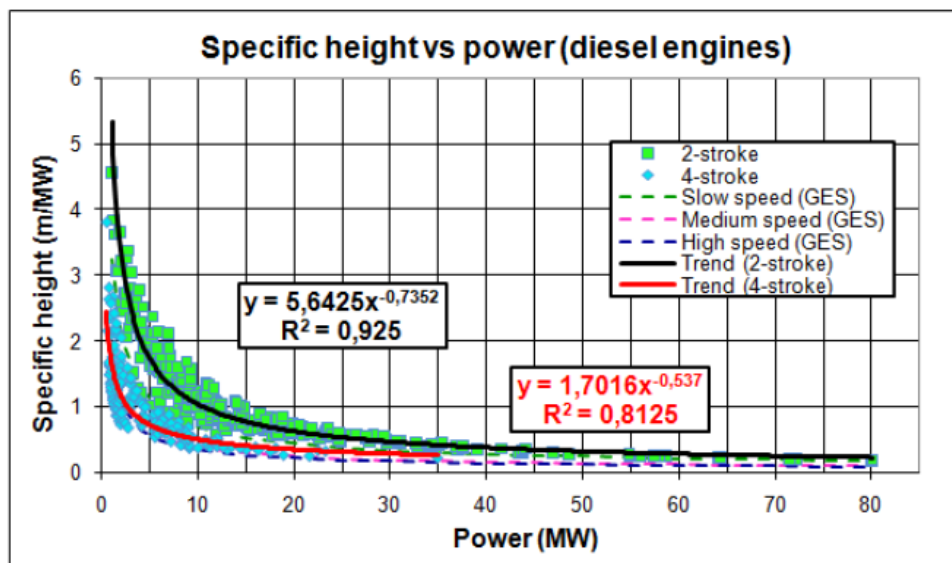


Figure 2.3 Specific height of diesel engines as a function of power, reference [13]

One of the weaknesses of the ‘black box method’ is discussed by *Hyde and Andrews* [8] that the ‘black box’ method, as the name implies, is like a ‘black box’ with parametrical input to obtain the target dimension. As a result, the physical meaning behind the equations based on ‘black box’ method is not clear. In contrast, the dimension prediction approach based on the first principle avoids this misgiving

caused by such 'black box' approach. *Stapersma* and *de Vos* [1] also state that the first principle approach means the expressions of components dimensions have more physical meaning than 'black box' method. Stated otherwise, the fidelity of the 'black box' models is low compared to the first principle based models.

Besides that, the second weakness of 'black box' method is that database could not contain all kind of applicable fitting dimensions of components, i.e. insufficient richness or range of database. Ship designers would probably come across failing to find a suitable size of the component from manufacturer database according to specific requirements by the ship owner. In addition, in order to maintain the database, a large amount of work on updating and maintaining data of machine is unescapable. For instance, the database of electric motor applied in 'AES decision model' by *Frouws* [15] is a European database called Eurodeem created by Joint Research Centre which needs continually updating new data. The expression probably loses accuracy over time caused by infrequently data updating. For instance, in the thesis of *Van Es* [13], the initial plan of making dimension prediction model is based on 'AES decision model'. However *Van Es* found a lot of relationships between machine dimension and power output did not fit the recent data anymore, thus a new model based on current data needs to be refined. Unfortunately, there is still a risk left for some designers who don't know the expression of machine relationship in 'AES model' is not accurate enough anymore.

The third weakness is the problem of extrapolation. Due to the extension of power requirements of some marine components (diesel engine, electric machine) on board, larger dimension of components is accordingly expected. However, existing database does not contain any extension of components dimension since these larger components did not exist in the past and even extrapolation of database-fit may not be valid. Theoretically, the mathematical expression between the dimension of machine and power output is based on existent manufacturer data in the database.

Due to some information is limited and unclear physical meaning, the degree of reliability of the mathematical expression is not high enough. Consequently, the expression with low degree of reliability would probably not be valid for extrapolation of non-existing data in the database.

The fourth weakness of 'black box' method is that there is a risk of interpolation of non-linear effects. Figure 2.4 derived in *Van Es* thesis [13] illustrates the relationship between the specific weight and speed of diesel engine based on 'black box' method. The red line goes through the plots is the trend line across all speed types. If we zoom into the figure, we can find the plots in the circle representing the medium speed diesel engines are mostly above the trend line. This is an example of non-linear effect which would lead an underrated evaluation of the specific weight of medium speed diesel engine.

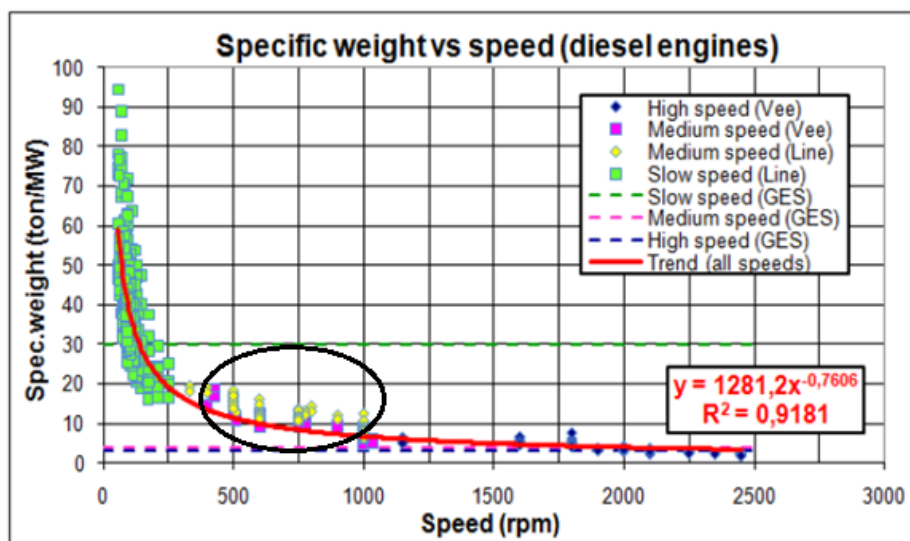


Figure 2.4 Relationship between specific weight and speed of diesel engine, reference[13]

Another example is shown in Figure 2.3 which provides the overview of the specific height of diesel engine as a function of required power. Obviously, the plots in the figure are divided into two groups which are two-stroke engines and four-stroke

engines separately. Accordingly, there are also two trend lines across the plots when applying regression analysis. However, if the designers don't know the approach need to divide diesel engine into two stroke engine and four stroke engines these two types to analyze, a single trend line would be drawn across the spots in the graph. The consequence of the single line would probably be drawn in the middle between red line and black line and that would lead to a underrated estimation of the specific height of two stroke diesel engines or over estimating that of the four-stroke diesel engines. Actually, the reason of this non-linear effect is because of the different construction type of two-stroke diesel engines and four-stroke diesel engines. Four-stroke engines are usually trunk piston engines and two-stroke engines are usually crosshead engines.

In comparison with the construction type of crosshead engine, the shape of trunk engine is more compact and usually built with two lines of cylinders in a V-configuration (as discussed by *Stapersma* [16]). Hence, the dimension of two types of diesel engines is different as a function of same power output. Similar construction situation influencing the dimensions of equipment is also encountered in electric machines. For a small electric machine, an open cooling fan at the free end of the machine and cooling vanes around housing is enough as a cooling system. However, for a larger electric machine a heat exchanger is mounted on the machine for cooling is needed (see *Stapersma* and *de Vos* [1]). Theoretically, without considering these two different cooling methods of electric machines, this would also probably cause non-linear effects when 'black box' method is used to build dimension prediction model. In contrast, the 'first principle' dimension prediction model has already taken into account the constructional disturbance which obliges designers to consider the type of machine during the early design stage. For instance, the dimension prediction model for diesel engines is classified into 'L engines' and 'V engines' which avoids usage of incorrect fit-functions.

Based on the weaknesses of 'black box' method of dimension prediction which have been discussed, a more fundamental model for describing the dimension of components need to be derived (mentioned by *van Es and de Vos* [17]). It is important to note that regression analysis is not denounced completely. The 'first principle' method still needs information from manufacturers in the database. For instance, evaluating the size of the overall machine from the dimension of core machine still needs the manufacturer data. In contrast with 'black box' method, the 'first principle' method tries to develop the expressions of components dimension as well as the selection of main parameters which have a large influence on the final overall dimensions of components [1]. In principle, the main specific parameters (e.g. Circumferential Lorentz stress, Mean effective pressure) are represented in the mathematical expression of components' power output. In practice, the values of these main parameters are in a certain range which also implies the range of machine dimension. Ultimately, this range of dimensions provides an overview of selection for ship designers in early stage ship design. In the next section, more information about the 'first principle' approach will be discussed.

### **2.3. Methodology of the 'first principle' approach**

Section 2.2 discussed the 'black box' method of marine components dimension prediction and the weaknesses of the 'black box' method compared with the 'first principle' method. In this section, the detailed methodology and whole process of the 'first principle' approach will be discussed and that is served as a guide for new applications in later chapters in this thesis. The main idea and the process of this new sizing methodology are basically summarized from the paper 'Dimension prediction models of ship system components based on first principles' written by *Stapersma and de Vos*. The entire content of the paper is attached in Appendix A.

## General process

The basic idea of 'first principle' dimension prediction model of main marine components (diesel engine, electric machine, gearbox, heat exchanger, etc) is predicting the whole dimension of a machine through sizing the core of it to the required power output or capacity by first principle relationship. In practice, the required power output/capacity is more or less fixed by mission or the size of ships which also underlying to the dimension of the core of the machine [1]. The core of the machine normally consists of a primary element and a secondary element. The dimension of the primary element is evaluated by the relationships with required power output/capacity through basic physical first principles. In the next step, the size of the secondary element is usually evaluated by geometrical analysis based on the dimension of the primary element. Combine these two elements together, the core of the machine can be achieved. Theoretically, the core dimension represents the significant part of the actual overall dimension of the machine or at least, the minimum dimensions of the machine for the required power output/capacity. The ultimate step is evaluating the whole dimension of the machine based on the core dimension using regression analysis. The explanation above is the general process of the dimension prediction method based on the first principle and the process is also summarized by Figure 2.5 below:

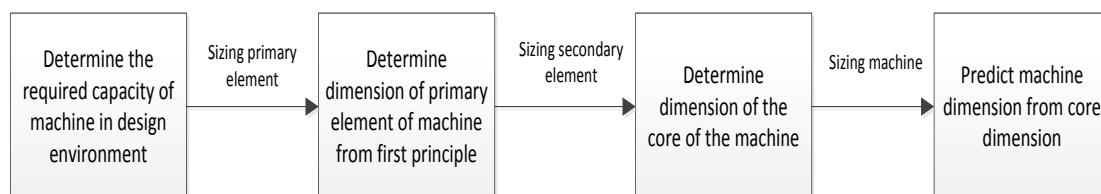


**Figure 2.5 General process of dimension prediction of components based on first principles, reference[1]**

From this figure it can be seen that the approach requires an estimate of the required power output or capacity of the machine under consideration as a starting point. Normally this capacity will be derived from a load balance or alternative method for calculating power usage. A load balance lists all users of a certain energy distribution system (mechanical, electrical, thermal, etc.) and their required powers in different operational modes. This leads to a required power/capacity of suppliers of a specific energy form. In the following part, the process of building up the 'first principle' model will be illustrated. The examples selected for supporting the illustration are from the paper written by *Stapersma* and *de Vos* [1].

## **Sizing the primary element**

As discussed before, the strategy of sizing primary element dimension is based on basic physical first principles. The marine components investigated by *Stapersma* and *de Vos* are diesel engine, electric machine and gearbox. Take a diesel engine for example, the primary element of the machine is the cylinder since a mathematical relationship between the dimension of a cylinder and the power output is founded. As a matter of fact, the mathematical relationship is not only limited to power output of the machine but also other energy flow (e.g. heating capacity for heat exchangers). For these three investigated machines, the types of the energy flow are all rotating mechanical power output.

Thus, the power output of these three components is all related to the torque and angular velocity of the machine. The basic equation of these three components is:

$$P=M \cdot \omega=2\pi \cdot M \cdot n \quad (2.1)$$

Where  $P$  (W) is power output,  $M$  (Nm) is torque and  $\omega$  (rad/s) is the angular velocity and  $n$  (rps) is rotational velocity in revolutions per second.

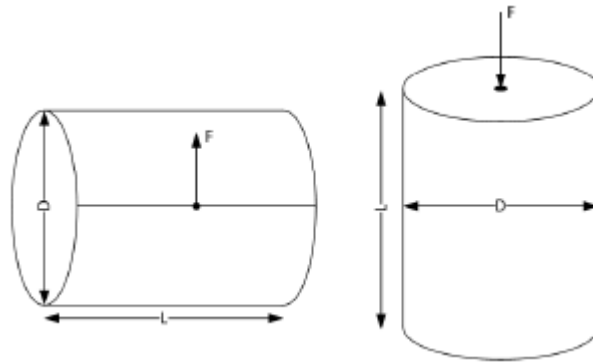


**Figure 2.6 Cylindrical volumes - left depicting a rotor of an electric machine or pinion/wheel of a gearbox and right depicting a diesel engine cylinder**

Actually, the torque ( $M$ ) delivered by these three machines are essentially from primary elements. For electric machine and gearbox, the forces are acted on the circumference surface of a cylinder shape. And for a diesel engine, the torque output is determined by the force is acted on the top of a piston. As illustrated by *Stapersma* and *de Vos*, the forces  $F$  in these three machines can be expressed as a mean shear stress ( $\tau$ ) and mean pressure ( $p_{me}$ ) in  $N/m^2$  which are the results of the force  $F$  divided by an area  $A$ . It is expected that there are physical limits to this mean shear stress and mean effective pressure depending on material characteristics. This means it is also expected that actual values for the mean shear stress and mean pressure can be reasonably estimated as they will be in a confined space near the upper limit. Thus, the main parameters (shear stress or mean pressure) contribute to establishing the first principle relationship between power output and dimension of the machines. For an electric machine, this 'specific force  $F$ ' acting on the circumference surface of a rotor (primary element) is called ElectroMotive Force (EMF). For gearbox the 'specific force  $F$ ' is called tooth force (TF) which is caused by the mechanical interaction between pinion and gear and for diesel engine is force on the piston ( $F_{piston}$ ). The detailed expressions about how the first principle relationships are built up are shown in Appendix A.

## Sizing the secondary element and core of the machine

As the statement in the paper, the dimension of the secondary element is determined by the geometrical relationship with the primary element. Furthermore, the combination of primary element and secondary element is the core part of the machine which would reflect the main information of the machine functionally and geometrically. Therefore, selection of secondary element is essential for building up the overall dimension prediction model. Take diesel engine, electric machine and gearbox for example, the secondary elements selected by *Stapersma* and *de Vos* for these three marine components are crankshaft, stator and wheel separately.

For an electric machine, Figure 2.7 shows the schematic of the core construction of the machine. From the Figure 2.7, we can find the shapes of the primary element and secondary element are actually both cylindrical. The primary element (rotor) is surrounded by the secondary element (stator) in the machine. In order to evaluate the dimension of the secondary element based on the primary element, a manufacturer factor 's' which is the rotor/stator diameter ratio ( $D_R/D_S$ ) is introduced.

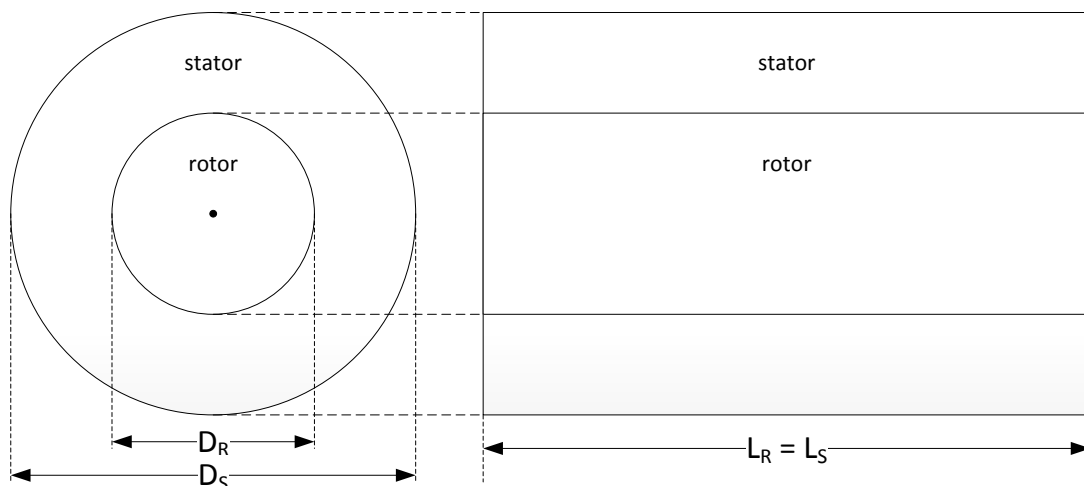
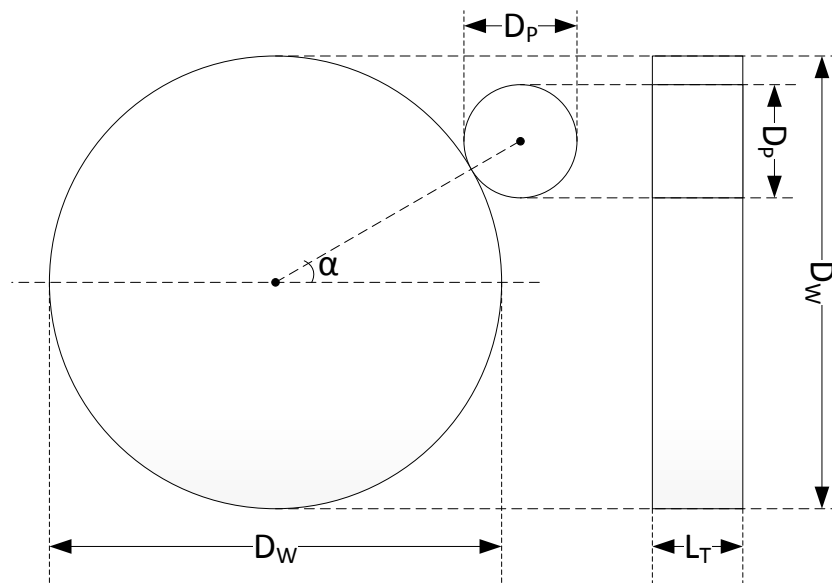


Figure 2.7 Schematic of electric machine core construction, reference[1]

Based on the schematic of the core construction of electric machine, the dimension of core is:

$$\begin{aligned} L_{\text{core,EM}} &= L_S = L_R \\ W_{\text{core,EM}} &= D_S = D_R / s \\ H_{\text{core,EM}} &= D_S = D_R / s \end{aligned} \quad (2.2)$$

For a gearbox, the configuration of core construction is shown in Figure 2.8. From this figure, we can see that there is an angle ' $\alpha$ ' determining the position of two elements. Actually, this angle ' $\alpha$ ' is characterized as the offset in the gearbox. For SISO (single input and single output) marine gearbox, the angle ' $\alpha$ ' is usually 90 degree for locating the gearbox far back in the ship possible .while for DISO (double input and single output) the angle ' $\alpha$ ' is set to 180 degrees to obtain more space between two machines [1].



**Figure 2.8 Schematic of gearbox core construction.**

After geometrical analysis based on the schematic of core construction, the mathematical description of core of gearbox is shown below:

$$\begin{aligned}
L_{\text{core,GB}} &= L_T \\
W_{\text{core,GB}} &= \max\left(\frac{D_P + D_W}{2} + \frac{D_P + D_W}{2} \cdot \cos(\alpha); D_W\right) \\
H_{\text{core,GB}} &= \max\left(\frac{D_P + D_W}{2} + \frac{D_P + D_W}{2} \cdot \sin(\alpha); D_W\right)
\end{aligned} \tag{2.3}$$

The core construction of the diesel engine is a little complicated compared with the other two components. Due to there are two configuration types of the diesel engine (Line-engine and V-engine), an angle ' $\alpha$ ' is introduced in Figure 2.9, as like gearbox, is used to determine different type of diesel engine. When the ' $\alpha$ ' becomes 0 degree, the type of diesel engine is L-type otherwise the type would be a V-type engine. Besides that the construction type of engine is also divided into two types: trunk piston type and crosshead type construction. A parameter 'ct' is introduced in the equation to characterize the construction type: for ct=1 is crosshead type engines and ct=0 is trunk piston type engines. According to the geometrical relationship in Figure 2.9, the expressions of core dimension of diesel engine is concluded that:

$$\begin{aligned}
L_{\text{core,DE}} &= i \cdot D_B \quad \text{for L engines} \\
L_{\text{core,DE}} &= \frac{i \cdot D_B}{2} \quad \text{for V engines} \\
W_{\text{core,DE}} &= 2 \cdot \text{MAX}\left(\left(\frac{L_S}{2} + (1+ct) \cdot \sin\left(\frac{\alpha}{2}\right) + \frac{D_B}{2} \cdot \cos\left(\frac{\alpha}{2}\right)\right); \frac{L_S}{2}\right) \\
H_{\text{core,DE}} &= \frac{L_S}{2} + \text{MAX}\left(\left(\frac{L_S}{2} + (1+ct) \cdot L_S\right) \cdot \cos\left(\frac{\alpha}{2}\right) + \frac{D_B}{2} \cdot \sin\left(\frac{\alpha}{2}\right); \frac{L_S}{2}\right)
\end{aligned} \tag{2.4}$$

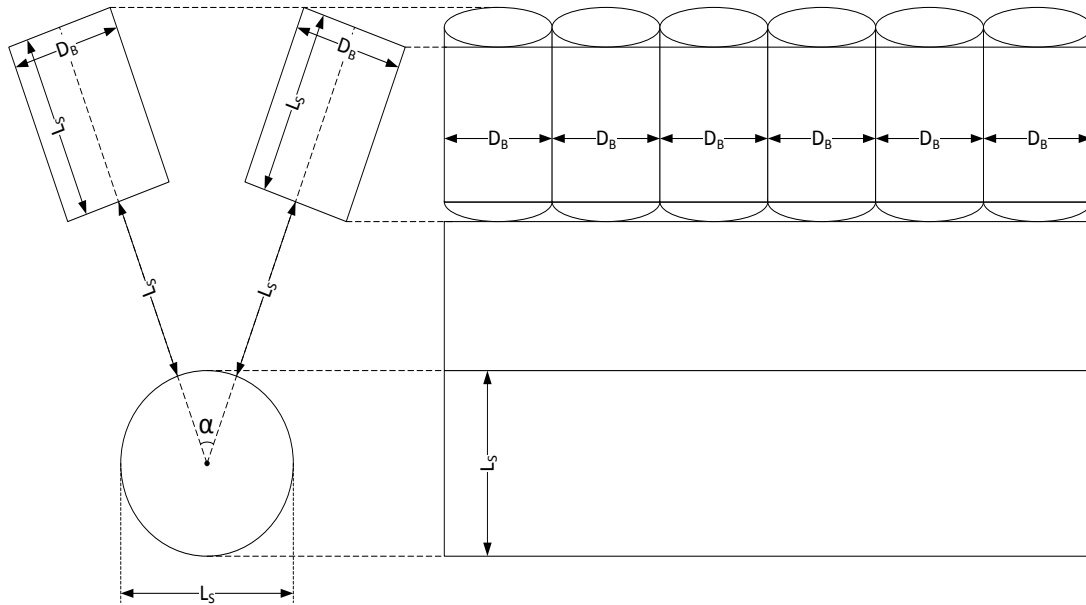


**Figure 2.9 Schematic of diesel engine core construction**

The more detailed analysis and illustration are provided in Appendix A.

## Sizing the whole machine dimension

The idea behind sizing the actual dimension of the whole machine is basically using regression analysis. Theoretically, the relationship between the core dimension and the whole machine dimension could be applied using different options such as polynomial function, power laws and even Fourier series. (As discussed by *Stapersma and de Vos* [1]). Since the core part of a machine, selected using the ‘first principle’ method, has already been counted a significant part of the whole machine, a single but effective relation is preferred. As a result, linear function probably is an effective option to represent the relationship between core dimension and the overall dimension of the machine. The mathematical relationship could be expressed as:

$$\begin{aligned}
 L_{\text{machine}} &= A_1 \cdot L_{\text{core}} \\
 W_{\text{machine}} &= B_1 \cdot W_{\text{core}} \\
 H_{\text{machine}} &= C_1 \cdot H_{\text{core}}
 \end{aligned}
 \tag{2.5}$$

In equation (2.5), ' $L_{\text{machine}}$ ', ' $W_{\text{machine}}$ ' and ' $H_{\text{machine}}$ ' are the machine's overall length, width and height separately. The ' $A_1$ ', ' $B_1$ ' and ' $C_1$ ' are the fitting factors of the relationship. ' $L_{\text{core}}$ ', ' $W_{\text{core}}$ ' and ' $H_{\text{core}}$ ' are the dimension of the core element of the machine.

In the following chapters, the methodology will be applied to evaluate the dimension of shell and tube heat exchangers, plate heat exchangers and centrifugal pumps. And check whether the sizing model is a 'rubber' design model with general applications. In order to apply this 'first-principle' model to other auxiliary marine equipment, some literature review based on machine working principle and relevant research will be done in the next section.

## **2.4. Literature review of marine components**

In this section, the working principle and performance, which need to be known for the establishment of dimension prediction model of the new components (shell and tube heat exchangers, plate heat exchangers and centrifugal pumps) will be introduced. Underneath the working principles and other relevant information of these components is summarized based mostly in handbooks on relevant topics.

### **2.4.1. Shell and tube heat exchanger**

In order to build up the dimension prediction model for shell and tube heat exchangers, a literature review is necessary. The literature review comprises working principle, design process, correlation of overall heat transfer coefficient etc. The basic working principle of shell and tube heat exchangers can be found in several books, such as [18], [19] and [20] and a detailed explanation is presented in Chapter 4. The basic working principle of shell and tube heat exchangers is that heat transfer takes place between a hot fluid flowing through a bundle of tubes and a cold fluid flowing through the shell surrounding the tubes or vice versa. The heat transfer process occurs in the

heat exchanger at the surface of the bundle of tubes. A first principle relationship could be built up between heat flow and surface area of the tubes in shell and tube heat exchangers. Accordingly the dimensions of the primary element (tubes) in the dimension prediction model are determined.

After that, the literature of construction type and detailed geometry description of tubes need to be reviewed as well. This is necessary for dimension prediction of the secondary element: the shell. The construction types of shell and head of shell and tube heat exchanger are different and TEMA [21] set the standard of them. Different types of shell and head combined together build up different shell and tube heat exchangers for different applications. *Thulukkanam* [19] in his book elaborates on the detailed geometry and layout pattern of tubes. Figure.2.10 gives the three types of tube layout in the tube bundle. The layout pattern will influence the number of tubes which are mounted on the tube sheet.

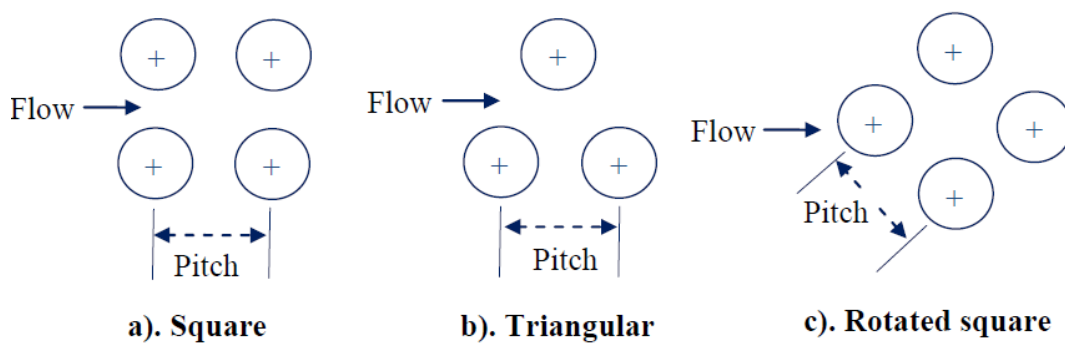


**Figure 2.10 Shell and tube heat exchanger tube layouts**

During the design process of shell and tube heat exchangers, correlations are normally used for rating heat transfer performance of shell and tube heat exchangers and the most commonly used correlations are based on Kern Method [22] and Bell-Delaware Method [20]. These two methods could be employed to estimate shell side heat transfer coefficient which is part of overall heat transfer coefficient ( $U$ ). Compared with Kern Method, the Bell-Delaware method is more accurate and can

provide detailed design process (as discussed by *Rehman* [23]). The Bell-Delaware method can predict the pressure drop and heat transfer coefficient with high accuracy, however the process of this method requires many details which usually are not available in the preliminary design stage. A simplified version of Bell-Delaware is presented by *Serth* [20] which is more straightforward and more suitable for building up the model in early stage. Besides that, the method of calculating the tube side heat transfer coefficient ( $h_i$ ) is presented in the book written by *Stappersma and Woud* [18] as well, who divided the flow into laminar flow and turbulent flow and considered it separately.

References [19, 24] illustrate an empirical formulation to estimate the diameter of the shell based on tube diameter and the number of tubes. The details of this empirical formulation will be presented in Chapter 4 later. References [19, 20, 24] also introduce the whole process of designing shell and tube heat exchangers. Their process correlates well with the basic ideas behind the marine equipment dimension prediction model.

## **2.4.2. Plate heat exchanger**

The basic working principle of plate heat exchanger is similar to the shell and tube heat exchanger, only heat transfer takes place through corrugated heat transfer plates (as discussed by *Kakac et al.* [25]). Accordingly, the primary element of plate heat exchangers is the plate which is used for building up a relationship between the thermal power and geometry of the plate. *Muley and Manglik* [26] in their paper introduce a review of different plate geometries and focus on the corrugated heat transfer plate which is most commonly used in plate heat exchangers. Deeper research of corrugated plate is done by *Focke et al.* [27], who found the inclination angle and flow direction are the main factors influencing the thermal hydraulic performance of plate heat exchangers. The detailed configuration of heat transfer

plate is introduced by *Vishal R and Matawala* [28]. As shown in Figure 2.11, there are two categories of configurations which are intermating throughs (a) and chevron throughs (b and c) respectively. In practice, the chevron type of plates is most commonly used in manufacturer. As discussed by *Shah et al.* [29], the configuration is pressed equally so that the spacing and the plates are assembled together with opposite direction of chevrons as shown in Figure 2.11(b). The typical depth of chevron throughs is 3-5 mm. The design of chevron pattern plate could increase the performance of heat transfer [29].

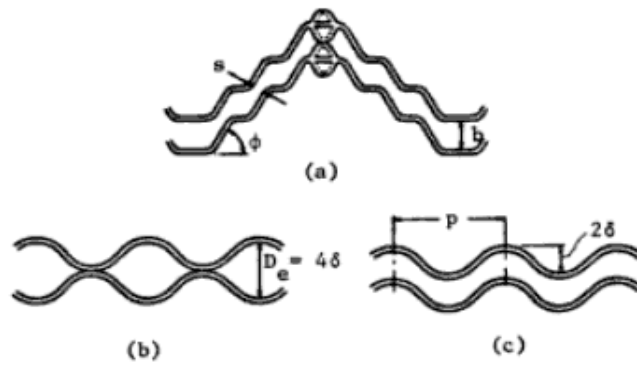


**Figure 2.11 Cross section of two neighboring plates (a) Intermating throughs, (b) and (c) Chevron throughs**

As same as shell and tube heat exchangers, there are also several methods of calculating the overall heat transfer coefficient of plate heat exchangers e.g. [18, 25, 28]. In the researched literature, a lot of effort has been spent on improving the correction factor of heat transfer coefficient. In Chapter 5, the author will employ a suitable method in dimension prediction model for plate heat exchangers.

### 2.4.3. Centrifugal pump

References [18, 30, 31] illustrate the general knowledge of the centrifugal pumps including working principle, machine configuration, design process, application, etc. From the references mentioned above, the author identified the main parts of a centrifugal pump which are an impeller and a volute (casing). The fluid is sucked into the pumps driving by the rotating impeller and accelerated by the impeller. The volute cross section increases gradually in the flow direction that could reduce the velocity of fluid and convert into pressure [18]. The design approaches of pump impeller are presented in several papers, such as *Wu et al.* [32] employ novel design approach which combines manufacturing process and numerical simulation, *Wen-Guang* [33] uses a singularity method to design the blades of pump impellers and *Westra* [34] employs inverse-design and optimization method to design the pump impeller. When designing the geometry of pump volute, the Stepanoff theory is normally used which is proposed by *Stepanoff* [35] in 1957. The Stepanoff theory assumes the velocity of flow in volute is constant when designing the cross-sectional area of the volute. The cross-sectional area is changed based on the divergence angle (as shown in Figure 2.12) in order to maintain the constant flow velocity.

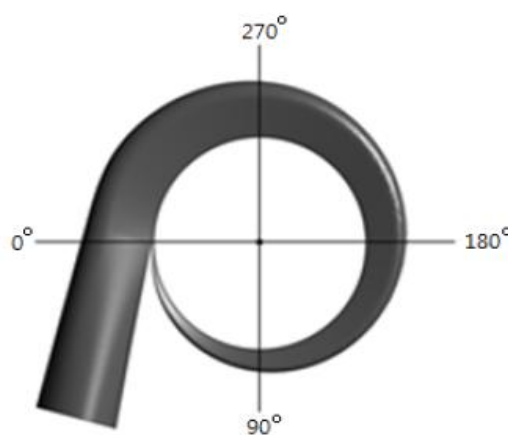


**Figure 2.12 Angle position with volute geometry**

The flow and loss mechanisms in pump volute are analyzed by *Van der Braembussche*, who discusses the advantages and disadvantages of different volute geometries, the relations between the flow and geometry, the impact of downstream and upstream impeller and the model of predicting mechanical loss within the volute [36].

*Tiwari and Kumar* in their paper analyze the losses in centrifugal pumps. The mathematical analysis is done through estimation of geometrical parameters of centrifugal pumps to predict the performance curve [37]. Similar research of performance prediction of centrifugal pumps has been developed by *Dick et al.* [38].

# 3. Generating Results of ‘Black Box’ Method

---

In this chapter, author is going to generate results of the ‘black box’ method applied to shell and tube heat exchanger, plate heat exchanger and centrifugal pump. The generated results will be used to compare with the results generated by ‘first principle’ method in Chapters 4, 5, 6.

## 3.1. Introduction

The ‘black box’ method is assumed to be based on regression analysis performed on manufacturer information contained in a database. The goal of regression analysis in this case is to convert discrete points in the database to a continuous ‘fit-function’ that enables dimension prediction within, or even outside, the range of the database. This continuous fit-function is much easier to implement in a computer program than the database itself, which could be one reason for applying regression analysis to find the fit-function. Furthermore, a generally applicable mathematical relationship can be found in this way which can be used in a conceptual ship design environment to quickly find dimensions of equipment without having to ask manufacturers for this information. As discussed in the literature review it is expected that this ‘black box’ method based on regression analysis is applied regularly in current ship design approaches. As implied, a ship designer could alternatively simply ask a manufacturer for the dimensions of a certain type of machine or equipment given a certain specification. This approach however may take longer than the time available.

In order to be able to compare the new ‘first principle’ method for dimension prediction with the ‘black box’ method, the ‘black box’ method is mimicked here to generate results from a regression analysis based dimension prediction approach.

The 'black box' method is mimicked here by plotting 'input-data' (power/speed/capacity/mass flow) against 'output-data' which are the dimensions. By doing so a fit-function is found that predicts dimensions without requiring any knowledge of the equipment. Whether the fit-functions that are found in this way can really be applied in an actual ship design environment depends on the required accuracy, the available time, etc.

### 3.2. The generated results by 'black box' method

In this section the mathematical relationship between the 'input-data' (power output/heat capacity) and dimensions of the machine will be explored based on 'black box' method. The trend-line across the plots is generated using regression analysis. The accuracy of the fitted trend-line is indicated by the coefficient determination, called  $R^2$  which is in the range of (-1,1). In the range of  $R^2$ , '-1' is the perfect negative correlation, '1' is the perfect positive correlation and '0' is no correlation. Thus the higher ' $R^2$ ' value implies the higher accuracy of the trend-line mathematic relationship and vice versa. The generated results of 'black box' method are shown below:

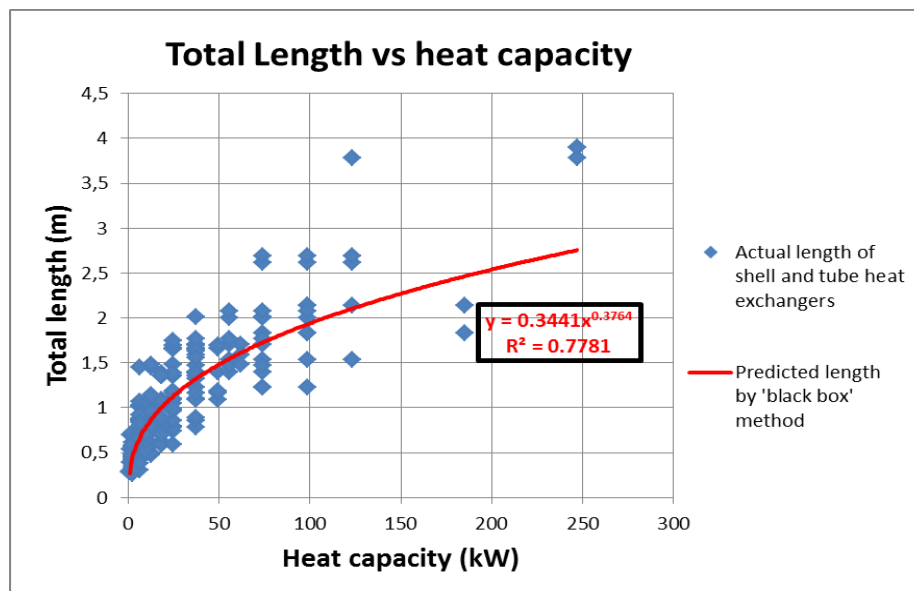
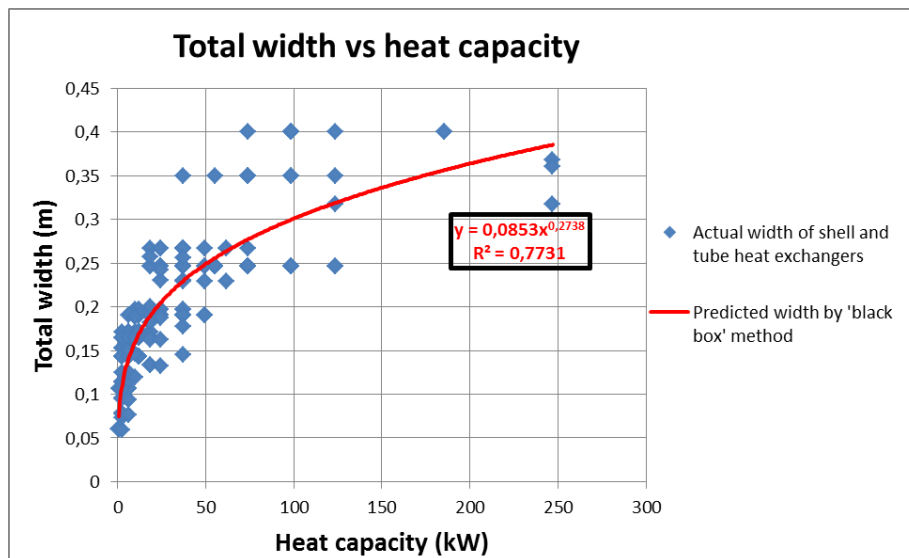


Figure 3.1 Total length of shell and tube heat exchangers as a function of heat capacity

It can be seen in Figure 3.1, the 'x-axis' represents the heat capacity of the heat exchangers and the 'y-axis' represents the dimensions of the shell and tube heat exchangers. The power relationship is applied to the red trend-line across the plots. The 'R<sup>2</sup>' value is approximate 0.78. Again, in specific cases the required accuracy and available time may be different, so nothing can be concluded here on whether this accuracy is sufficient or not.



**Figure 3.2 Total width of shell and tube heat exchangers as a function of heat capacity**

The situation of the width is similar with that of length. As shown in Figure 3.2, the 'R<sup>2</sup>' value is approximate 0.77.

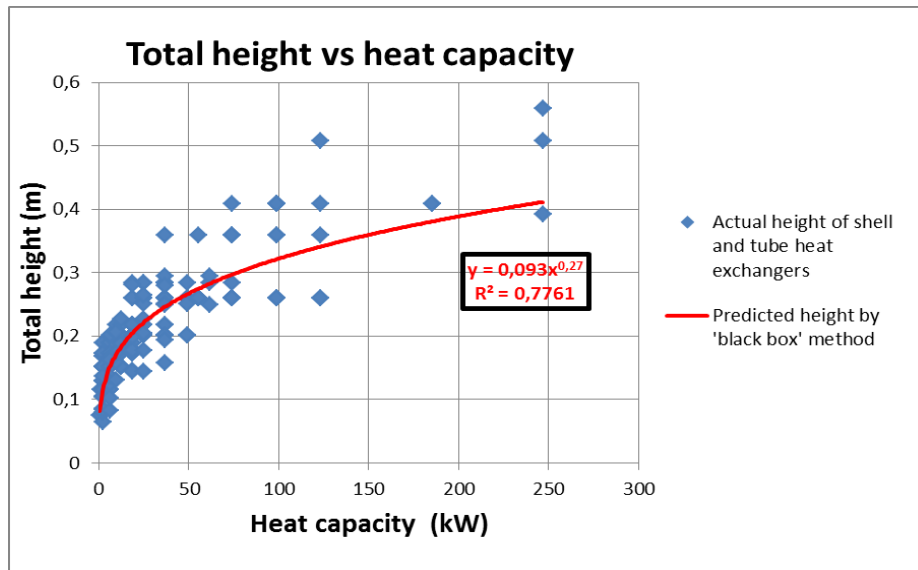


**Figure 3.3 Total height of shell and tube heat exchangers as a function of heat capacity**

Since the shape of the shell and tube heat exchanger is cylindrical, the dimensions of the width and height are close. It can also be proved in figures where the plots in Figure 3.2 and 3.3 are similar. The 'R<sup>2</sup>' value in Figure 3.3 is approximate 0.78 which is also close to that of width correlation shown in Figure 3.2.

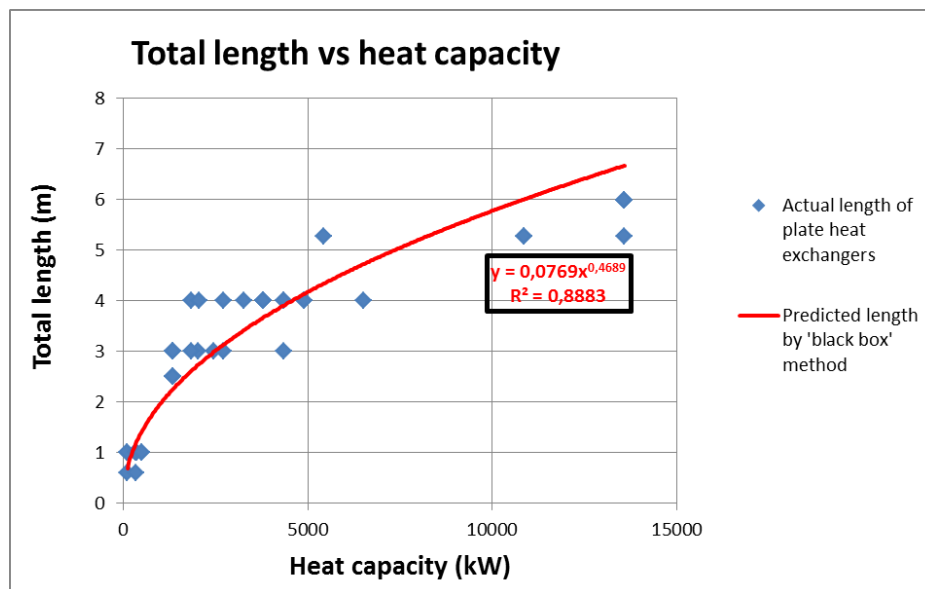


**Figure 3.4 Total length of plate heat exchangers as a function of heat capacity**

Figure 3.4 shows the results of the plate heat exchangers based on 'black box method'. As same as shell and tube heat exchangers, the power relationship is applied of the dimension correlation. The 'R<sup>2</sup>' value of the trend-line is around 0.89. It can be seen in Figure 3.4, a same length of the plate heat exchanger matches different heat capacity. That is due to the construction of the plate heat exchanger whose heat transfer plates could be removed or added with the same overall length. Therefore, the construction type of the plate heat exchanger influences the results of the 'black box' method.

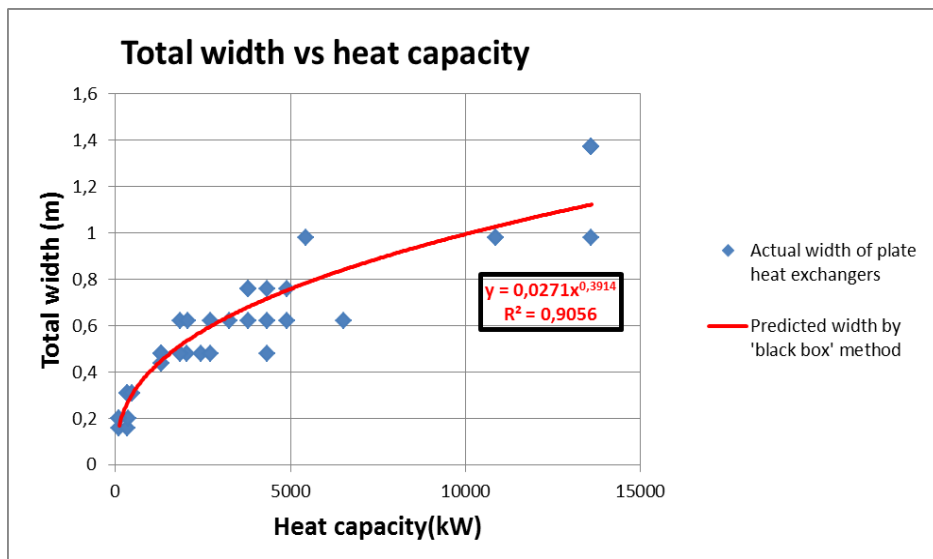


**Figure 3.5 Total width of plate heat exchangers as a function of heat capacity**

The result of width correlation is better than that of length. The 'R<sup>2</sup>' value of the trend-line is approximate 0.91.

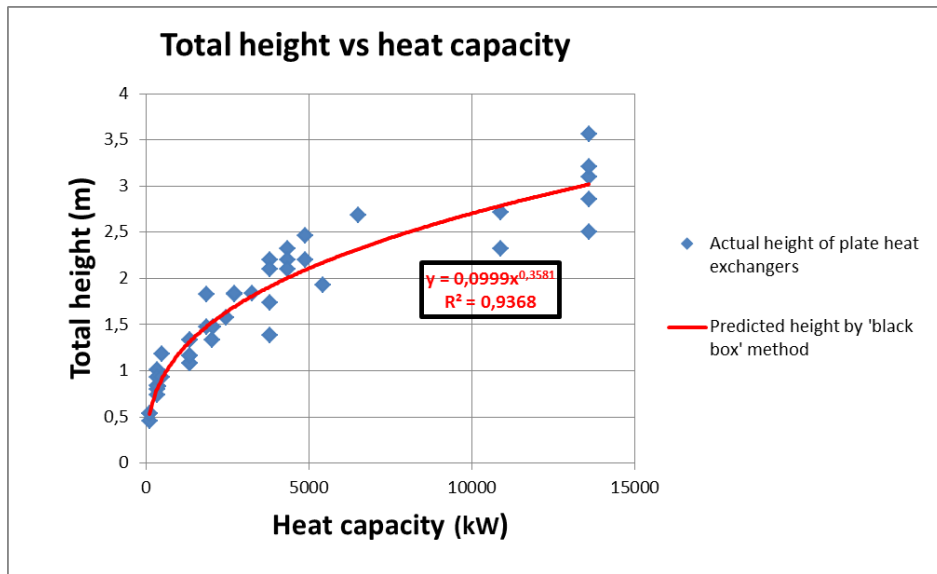


Figure 3.6 Total height of plate heat exchangers as a function of heat capacity

It can be seen in Figure 3.6, the results of total height better than width and length whose 'R<sup>2</sup>' value of the trend-line is approximate 0.94.

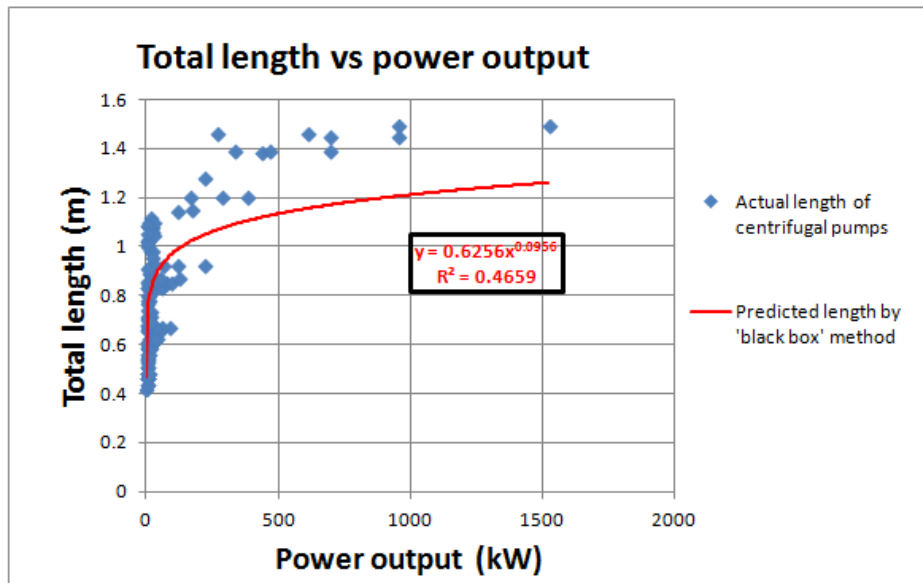


Figure 3.7 Total length of centrifugal pumps as a function of power output

Figure 3.7 shows the generated fit-function for dimension prediction of centrifugal pumps' total length as a function of power output. The 'R<sup>2</sup>' value of the trend-line is around 0.47 which means low accuracy for dimension prediction. This is most

probably caused by the fact that the electric motor driving the pump is included in the overall length as the gathered information did not allow for finding the length of the centrifugal pump only.

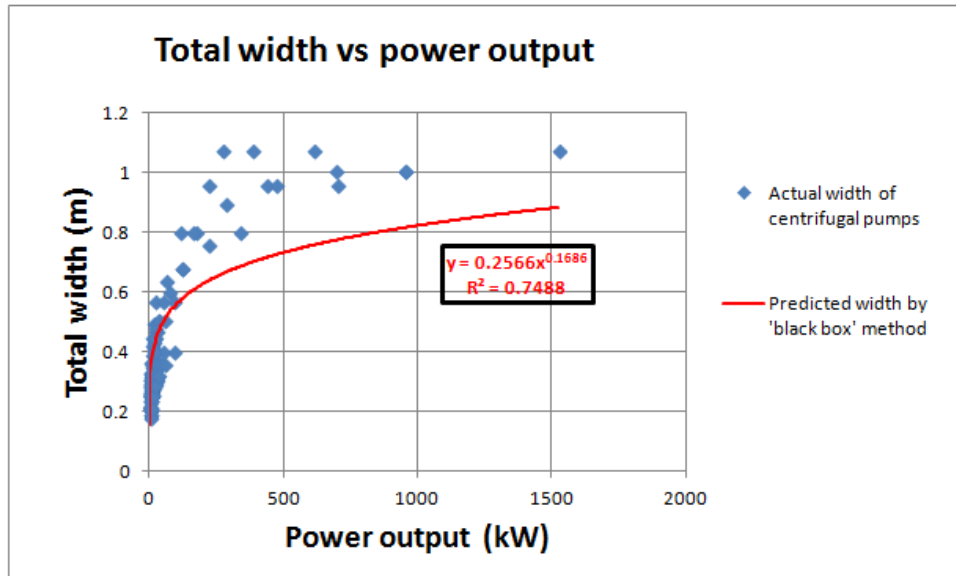


Figure 3.8 Total width of centrifugal pumps as a function of power output

The situation of the width correlation is better compared with length correlation whose 'R<sup>2</sup>' value of the trend-line is approximate 0.75 read from the figure above.

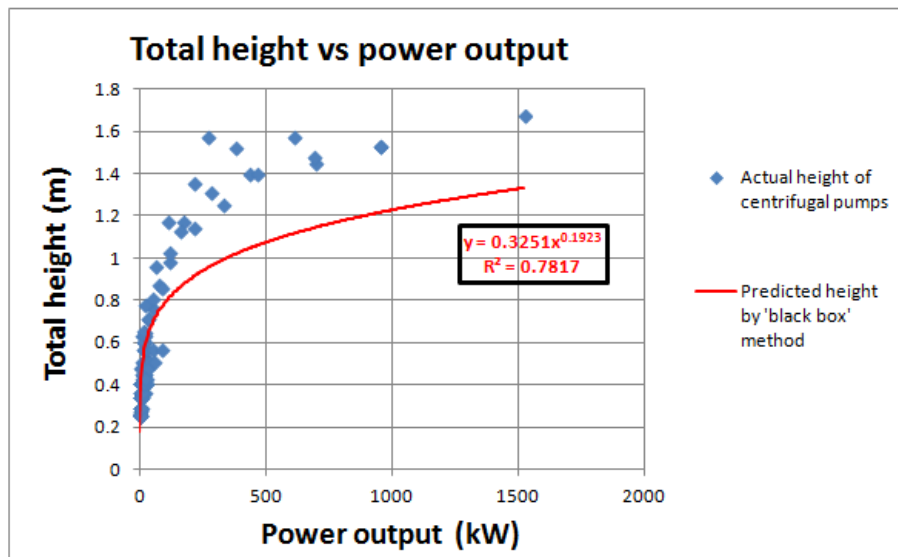


Figure 3.9 Total height of centrifugal pumps as a function of power output

As shown in Figure 3.9, the 'R<sup>2</sup>' value of the trend-line is approximate 0.78 using the power relationship. It can be seen in the figure, some plots are above the red trend-line rather than on the trend-line.

### **3.3. Discussion**

From the results, it can be seen that the 'black box' method enables dimension prediction without requiring knowledge of the working principles of the equipment / machines under consideration. But whether the accuracy is high enough remains to be seen and depends on the specific situation in which the 'fit-function' will be applied. Another consideration is the fidelity of the models as already discussed in Chapter 2. The low fidelity of the 'black box' method means there is a risk for finding a fit-function that overlooks 'something', like e.g. a non-linear effect. For instance, it remains a question whether or not the author would have understood the reason for the poor accuracy of the centrifugal pump length fit-function if the first principle based approach would not have been applied. But perhaps more importantly, in an actual ship design environment the "meta-data" of the fit-function, i.e. the low accuracy and the reason for it, may be lost when the fit-function is transferred between persons. If this risk is considered unacceptable, the fidelity of the models needs to be raised. This is done by applying the 'first principle' method, which is the subject of the subsequent chapters.

The 'first principle' method is something like a 'deeper dig' method of sizing marine components which is a physical-based method establishing the relationship between machines' working principle and the dimensions of them. Compared with the 'black box' method, the 'first principle' method demands engineers to know basic knowledge about the machines and decide the variables of the mathematical expressions.

In the following chapters, the author will establish the 'first principle' models for shell and tube heat exchangers, plate heat exchangers and centrifugal pumps. The results

produced by 'first principle' method and 'black box' method will be compared as well.

## 4. Shell and Tube Heat Exchanger

---

A heat exchanger is a heat transfer device that exchanges heat between two or more process fluids [19]. Heat exchangers are applied in plenty of marine systems for cooling or heating purposes. Among different types of heat exchangers, shell and tube heat exchangers are commonly used in marine systems. In this chapter, the working principle and configurations of shell and tube heat exchangers (STHE) will be introduced. Furthermore, based on the working principle and configuration of STHE, the primary element and secondary element of STHEs will be determined. After that, the dimension prediction models based on first principle will be established for STHE. Ultimately, implementation of the model and results discussion will be presented.

### 4.1. General information of shell and tube heat exchangers

Shell and tube heat exchanger is a common versatile type of heat exchanger; it can be applied for cooling lube oil of an engine or gearbox, cooling of fresh water by sea water, heating fuel oil in bunkers, etc. A tube bundle is one of the main parts of STHE, which is enclosed by a cylindrical shell. During the working process, one fluid flows through the cylindrical shell from one side to another, while the other fluid flows through the tubes from one head to another. Heads at one or both ends of the tube bundle act as manifolds distributing the fluid flow over the tubes in the bundle [18]. The two fluids with different temperatures undergo a heat transfer process through the wall of the tubes. According to the direction of two flows in STHE, the same direction of flow is called parallel flow; while the opposite direction is called counter flow.

The type of STHE on the type of construction can be classified as the straight-tube type and the U-tube type. As Figure 4.1 shown, the tubes of the straight-tube heat exchanger are straight and the ends of each tube are welded into the two tube sheets

on each side which separate the shell-side and tube-side fluids. The tube sheets are welded to the shell. The flow arrangement of straight type could be single-pass or multi-pass. However, for U-tube type heat exchanger a single pass is not possible because the shape of U-bundle makes the fluid in the tubes traverse through the tube bundle twice.

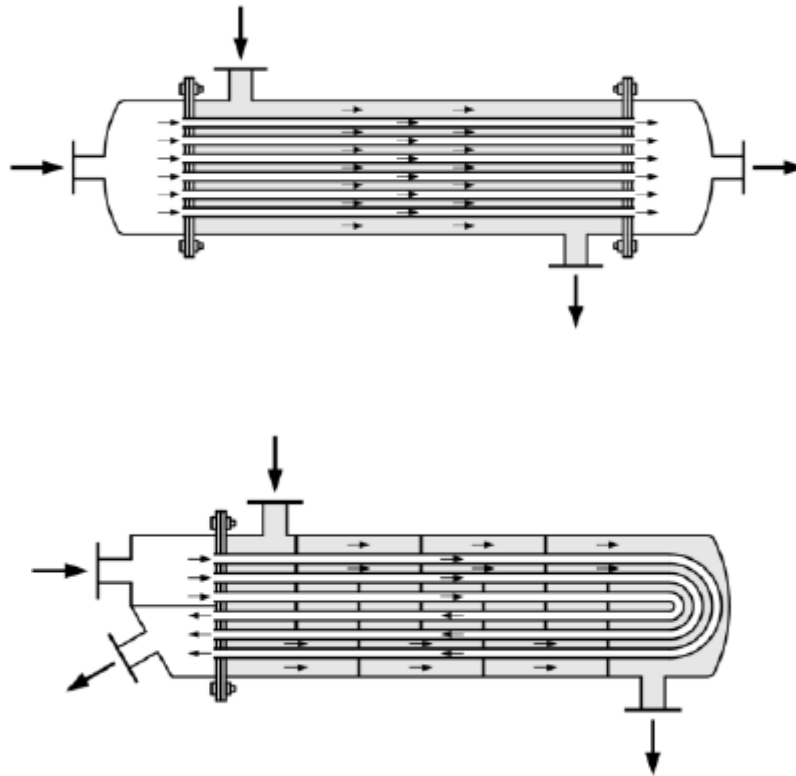


Figure 4.1 Straight-tube heat exchanger and U-tube type heat exchanger

## 4.2. Configuration of shell and tube heat exchanger

Before selecting the primary and secondary element of the component according to the sizing methodology, the detailed configuration and mechanical feature of shell and tube heat exchangers need to be discussed in advance.

The principle components of STHE are:

- shell
- tubes
- baffles
- tube sheets
- heads
- nozzles

Other components include pass partition, tie rods and spacers, support saddles, sealing trips etc [39]. Figure 4.2 gives an overall description of components within a STHE. According to Figure 4.2, it can be concluded that a STHE basically can be divided into three major parts: shell, tube bundle and heads. Due to the tube bundle is totally contained inside the shell, it is also reasonable dividing STHE into shell and heads these two parts.

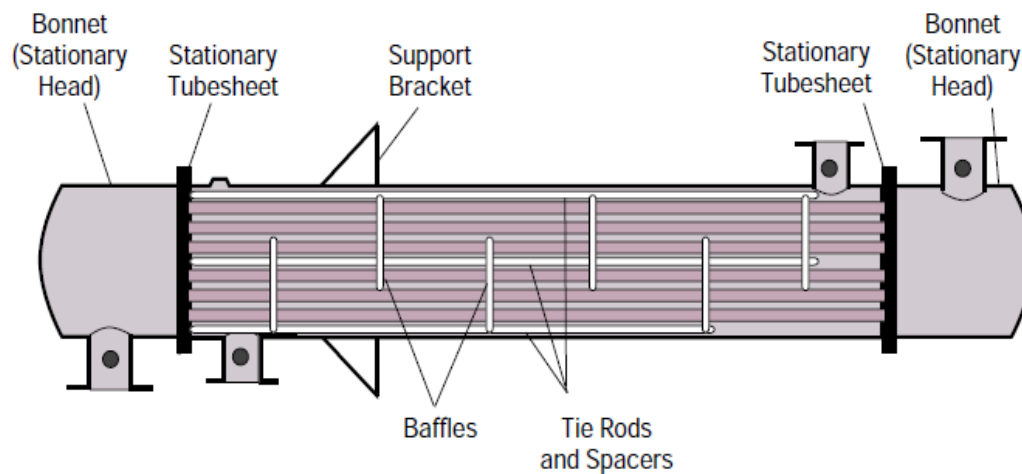


**Figure 4.2 Configuration of a shell and tube heat exchanger**

### 4.3. Sizing the primary element of shell and tube heat exchanger

As the methodology introduced before, the core of machine consists of the primary and secondary elements. In this section, we will select the primary element of STHE and establish a sizing model.

According to the heat transfer process of STHE, the boundary between the hot fluid and cold fluid is the wall of tubes. The fluid on the cold side gains energy by heat transfer from the wall while the fluid on the hot side loses energy to the wall [18]. Therefore, the total heat transfer area would be the total surface area of a bundle of tubes which actually is the total surface area of tubes' wall. Therefore, in order to make a relationship between the dimension and thermal energy, it is reasonable to choose tubes as the primary elements. In the following part, the dimension prediction model of the primary element (tube) will be introduced.

Start with three basic heat transfer equations:

$$\dot{Q} = \dot{m}_{\text{hot}} \cdot C_{p,\text{hot}} \cdot (T_{\text{hinlet}} - T_{\text{houtlet}}) \quad (4.1)$$

$$\dot{Q} = \dot{m}_{\text{cold}} \cdot C_{p,\text{cold}} \cdot (T_{\text{coutlet}} - T_{\text{cinlet}}) \quad (4.2)$$

$$\dot{Q} = U \cdot A \cdot \Delta T_m \quad (4.3)$$

Where ' $\dot{Q}$ ' is heat transfer rate (W), ' $\dot{m}_{\text{hot}}$ ' and ' $\dot{m}_{\text{cold}}$ ' are the mass flow of hot fluid and cold fluid separately (kg/s), ' $C_p$ ' is the specific heat of the fluid (J/kg K), the temperature ' $T_{\text{cinlet}}$ ', ' $T_{\text{hinlet}}$ ', ' $T_{\text{coutlet}}$ ' and ' $T_{\text{houtlet}}$ ' are the inlet and outlet temperature of hot and cold fluid respectively (K), ' $U$ ' is overall heat transfer coefficient (W/m<sup>2</sup>K), ' $A$ ' is heat transfer area (m<sup>2</sup>) and ' $\Delta T_m$ ' is the mean temperature difference between hot

fluid and cold fluid (K).

In the equation (4.3), the heat transfer area 'A' can be defined in terms of hot fluid surface area or cold fluid. That also means the heat transfer area can be based on either the inside surface or outside surface of tubes [20]. For the sake of checking manufacturer data in the following part, the outside surface is obviously a better choice. Since the outside diameter of the tube is normally provided by the manufacturers. So the heat transfer area can be expressed:

$$A = \pi \cdot d_o \cdot l_{\text{tube}} \cdot N_t \quad (4.4)$$

Here 'd<sub>o</sub>' is the outside diameter of a tube (m), 'l<sub>tube</sub>' is the length of a tube (m) and 'N<sub>t</sub>' is the number of tubes in the tube bundle.

'ΔT<sub>m</sub>' in the basic equation (4.3), based on LMTD method [19] can be expressed as the logarithmic mean temperature difference:

$$\Delta T_m = \Delta T_{\ln} = \frac{\Delta T_2 - \Delta T_1}{\ln(\Delta T_2 / \Delta T_1)} \quad (4.5)$$

Where ΔT<sub>1</sub> and ΔT<sub>2</sub> are the temperature differences at the two ends of the exchanger and equation (4.5) is valid regardless of whether counter flow or parallel flow is employed [20]. In the design process of STHE, the inlet and outlet temperature for both fluids are basically set by designers.

In the next part, the author will establish the model for calculating the overall heat transfer coefficient (U) in equation (4.3) and there are two approaches will be discussed.

## Approach 1 of evaluating overall heat transfer coefficient (U)

The first approach of evaluating the overall heat transfer coefficient (U) in equation (4.3) is checking the data table of typical value of the overall heat transfer coefficient of shell and tube heat exchangers which can be found in some handbook or on internet (e.g. *Serth* [20]). The data table is also provided in Appendix B.

## Approach 2 of evaluating overall heat transfer coefficient (U)

The second approach is evaluating 'U' from equation (4.6) below

$$\frac{1}{U} = \frac{1}{h_o} + R_{f,o} + \frac{d_o \cdot \ln(d_o/d_{in})}{2k} + \frac{R_{f,i} \cdot d_o}{d_{in}} + \frac{d_o}{h_i \cdot d_{in}} \quad (4.6)$$

Where :  $h_o$  = shell-side heat transfer coefficient ( $W/m^2 K$ )

$h_i$  = tube-side heat transfer coefficient ( $W/m^2 K$ )

$R_{f,o}$  = fouling factor for shell-side fluid ( $m^2 K/W$ )

$R_{f,i}$  = fouling factor for tube-side fluid ( $m^2 K/W$ )

$k$  = thermal conductivity of the tube wall ( $W/m K$ )

$d_o$  = tube outside diameter (m)

$d_{in}$  = tube inside diameter (m)

The parameters in equation (4.6) will be discussed separately in the following part.

## **Fouling factor ( $R_f$ ) and thermal conductivity ( $k$ )**

Theoretically, the value of thermal conductivity ( $k$ ) is dependent on the property of the material, thereby applying an empirical value of thermal conductivity in early stage ship design is efficient. Fouling factors ( $R_{f,o}$ ,  $R_{f,i}$ ) are determined by a number of mechanisms either alone or in combination such as corrosion, crystallization, decomposition, polymerization, sedimentation, biological activity etc [20]. As same as thermal conductivity, using a typical value of fouling factor based on category of fluid for evaluating overall heat transfer coefficient is rational and plausible. The typical value of fouling factor and thermal conductivity can be checked in some references (e.g.[20, 21]).

## **Diameters: $d_{in}$ and $d_o$**

The value of inside diameter ( $d_{in}$ ) and outside diameter ( $d_o$ ) usually could be checked by manufacturer information. However, due to the limited resource of published data from the manufacturer, the inside diameter of a tube usually is normally difficult to be checked. According to some reference [40], a typical geometrical factor is usually used:.

$$d_{in} = 0.8d_o \quad (4.7)$$

## **Heat transfer coefficient $h_o$ and $h_{in}$**

Before evaluating the heat transfer coefficient of the tube ( $h_i$ ) and shell heat transfer coefficient ( $h_o$ ), the condition of fluid needs to be considered in advance.

For laminar flow through the tube ( $Re_d < 2300$ ). This may happen for oil flowing through the tubes [18].

$$h_i = \left( \frac{k}{d_{in}} \right) \left[ 3.66 + \frac{0.0668 \cdot \frac{d_{in}}{l_{tube}} \cdot Pr \cdot Re_d}{1 + 0.04 \left( \frac{d_{in}}{l_{tube}} \cdot Pr \cdot Re_d \right)^{\frac{2}{3}}} \right] \quad (4.8)$$

For turbulent flow through the tubes ( $Re_d > 10^4$ ). This may happen for water or gas flowing through the tubes [18].

$$h_i = \left( \frac{k}{d_{in}} \right) \cdot 0.023 \cdot Re_d^{0.8} \cdot Pr^{1/3} \cdot \left( \frac{\mu_t}{\mu_w} \right)^{0.14} \quad (4.9)$$

In equations (4.8) and (4.9), 'Pr' is the Prandtl number which is a dimensionless number defined as the ratio of kinematic viscosity to thermal diffusivity. 'Re' is the Reynolds number which is also dimensionless, ' $\mu_t$ ' is the fluid viscosity evaluated at the average bulk fluid temperature in tubes and ' $\mu_w$ ' is fluid viscosity evaluated at an average wall temperature.

When it comes to shell-side heat transfer coefficient (' $h_o$ '), there are a number of methods and research (e.g. Kern Method, Bell-Delaware Method, Wills-Johnston Method etc) which have been proposed [41]. Among these methods, the Bell-Delaware method is conceptually simple and accurate. The method which will be used in this project is the simplified version of Delaware Method which is straight forward and avoid being deep down in mass of details. (as discussed by *Serth* [20]) Another advantage of the simplified version method is using one equation which could include both laminar and turbulent flowing condition through the shell side.

The heat transfer coefficient of shell-side ' $h_o$ ' is expressed as follows:

$$h_o = j_H \left( \frac{k}{De} \right) Pr^{1/3} \left( \frac{\mu}{\mu_w} \right)^{0.14} \quad (4.10)$$

In the equation (4.10), the parameter 'De' is the equivalent diameter can be defined:

$$De = \frac{4 \times \text{channel flow area}}{\text{wetted surface}} = \frac{4A_c}{P_w} \quad (4.11)$$

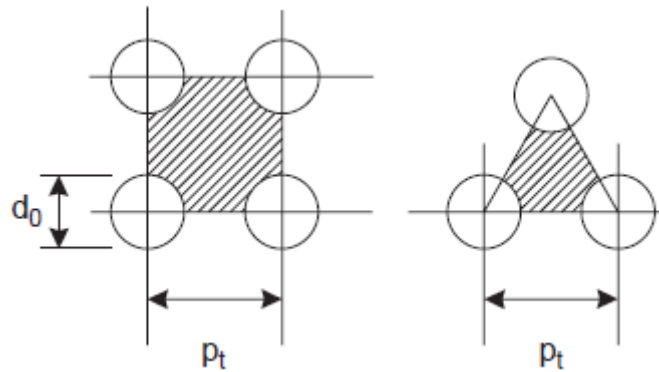


**Figure 4.3 Equivalent diameters for square pitch arrangement and triangular pitch arrangement, reference[42]**

And calculate the shell-side equivalent diameter 'De' as shown in Figure 4.3. For a square pitch arrangement:

$$De = \frac{4(P_t^2 - \frac{\pi d_o^2}{4})}{\pi d_o} = \frac{1.27}{d_o} (P_t^2 - 0.785 d_o^2) \quad (4.12)$$

For triangular pitch arrangement:

$$De = \frac{4(\frac{P_t}{2} \cdot 0.87 P_t - \frac{1}{2} \cdot \frac{\pi d_o^2}{4})}{\frac{\pi d_o}{2}} = \frac{1.10}{d_o} (P_t^2 - 0.917 d_o^2) \quad (4.13)$$

In the equations (4.12) and (4.13) the parameter 'P<sub>t</sub>' is the tube pitch (m) which defined the center-to-center distance between adjacent tubes in the tube bundle.

In equation (4.10) 'j<sub>H</sub>' is the correction for the shell-side heat transfer coefficient and

can be calculated from:

$$j_H = 0.5 \left(1 + \frac{B}{D}\right) (0.08 \text{Re}^{0.6821} + 0.7 \text{Re}^{0.1772}) \quad (4.14)$$

Where 'D' is the shell diameter (m), 'B' is baffle spacing (m). Reynolds number 'Re' in equation (4.14) is defined as:

$$\text{Re} = \frac{G_s \cdot D_e}{\mu} \quad (4.15)$$

'G<sub>s</sub>' in equation (4.15) is the shell-side mass velocity (kg/m<sup>2</sup>s) which is defined as:

$$G_s = \frac{\dot{m}_t}{a_s} \quad (4.16)$$

The parameter ' $\dot{m}_t$ ' in equation (4.16) is fluid flow rate on the shell-side (kg/s). Then the shell side cross flow area ' $a_s$ ' (m<sup>2</sup>) in equation (4.16) is given by

$$a_s = \frac{D \cdot C \cdot B}{P_t} \quad (4.17)$$

'C' is the spacing between tubes (m) which equals tube pitch minus tube outside diameter. After discussing each parameter in equation (4.10), the shell-side heat transfer coefficient ( $h_o$ ) can be evaluated.

The equations and explanations above are the whole procedure of evaluating heat transfer coefficient of both tube-side and shell-side. Since the variables in equation (4.6) have been evaluated, the overall heat transfer coefficient 'U' can be determined. After that the dimension prediction model could be built up.

Go back to the initial equation (4.3) and (4.4), the relationship between the dimension

of tube and heat flow rate could be built:

$$\boxed{\dot{Q}=U \bullet \Delta T_m \bullet \pi \bullet d_o \bullet l_{tube} \bullet N_t} \quad (4.18)$$

Combine equations (4.1), (4.2) and (4.4) together, we can get another way to express the dimension of tubes.

$$\frac{\dot{m}_{hot} \bullet C_{Ph} \bullet (T_{hinlet} - T_{houtlet})}{U \bullet \Delta T_m} = \frac{\dot{m}_{cold} \bullet C_{Pc} \bullet (T_{coutlet} - T_{cinlet})}{U \bullet \Delta T_m} = \pi \bullet d_o \bullet l_{tube} \bullet N_t \quad (4.19)$$

Due to the fact that designers are usually interested in the shape factor 'λ' ( $\lambda=l_{tube}/d_o$ ), we would introduce it into equation (4.18). And then equation (4.18) changes into:

$$\frac{\dot{Q}}{N_t \bullet \Delta T_m} = U \bullet \sqrt[3]{16\pi \bullet \lambda \bullet V^2} \quad (4.20)$$

The 'V' in equation (4.20) is the volume of per tube in the tube bundle. Based on equation (4.18) the expression about length ( $l_{tube}$ ) and outside diameter ( $d_o$ ) of tubes using shape factor 'λ' can be shown below:

$$l_{tube} = \sqrt[3]{\frac{\dot{Q}^3 \bullet \lambda}{4\pi^2 \bullet V \bullet \Delta T_m^3 \bullet U^3 \bullet N_t^3}} \quad (4.21)$$

$$d_o = \sqrt[3]{\frac{\dot{Q}^3}{4\pi^2 \bullet V \bullet \Delta T_m^3 \bullet U^3 \bullet N_t^3 \bullet \lambda^2}} \quad (4.22)$$

After establishing the dimension prediction model of the primary element, it can be concluded that there is indeed a first principle relation between the heat flow rate and the size of primary element which is characterized by its diameter ( $d_o$ ), length ( $l_{tube}$ ) and quantity ( $N_t$ ). The previous dimension model built by *Stapersma* and *de Vos* for

diesel engine, electric machine and gearbox whose equations all relate the power output to torque and angular speed. Compared with that, the model equation of heat exchanger is actually in thermal domain relating heat flow ( $U \bullet A$ ) and temperature difference ( $\Delta T_m$ ) which represent 'flow' and 'effort' variables separately.

From equation (4.18) we can see that heat flow rate ( $W$ ) of the shell and tube heat exchanger depends on:

- The overall heat transfer coefficient 'U' in  $W/m^2 K$  which is determined by manufacturer of the STHE, influenced by the fluid property, material limitation and the inside configuration of the STHE
- The characteristic temperature difference ' $\Delta T_m$ ' which is determined by manufacturers based on the property of fluid and requirement from working operation.
- Characteristic dimension of primary element (tubes) of STHE

#### **4.4. Sizing secondary element and core of shell and tube heat exchanger**

After the model of sizing primary element (tubes) of shell and tube heat exchanger has been built in Section 4.3, the next step is merited to size the secondary element and evaluate the core dimension of the shell and tube heat exchanger. In this section, the framework model for sizing secondary element (shell) will be established and also the model of core dimension based on a combination of the primary and secondary elements will be built.

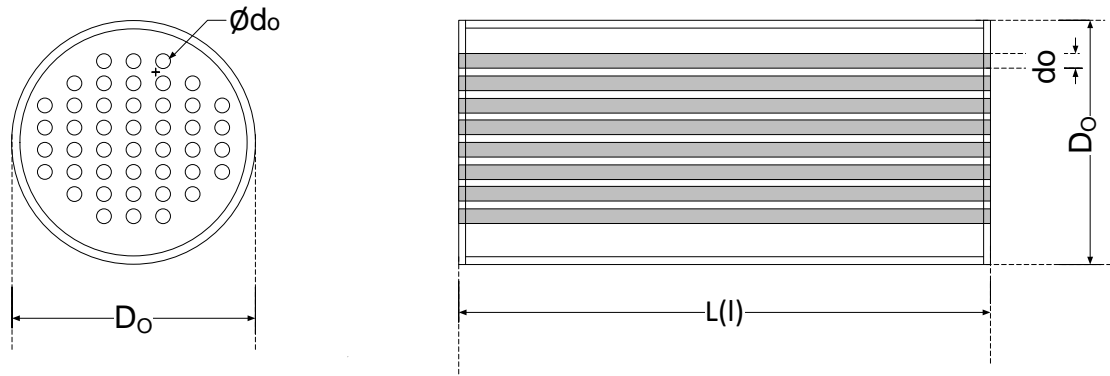


**Figure 4.4 Core construction of shell and tube heat exchanger**

Figure 4.4 above gives the schematic of the core construction of a shell and tube heat exchanger. In practice, the shape of the secondary element (shell) is cylindrical which is the same as that of the primary element (tube). So the diameter of shell is regarded as an essential dimension parameter for sizing. Accordingly the next step is evaluating the outside diameter of the shell ( $D_o$ ) based on outside tube diameter ( $d_o$ ).

There are two different estimation methods of sizing shell outside diameter ( $D_o$ ). The first estimation method is using empirical formulation and the second method is introducing a 'manufacturer parameter' to evaluate. The second method is kind of similar to the method of evaluating stator diameter based on rotor diameter which states in reference [1].

## Empirical estimation method

This method is presented in the handbook written by *Thulukkanam* [19] for roughly estimating tube counts in fixed tube sheet and this empirical formulation could be developed for calculating shell diameter. The original formulation is:

$$N_t = \frac{0.7854 D_{ctf}^2}{C_1 \cdot P_t^2} \quad (4.23)$$

Where ' $N_t$ ' is the number of tubes.  $C_1$  is a tube layout parameter,  $C_1=1.0$  for square

(90°) and rotated square (45°) and  $C_1=0.866$  for triangular (30°). The type of tube layout in tube bundle can be found in Figure 2.10. As the manufacturing standard, the minimum tube pitch is 1.25 times of tube diameter ( $P_t=1.25d_o$ ) and designers usually prefer employ value of 1.25 for heat exchanger preliminary design because it leads to the minimum shell diameter for given number of tubes [21, 39]. 'D<sub>ctl</sub>' (m) in equation (4.23) is the centerline tube limit diameter (m) [24]. Manipulate equation (4.23) and introduce the tube outside diameter, the new equation would be:

$$D_{ctl} = \sqrt{\frac{N_t \cdot C_1 \cdot (1.25d_o)^2}{0.7854}} \quad (4.24)$$

And the relationship between D<sub>ctl</sub> and D<sub>o</sub> is:

$$D_o = D_{ctl} + d_o + L_{bb} + 2T_s \quad (4.25)$$

Where 'L<sub>bb</sub>' is tube bundle-to-shell clearance (m) and 'T<sub>s</sub>' is the thickness of shell wall (m) and the final equation of shell outside diameter as follows:

$$D_o = (\sqrt{1.989N_t \cdot C_1 + 1})d_o + L_{bb} + 2T_s \quad (4.26)$$

## Manufacturer parameter method

This method introduces a 'manufacturer parameter' S<sub>STHE</sub> and  $S_{STHE} = A_s/A_t$ . 'A<sub>t</sub>' is the total cross-sectional area of tubes on the tube sheet (m<sup>2</sup>) and 'A<sub>s</sub>' is the shell cross-sectional area (m<sup>2</sup>). The parameter 'S<sub>STHE</sub>' can be expressed:

$$S_{STHE} = \frac{\frac{\pi D_o^2}{4}}{\frac{\pi d_o^2}{4} \cdot N_t} = \frac{D_o^2}{d_o^2 \cdot N_t} \quad (4.27)$$

In practice, the value of S<sub>STHE</sub> is within a certain range depending on manufacturer

standard. The author employed available the manufacturer data into equation (4.27) found the range of  $S_{STHE}$  is approximately 2.28-3.27 and typical value of  $S_{STHE}$  for evaluating the shell diameter could be 2.6 for dimension prediction in the early stage ship design.

Ultimately, the shell diameter can be expressed as:

$$D_o = \sqrt{d_o^2 \cdot N_t \cdot S_{STHE}} \quad (4.28)$$

Compare these two methods, the method employed by the author in our dimension prediction model is the manufacturer parameter method. In practice, there are some weaknesses of the empirical method model in the process of implementing the manufacturer data from database to dimension prediction model. The first weakness is uncertainty. As stated above, the length of tube pitch 'P<sub>t</sub>' is evaluated through empirical formulation  $P_t = 1.25d_o$ , which is the minimum manufacturer standard. However, in some design situations the tube pitch may be increased to a higher value for reducing shell-side pressure drop such as in the case of a cross-flow shell [39]. The second weakness is some detailed manufacturer data (e.g. layout pattern of tubes on tube sheet ( $C_1$ ), the thickness of shell wall ( $T_s$ )) usually is not available and that would make difficulty on implementing data into our dimension prediction model. While the second method gets rid of mass of details and easy to implement. Therefore, the second method is more suitable for dimension prediction in the preliminary design stage. Based on these, the second method is selected for implementing in our model. In the next part, the evaluation of the length of the secondary element (shell) through dimension of the primary element (tube) will be explained.

Based on the construction feature of a shell and tube heat exchanger in Figure 4.4, the length of tubes ( $l_{tube}$ ) is equal to the length of shell ( $L_{shell}$ ). So the length of shell ( $L_{shell}$ ) in terms of length of tube ( $l_{tube}$ ) could be:

$$L_{\text{shell}} = l_{\text{tube}} \quad (4.29)$$

According to the schematic construction diagram in Figure 4.4, tube bundle is always contained within the casing of shell. Therefore, the core dimension of a shell and tube heat exchanger could be regarded as the shell dimension. According to the cylindrical shape of the shell, the width and height of shell are virtually both equal to the outside diameter of shell ( $D_o$ ). The following expression is utilized for sizing core of a shell and tube heat exchanger.

$$\begin{aligned} L_{\text{core,STHE}} &= l_{\text{tube}} \\ W_{\text{core,STHE}} &= \sqrt{d_o^2 \cdot N_t \cdot S_{\text{STHE}}} \\ H_{\text{core,STHE}} &= \sqrt{d_o^2 \cdot N_t \cdot S_{\text{STHE}}} \end{aligned} \quad (4.30)$$

## 4.5. Sizing the whole shell and tube heat exchanger

After establishing the dimension model for the core of shell and tube heat exchanger, the question becomes how to evaluate the whole dimension of the machine based on the core dimension. Figure 4.5 is a typical construction of a shell and tube heat exchanger from the API manufacturer. From Figure 4.5, it can be seen that the whole shape of a shell and tube heat exchanger could also be regarded as cylindrical which resembles the shape of shell. The overall length of the machine is larger compared with length of the shell that because a head chamber is installed at the end of the shell. In addition, the nozzles mounted on the surface of shell influence the total height of a shell and tube heat exchangers.

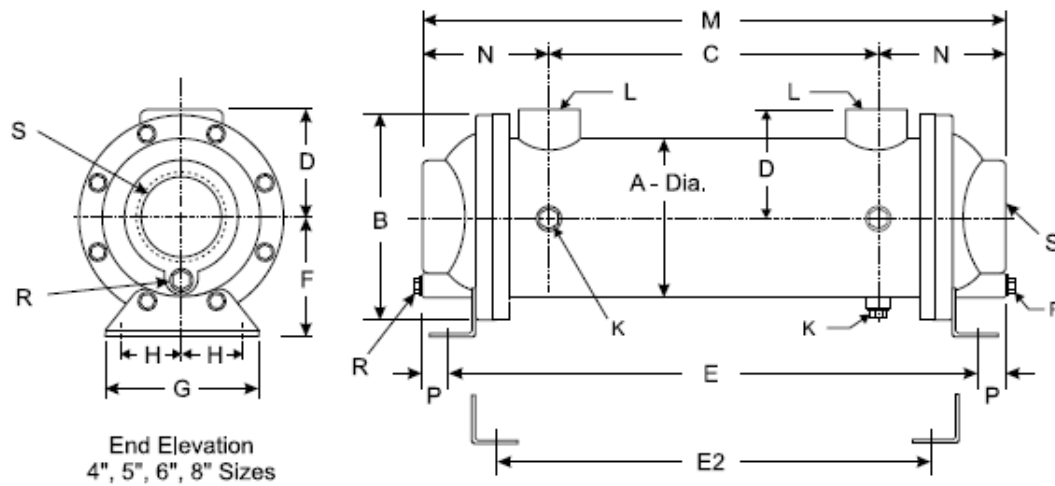


**Figure 4.5 Typical shell and tube heat exchanger construction. Source: online API**

**Basco Type 500 straight tube heat exchanger**

As the methodology described in Chapter 2, a shell and tube heat exchanger dimension related to core dimension with linear relationship:

$$\begin{aligned}
 L_{STHE} &= A_1 \cdot L_{core,STHE} \\
 W_{STHE} &= B_1 \cdot W_{core,STHE} \\
 H_{STHE} &= C_1 \cdot H_{core,STHE}
 \end{aligned}
 \tag{4.31}$$

The constant value  $A_1$ ,  $B_1$ ,  $C_1$  represents as a function of the fitting degree that the core dimension differs from the actual machine dimension. In order to determine the constant value, regression analysis based on manufacturer data from the database would be employed. As the dimension of shell takes over the major part of the machine, it could rationally foresee the constant value is not large. In the next section, the manufacturer data will also be implemented into the model to evaluate the constant value  $A_1$ ,  $B_1$ ,  $C_1$  in equation (4.31).

## 4.6. Model implementation and results discussion of STHE

The model implementation is executed in Microsoft Excel which is efficient and convenient for data input and graph generation. Furthermore, Microsoft Excel is commonly used in the engineering field and being superior to other software on getting started and data collection by designers. Based on the basic equations (4.1), (4.2) and (4.3), there are 11 parameters in the model which are overall heat transfer coefficient ( $U$ ), mass flow rate of hot and cold fluid ( $\dot{m}_{hot}$ ,  $\dot{m}_{cold}$ ), specific heat of hot and cold fluid ( $C_{P,hot}$ ,  $C_{P,cold}$ ), inlet and outlet temperature of hot and cold fluid ( $T_{hinlet}$ ,  $T_{houtlet}$ ,  $T_{cinlet}$ ,  $T_{coutlet}$ ), the heat transfer rate ( $\dot{Q}$ ) and the heat transfer area ( $A$ ). In order to know all the value of the parameters in these three equations, any 8 parameters within the 11 parameters need to be given or set by the marine engineers. Thus, there are 165 cases would be raised by the model with different combinations of these 11 parameters. Here need to be noticed that not all the cases are with regard to the dimension prediction within these 165 cases. Some cases could also be used for heating performance prediction of heat exchangers based on the given dimension of the machine. And some specific cases could also predict the property of the hot or cold fluid as well. Since different cases could be applied to the different purpose, the cases related to dimension prediction of the shell and tube heat exchangers are basically interesting in this project.

In view of the application of shell and tube heat exchanger on board, we choose lubrication oil cooling heat exchangers to investigate. The manufacturer information of the oil cooling heat exchangers is mostly collected online from different manufacturers (e.g. API, Alfa Laval and Dolphin) and which cover various types of dimensions.

In order to implement the dimension prediction model, some requisite preliminary

assumption should be made in advance. For lubrication oil cooling heat exchanger, the hot fluid is of course lubrication oil and cooling medium is fresh cooling water. It can be seen in Table 4-1, for the design purpose, lube oil is designed to be cooled from 60°C to 49°C and temperature of cooling water increases from 29.5°C to 35°C accordingly.

**Table 4-1 Designed temperature change of fluids in shell and tube heat exchanger**

<u>Lubrication oil coolers</u>		
<b>Hot fluid: <i>Lube oil</i></b>	<b>°C</b>	<b>K</b>
Inlet temperature	60	333.15
Outlet temperature	49	322.15
<b>Cold fluid: <i>Fresh water</i></b>		
Inlet temperature	29.5	302.65
Outlet temperature	35	308.15

A number of shell and tube heat exchangers are collected in database and implemented in the dimension prediction model. The collected shell and tube heat exchangers vary in term of heat capacity, dimension, flow rate, etc.

After implementing the model with the manufacturer data, the results are shown below:

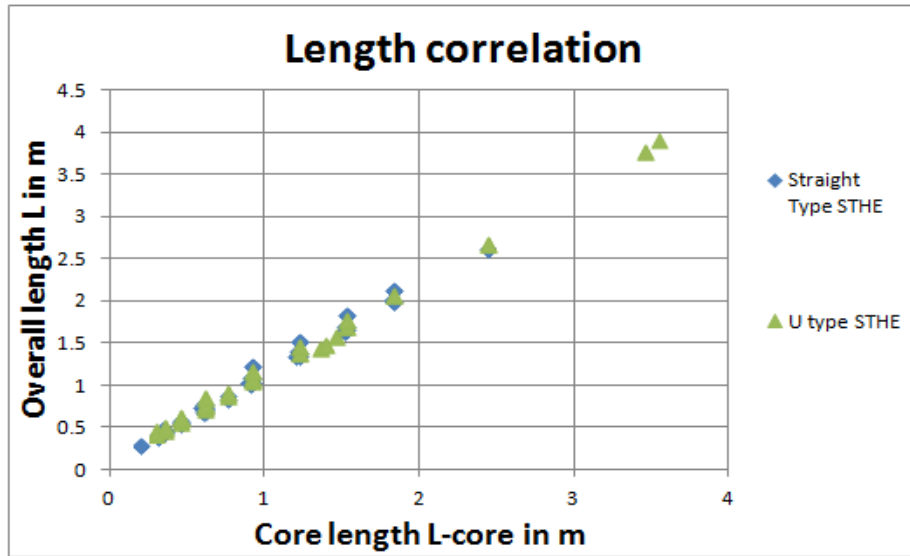


Figure 4.6a Correlation of actual length with theoretical core length for shell and tube heat exchangers

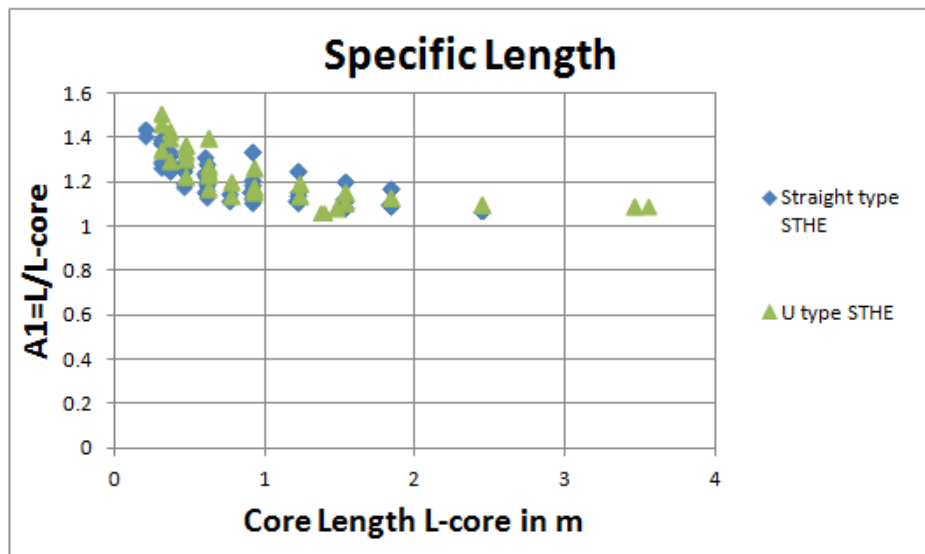


Figure 4.6b Correlation of specific length with theoretical core length for shell and tube heat exchangers

Length correlates well in Figure 4.6a for both straight-tube type and U-tube type heat exchangers. It can be seen in Figure 4.6b where the total length of the machine is approximately 1-1.5 times longer than the specific length of the core part of the shell and tube heat exchanger.

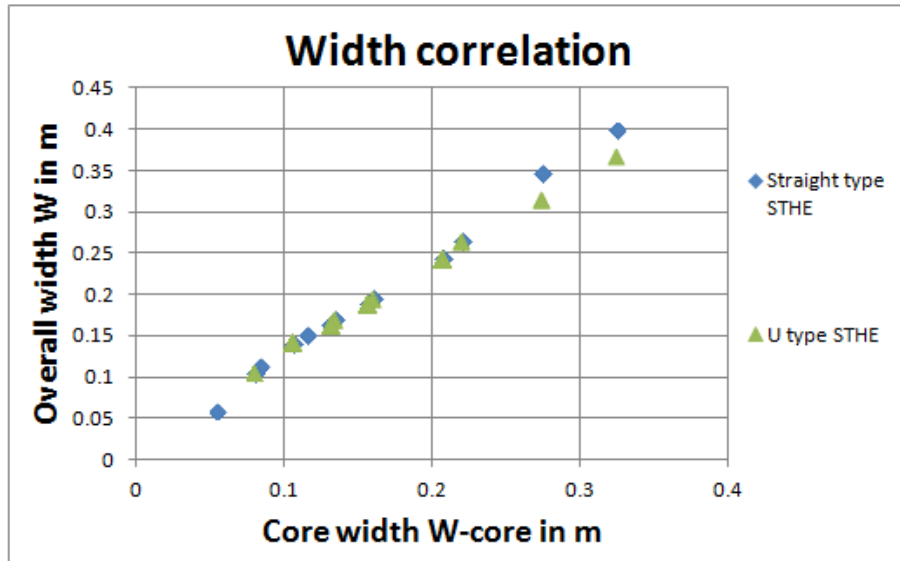


Figure 4.7a Correlation of actual width with theoretical core width for shell and tube heat exchangers

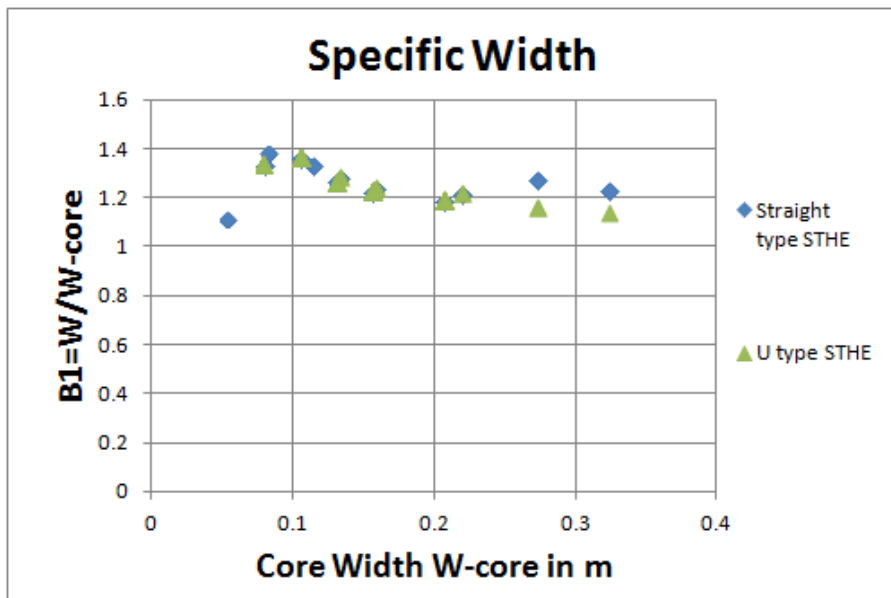


Figure 4.7b Correlation of specific width with theoretical core width for shell and tube heat exchangers

The results of width correlation also show approximate linear relationship in Figure 4.7a. Due to the shape of both core and overall shell and tube heat exchanger are cylindrical and the core part has already counted major part of the machine. The linear constant of the width are also in a confined range which is in the range of 1.1-1.4. The

disturbance happened on the width correlation is because the flange mounted between the head and shell of the heat exchanger. The width of the flange normally is larger than that of shell. The width of flange actually could be counted as the total width of the shell and tube heat exchanger.

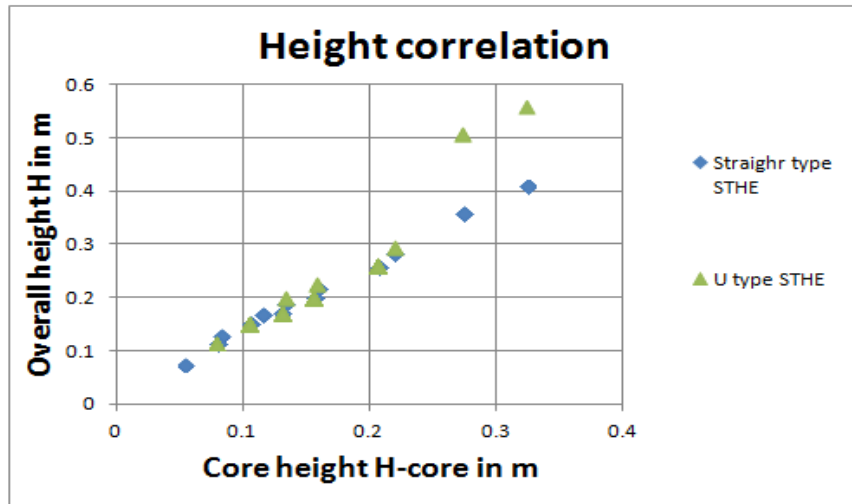


Figure 4.8a Correlation of actual height with theoretical core height for shell and tube heat exchangers

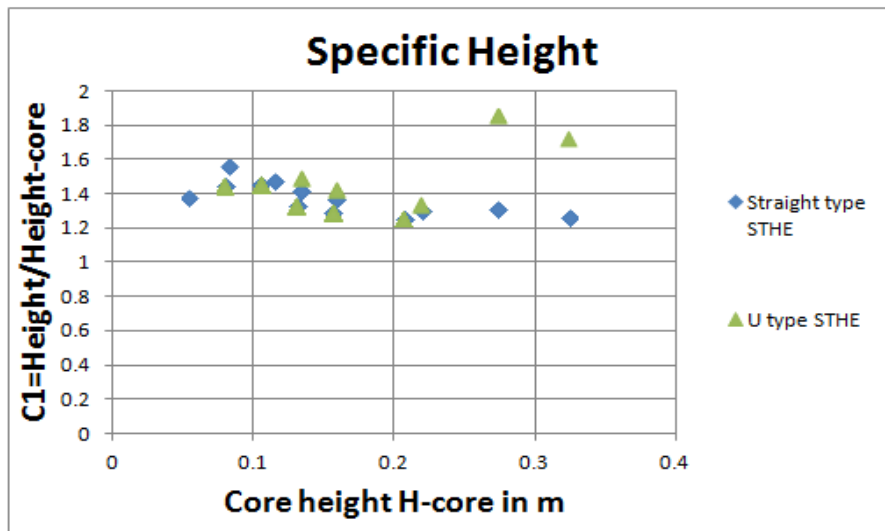
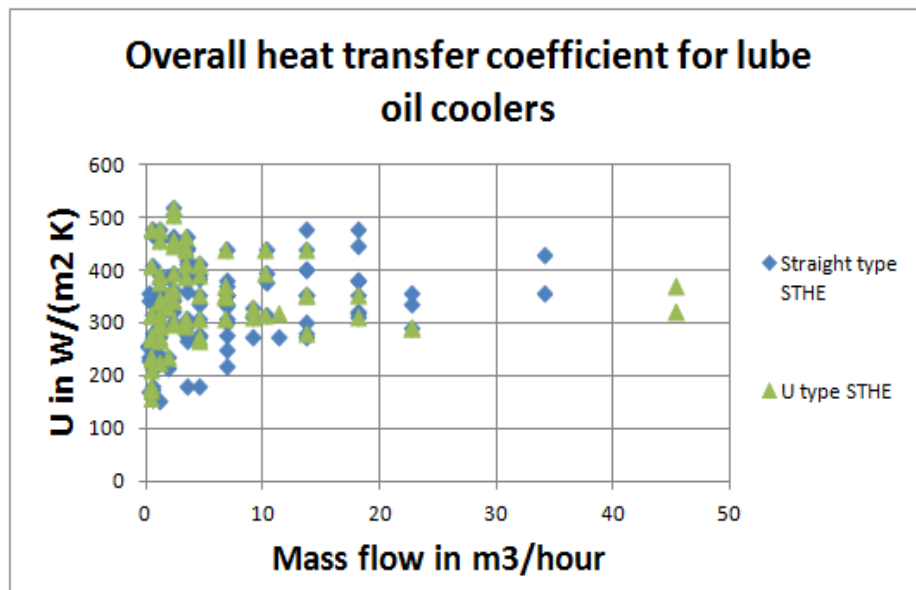


Figure 4.8b Correlation of specific height with theoretical core height for shell and tube heat exchangers

The height correlates linearly as well shown in Figure 4.8a, even though that is not that regularly linear like length correlation or width correlation. The reason of the disturbance happened on height correlation is the nozzles mounted on the shell where the hot or cold fluid flowing into the shell side. The height and the arrangement of the nozzle mounted on the shell and tube heat exchanger have the effect on the total height dimension of the machine. The height difference is mainly due to the mounted nozzles and the specifically details required by purchasers. It can be read from Figure 4.8b, the range of the linear constant  $C_1$  is around 1.2-1.8.



**Figure 4.9 Range of overall heat transfer coefficient for shell and tube heat exchangers**

As we discussed in Chapter 2, the selection of main machine parameter would have influence on the overall dimension of the machine. The range of the overall heat transfer coefficient is also essential to be studied. Figure 4.9 shows the value of overall heat transfer coefficient ( $U$ ) of different heat exchangers. Based on Figure 4.9, the ranges of overall heat transfer coefficient of normal straight-tube type and U-tube type lube oil coolers are similar which are approximately ranging from 150  $W/(m^2 K)$  to 510  $W/(m^2 K)$ . In fact, the different range of overall heat transfer coefficient is mainly due to the different fluid crossing the heat exchangers.

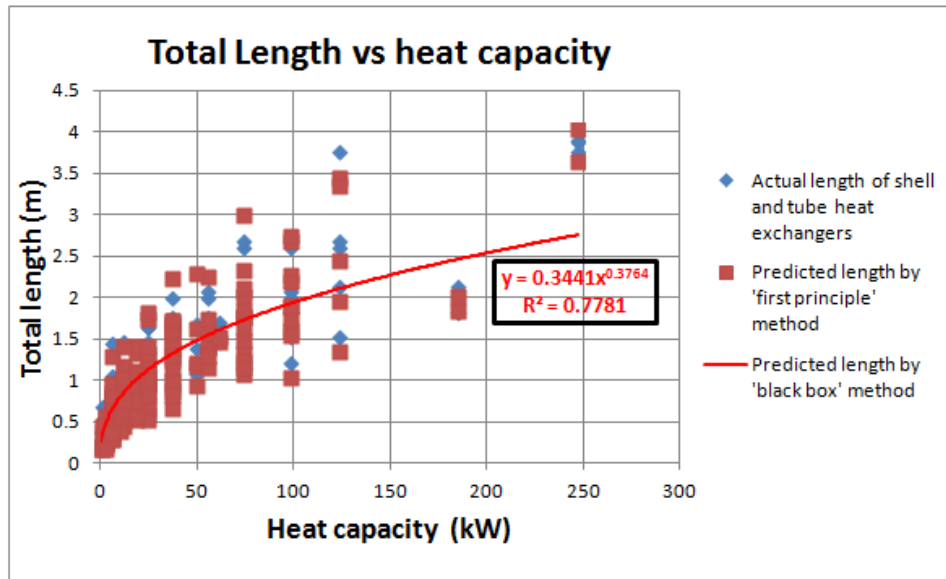


**Figure 4.10 Predicted length by 'black box' method and 'first principle' method against the actual length**

After establishing the 'first principle' sizing model of shell and tube heat exchangers, the author tries to compare this model with 'black box' method model of shell and tube heat exchangers. The red plots in the Figure 4.10 are the generated length dimension based on 'first principle' method. Based on the methodology, some presumptions need to be set in advance. First of all, the heat capacity of heat exchangers needs to be given which is the start point of the methodology. The overall heat transfer coefficient we choose an average value  $350 \text{ W}/(\text{m}^2 \text{ K})$ . The linear constant 'A<sub>1</sub>' we select 1.2 according to its range shown in Figure 4.6a. From Figure 4.10, it can be seen there are still deviations between the red plots (predicted length by 'first principle' method) and the blue plots (actual dimension). The reason of the dimension deviation could be known which is due to the variable settings. However, for the 'red trend' line generated by 'black box' method, the reason of the deviation is difficult to conclude using the generated power relationship. Therefore, from this point, the degree of the fidelity for 'first principle' model is higher than the 'black box' model.

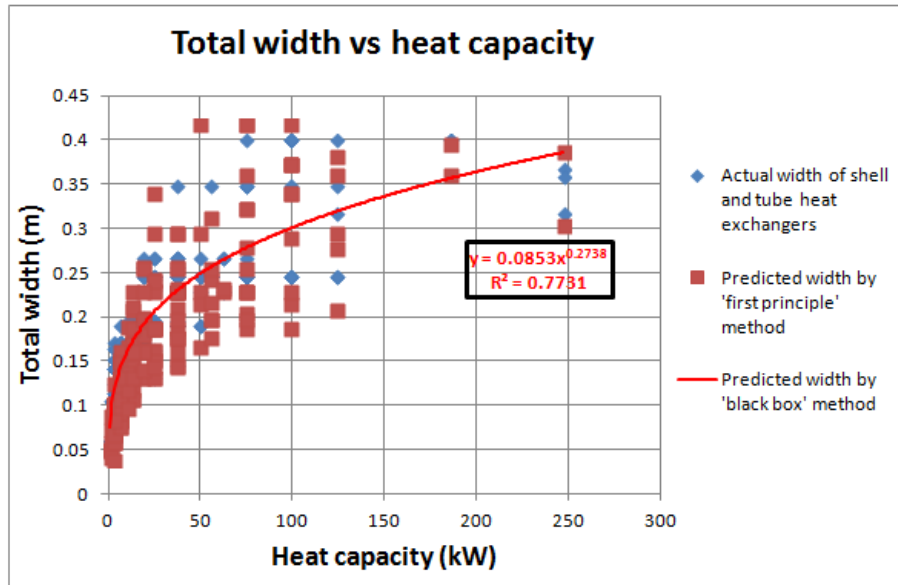


**Figure 4.11 Predicted width by 'black box' method and 'first principle' method against the actual width**

Figure 4.11 shows the predicted width of shell and tube heat exchanger which are represented as red plots. According to Figure 4.7b, the value of the linear constant 'B<sub>1</sub>' is set 1.2. The overall heat transfer coefficient (350 W/(m<sup>2</sup> K) ) is the same with that of predicted length dimension. The deviation existing between the red plots and blue plots is mainly caused by the overall heat transfer coefficient and the evaluated linear constant 'B<sub>1</sub>'. Take the red plot with 0.3 m in y-axis and 250 kW at x-axis for example, the actual overall heat transfer coefficient and linear constant are 374 W/(m<sup>2</sup> K) and 1.14 separately. When the author manipulates these two variable settings using the actual value, the deviation reduces dramatically. This trial proves the fidelity and flexibility of the 'first principle' model once again.

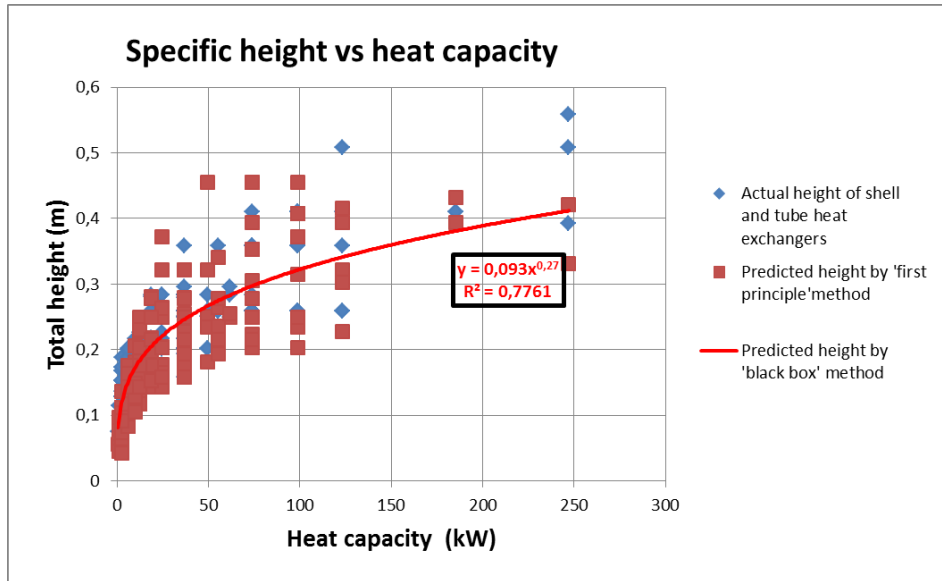


**Figure 4.12 Predicted height by 'black box' method and 'first principle' method against the actual height**

It can be seen in Figure 4.12, the situation of the predicted results resembles that in Figure 4.10 and Figure 4.11. The linear constant ' $C_1$ ' is set 1.3 according to the range shown in Figure 4.8b. Other variables are the same as which are set for length and width prediction.

## 4.7. Summary

This chapter mainly illustrates the process of establishing the 'first principle' model of shell and tube heat exchangers. Tubes and shell are selected as the primary element and secondary element in the sizing model. The heat overall transfer coefficient in the model is the 'main parameter' which could be evaluated in two approaches. The first approach is evaluating the value based on the experienced data which is normally used in preliminary design stage. Since in the preliminary design stage, the detailed information data of the shell and tube heat exchanger (e.g. baffle spacing, tube arrangement) is usually not available, employing the typical data for sizing the rough dimension of the machine is an efficient way. Compared with the first approach, the second approach of evaluating the overall heat transfer coefficient is more accurate,

however more input variables are also needed. Thus, the second approach is preferred to be applied in later ship design stage or detailed requirements of the machine are provided by the ship owner. Then a manufacture parameter ' $S_{STHE}$ ' is introduced to determine the size of the secondary element (shell) of a shell and tube heat exchanger. Finally, the overall dimension of the machine is evaluated based on the core of the machine (combination of the primary element and secondary element). From the results shown in the figures, approximate linear relationships between the dimension of core and overall dimension of the machine are exploited. In conclusion, the 'first principle' sizing model is successfully applied to shell and tube heat exchangers. In the end, the comparison between the 'first principle' method and 'black box' method are discussed. The deviation still exists between the predicted dimension by 'first principle' method and actual dimension. However, the reason of the deviation could be exploited and reduced by manipulating the specific variables compared with the 'black box' model. Therefore, it can be concluded that the degree of the fidelity of the 'first principle' model is higher than 'black box' model.

# 5. Plate Heat Exchanger

---

As same as shell and tube heat exchangers, plate heat exchangers (PHE) are also commonly employed in various industrial fields. There are four types of plate heat exchangers: Gasketed, Brazed Plate, Welded, and Semi-Welded. Among these four types, the gasketed plate heat exchangers are the most commonly used in marine applications. The reason is due to the plates could be easily removed for cleaning, expansion or replacing and that would also reduce the cost of maintenance. Therefore, the 'first principle' sizing model in this chapter is established based on the configuration of gasketed plate heat exchanger. What's more, it should be emphasized here that the plate heat exchangers discussed in the context specifically refer to gasketed plate heat exchangers. As the configuration of plate heat exchanger is greatly different from the shell and tube heat exchanger, rebuilding a dimension prediction model for a plate heat exchanger is necessary. In this chapter, firstly we will introduce the general information about plate heat exchangers. And then the primary element will be selected. Furthermore the dimension prediction model for plate heat exchanger will be built and implemented based on manufacturer data. Finally, the results of the model implementation, such as the relationship between the core dimension and whole dimension, a comparison between 'first principle' method and 'black box' method, etc will be discussed.

## 5.1. General information of plate heat exchanger

Plate heat exchangers were first commercially introduced in 1920's to meet the hygienic demand of dairy industry [43]. With the rapid development of plate heat exchangers in manufacturer which are widely used in a large range of heating and cooling application such as chemical process, food industry and of course in broad marine applications.

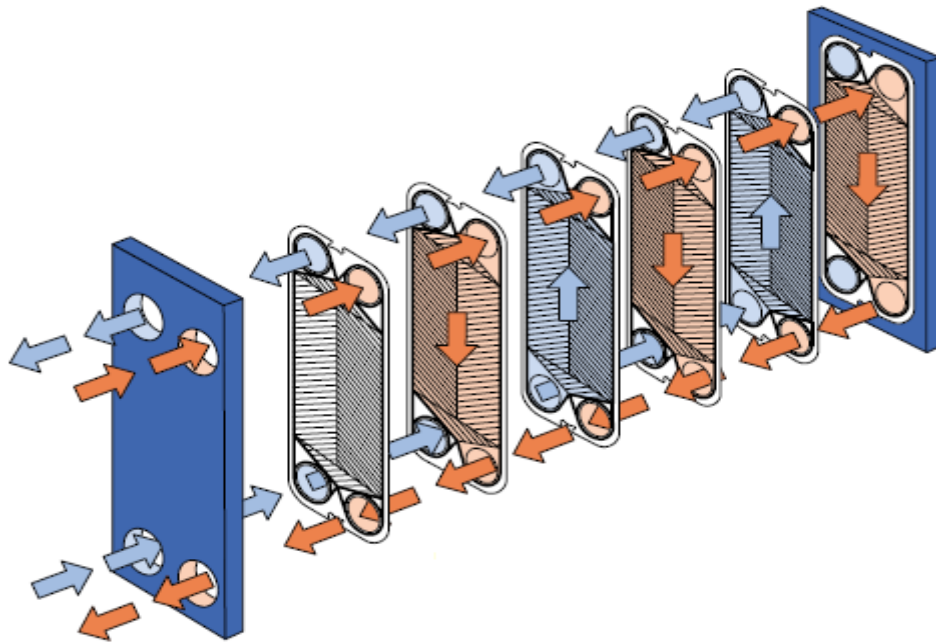
Compared with shell and tube heat exchangers, plate heat exchangers are more compact and efficient which are more propitious to save space and transfer heat energy. This is also a reason why plate heat exchangers partially substitute for shell and tube heat exchangers in some marine engineering systems. However in the case of high pressure fluid needed to be heated or cooled, shell and tube heat exchangers are still superior to plate heat exchangers [18].

Figure 5.1 is an example of the plate heat exchanger manufactured by Alfa Laval. As shown in Figure 5.1 and Figure 5.2, a plate heat exchanger basically consists of a series corrugated metal plates and two heavy frame plates for end cover [44]. For conventional plate-and-frame heat exchanger, each corrugated plate is mounted a gasket on one side which can lead cold and hot fluids distributed over separate plates without mixing. More details about corrugated plate geometry will be introduced in the following part. In manufacture application, stainless steel is commonly used material for plates.



**Figure 5.1 Example of plate heat exchanger assembly (Courtesy of Alfa Laval)**

Figure 5.2 gives a straightforward image of flow principle and heat transfer process occurred in plate heat exchangers. The gap between each plate forms a channel for fluids flowing across. Two fluids flow through alternate inter-plate and heat transfer process takes place across the plate [43]. The heat transfer area of two fluids is the surface area of plates in plate heat exchanger. According to the graphical description in Figure 5.2, it can be believed that with the equivalent volume, the heat transfer area of plate heat exchanger is much larger than that of the shell and tube heat exchanger. The flow arrangement set in plate heat exchanger could be the single pass, double pass and even multi-pass. Figure 5.2 is a typical single pass flow heat exchanger.



**Figure 5.2 Flow principle of plate heat exchanger**

## 5.2. Configuration of plate heat exchanger

Before selecting the primary and secondary element of a plate heat exchanger, we need to get knowledge about the configuration and construction details about a plate heat exchanger.

Figure 5.3 provides a detailed construction schematic for a plate heat exchanger. The numbered components in Figure 5.3 are [45]:

1. Fixed plate
2. Movable plate
3. Support column
4. Carrying bar
5. Lower plate guiding bar
6. Carrier roller
7. Tightening bolt and nuts
8. Fixing bolts
9. Rubber/ metal liners
10. Gaskets
11. Heat transfer plates
12. Name plate

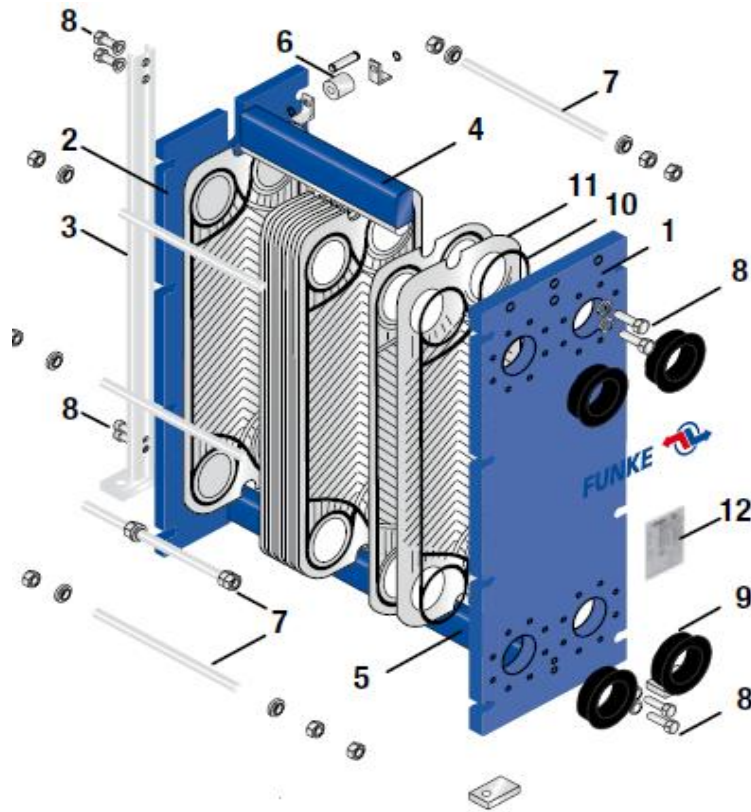


**Figure 5.3 Configuration of plate heat exchanger (Courtesy of FUNKE)**

Based on the manufacturer picture in Figure 5.3, the heat transfer plates take over the large part of the whole machine and real heat transfer process also takes place between each adjacent plate. According to this, not only for model establishing based on first principles but also in terms of practical configuration, heat transfer plates should be considered as the primary element of a plate heat exchanger. In the case of the plate heat exchanger, the author proposes the pack of heat transfer plates has already formed the primary part of plate heat exchanger which is shown in Figure 5.3 as well. Thus, no secondary element is necessary to be selected on establishing dimension model for plate heat exchanger. Consequently, the pack of heat transfer plates is the primary elements and geometrically forms the core part of plate heat exchanger as well.

### 5.3. Sizing primary element of plate heat exchanger

As the agreement states in Section 5.2, the heat transfer plate is selected as the primary element for our dimension prediction model. In the following part, the dimension model for sizing heat transfer plate will be built.

The basic equations are as same as the equations (4.1), (4.2) and (4.3), which stated in Chapter 4:

$$\dot{Q} = \dot{m}_{\text{hot}} \cdot C_{p,\text{hot}} \cdot (T_{\text{hinlet}} - T_{\text{houtlet}}) \quad (5.1)$$

$$\dot{Q} = \dot{m}_{\text{cold}} \cdot C_{p,\text{cold}} \cdot (T_{\text{coutlet}} - T_{\text{cinlet}}) \quad (5.2)$$

$$\dot{Q} = U \cdot A \cdot \Delta T_m \quad (5.3)$$

In equation (5.3),  $\Delta T_m$  (K) is expressed by Logarithmic Mean Temperature Difference (LMTD) for hot and cold fluid.

$$\Delta T_m = \Delta T_{\text{ln}} = \frac{\Delta T_2 - \Delta T_1}{\ln(\Delta T_2 / \Delta T_1)} \quad (5.4)$$

Here  $\Delta T_2 = T_1 - T_4$  and  $\Delta T_1 = T_2 - T_3$

Where  $T_1$  = Hot fluid inlet temperature

$T_2$  = Hot fluid outlet temperature

$T_3$  = Cold fluid inlet temperature

$T_4$  = Cold fluid outlet temperature

In practice, the fluid flow configuration in plate heat exchanger is usually counter-current flow which could make heat transfer process more efficient. Therefore, the author specifies  $\Delta T_1, \Delta T_2$  as counter flow configuration for further calculation.

Manipulating equation (5.3), total heat transfer area 'A' can be calculated:

$$A = \frac{\dot{Q}}{U \bullet \Delta T_m} \quad (5.5)$$

As perceived agreement in Section 5.2, the heat transfer area is formed by corrugated heat transfer plates. As a result, the total heat transfer area can also be like:

$$A = N_{ep} \bullet A_d \quad (5.6)$$

Here: 
$$N_{ep} = N_{tp} - 2 \quad (5.7)$$

In the equation (5.6), (5.7), 'A<sub>d</sub>' is the developed area per plate (m<sup>2</sup>) which is larger than the flat plate because of the corrugated pattern. 'N<sub>ep</sub>' is the effective number of heat transfer plates which is 2 less than the total number of heat transfer plates (N<sub>tp</sub>). The two subtracted plates are the first and the last plate which have fluid only on one side and they are noneffective in transferring heat [46]. Next, the detailed geometry of corrugated heat transfer plate will be discussed.

## Geometry of corrugated heat transfer plate

Figure 5.4 illustrates the detailed configuration of heat transfer plate and the right graph well presents the assembly between two adjacent plates. With the result of corrugation pattern, the heat transfer area between two plates increases remarkably in comparison to the original flat area.

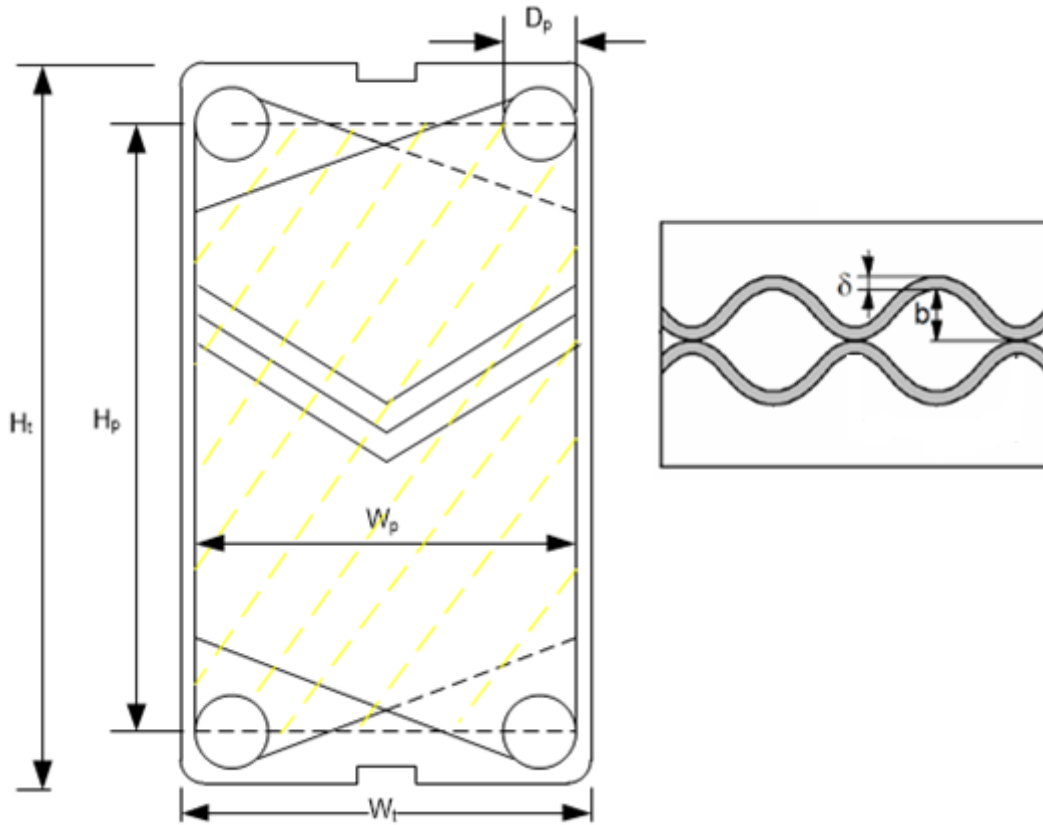


**Figure 5.4 Geometry of corrugated type plate**

In Figure 5.4,  $H_t$  is the total length of a plate (m);  $H_p$  is the height of a plate's projected area (m);  $W_p$  is the width of the projected area (m);  $W_t$  is the total width of the plate (m),  $D_p$  is the port diameter (m). According to Figure 5.4, some basic relations can be concluded:

$$H_t \approx H_p + D_p \quad (5.8)$$

$$W_p \approx W_t \quad (5.9)$$

In order to establish our model with available manufacturer information, here we assume  $H_t$  is approximately equal to the sum of  $H_p$  and  $D_p$ . The width  $W_p$  and  $W_t$  are approximately equal. Because of the gap between gaskets and the edge of the plate is considerably small, it is rational to neglect this less effective deviation for dimension

prediction in the preliminary design stage.

The yellow area shown in Figure 5.4 is the projected heat transfer area  $A_p$  where:

$$A_p = H_p \cdot W_p \quad (5.10)$$

However, due to the corrugated pattern the real effective heat transfer area is the developed area ( $A_d$ ). To express the increased area of the developed area, we introduce the enlargement factor ' $\phi$ ' which is the ratio of the actual effective heat transfer area ( $A_d$ ) specified by the manufacturer to the projected area ( $A_p$ ) [25].

$$\phi = \frac{A_d}{A_p} \quad (5.11)$$

Depending on the manufacturer standard, the enlargement factor  $\phi$  is in the range of 1.15-1.25, and the value 1.17 is usually used as a typical value for preliminary design stage (as discussed in reference [43, 47]).

The right part of Figure 5.4 illustrates the details of the connection between two plates where ' $\delta$ ' is the thickness per plate (m); ' $b$ ' represents the mean channel spacing (m).

The plate pitch between two plates ' $p_{PHE}$ ' (m) is defined as:

$$p_{PHE} = \delta + b \quad (5.12)$$

Furthermore, the plate pitch ' $p_{PHE}$ ' (m) can also be determined from the length of the compressed plate pack (between the head plate) ' $L_t$ ' (m) and the total number of the heat transfer plates [25]:

$$L_t = p_{PHE} \cdot N_{tp} \quad (5.13)$$

In our dimension prediction model, the length of the pack of plates ' $L_t$ ' is also

recognized as the length of the core of plate heat exchanger ( $L_{core}$ ).

After analysis of the detailed geometry of primary element (heat transfer plates), the next step is evaluating the overall heat transfer coefficient ( $U$ ) in basic equation (5.3). As same as what we have done in shell and tube heat exchanger model, there are also two approaches.

### **Approach 1 of evaluating overall heat transfer coefficient ( $U$ )**

The first approach of evaluating the overall heat transfer coefficient is through checking the experimental data table which provides a rough range of the overall heat transfer coefficient depending on different fluid. This method will offer designers a quick estimation about the overall heat coefficient for performance prediction in the preliminary design stage. The data table is also provided in Appendix B.

### **Approach 2 of evaluating overall heat transfer coefficient ( $U$ )**

This approach is based on the basic equation:

$$\frac{1}{U} = \frac{1}{h_h} + \frac{1}{h_c} + \frac{\delta}{k} + R_f \quad (5.14)$$

Where  $h_h$  is heat transfer coefficient in hot side ( $W/m^2 K$ );  $h_c$  is heat transfer coefficient in cold side ( $W/m^2 K$ );  $\delta$  is the thickness of plate (m);  $k$  is thermal conductivity ( $W/m K$ ) and  $R_f$  is the fouling factor of the plate ( $m^2 K/W$ ).

The method of dealing with fouling factor ' $R_f$ ' and thermal conductivity ' $k$ ' resembles what we have done in dimension model of shell and tube heat exchangers, using typical value based on plate material and type of fluid. This method could provide a quick and guided selection for ship designers in early stage ship design. The next step is evaluating the heat transfer coefficient on the hot side ( $h_h$ ) and cold side ( $h_c$ ).

In view of the configuration of plate heat exchanger, the plates holding hot fluid and cold fluid are exactly identical. Therefore, we will utilize one of the fluids to study and the process of calculating of another side will be the same. The basic equation of the heat transfer coefficient (h) is introduced below:

$$h = \frac{\text{Nu} \cdot k}{D_e} \quad (5.15)$$

In equation (5.15) 'Nu' corresponds to the Nusselt Number, 'De' is the equivalent diameter of the channel (m):

$$D_e = \frac{4 \times \text{channel flow area}}{\text{wetted surface}} = \frac{4A_c}{P_w} \quad (5.16)$$

$$D_e = \frac{4(b)(W_p)}{2(b+W_p\phi)} \approx \frac{2b}{\phi} \quad (5.17)$$

Here an approximation is made that  $b \ll W_p$ .

The Nusselt Number (Nu) of a plate heat exchanger in equation (5.15) is determined by:

$$\text{Nu} = 0.26 \cdot (\text{Re})^{0.65} (\text{Pr})^{0.4} \left( \frac{\mu_b}{\mu_w} \right)^{0.14} [42] \quad (5.18)$$

In the equation (5.18), 'Re', the Reynolds Number, is calculated depending on channel mass velocity  $G_s$  (kg/m<sup>2</sup>s), equivalent diameter  $D_e$  (m) and dynamic viscosity of the fluid  $\mu$  (kg/m s) as shown below:

$$\text{Re} = \frac{G_s \cdot D_e}{\mu} \quad (5.19)$$

In equation (5.19), the channel mass velocity  $G_s$  comes from equation (5.20):

$$G_s = \frac{\dot{m}_{\text{per}}}{b \cdot W_p} \quad (5.20)$$

Where  $\dot{m}_{\text{per}}$  (kg/s) is the mass velocity of fluid flowing in per channel which is calculated by:

$$\dot{m}_{\text{per}} = \frac{\dot{m}}{N_{\text{cp}}} \quad (5.21)$$

Where  $\dot{m}$  (kg/s) is the total mass rate entering into the plate heat exchanger and  $N_{\text{cp}}$  is the number of channel per pass and get from:

$$N_{\text{cp}} = \frac{N_{\text{tp}} - 1}{2N_p} \quad (5.22)$$

In equation (5.22) ' $N_{\text{tp}}$ ' is the total number of plates and ' $N_p$ ' is the number of passes.

Based on equations (5.19), (5.20), (5.21) and (5.22), the Reynolds number 'Re' in equation (5.18) can be calculated out. Then put the 'Re' value into equation (5.18). In equation (5.18) the Prandtl number and viscosity ratio are employed with typical value. After that, the Nusselt Number in equation (5.15) could be calculated using equation (5.18).

In equation (5.15) the thermal conductivity of fluid 'k' is the fluid property which could be checked in any hand books or database. As the calculation process of hot side heat transfer coefficient ( $h_h$ ) and cold side ( $h_c$ ) is same, the whole process of evaluation could be applied to both of them. In equation (5.14), other parameters have already discussed before, thus the overall heat transfer coefficient (U) could be calculated properly.

After calculating out the overall heat transfer coefficient, we can establish the detailed relationship between the geometry of heat transfer plate and the heat load according to equation (5.5) and (5.6).

$$\frac{\dot{Q}}{U \cdot \Delta T_m} = N_{ep} \cdot A_d \quad (5.23)$$

Based on equation (5.23) the developed heat transfer area could be expressed by:

$$A_d = \frac{\dot{Q}}{U \cdot \Delta T_m \cdot N_{ep}} \quad (5.24)$$

And then introduce the enlargement factor 'φ'. As expressed in equation (5.11) the plate projected area could be calculated by:

$$A_p = \frac{\dot{Q}}{U \cdot \Delta T_m \cdot N_{ep} \cdot \varphi} \quad (5.25)$$

When we go back to Figure 5.4, the total flat area of the plate could be expressed as:

$$A_{total} = H_t \cdot W_t \quad (5.26)$$

Through the geometrical analysis in Figure 5.4, the total the total flat area of the plate could also be calculated by:

$$A_{total} = A_p + D_p \cdot W_t \quad (5.27)$$

And then we introduce the shape factor of the plate 'λ' where:

$$\lambda = \frac{H_t}{W_t} \quad (5.28)$$

Combine equation (5.26), (5.27) and (5.28) together we can get:

$$\lambda \cdot W_t^2 = A_p + D_p \cdot W_t \quad (5.29)$$

Manipulate equation (5.29), the equation changes to:

$$\lambda \cdot W_t^2 - D_p \cdot W_t - A_p = 0 \quad (5.30)$$

Then the width of the plate could be calculated out:

$$W_t = \frac{D_p \pm \sqrt{D_p^2 + 4\lambda \cdot A_p}}{2\lambda} \quad (5.31)$$

In order to get the physical meaning of equation (5.31),  $W_t$  is always positive.

Therefore, the expression of width of the plate changes to:

$$W_t = \frac{D_p + \sqrt{D_p^2 + 4\lambda \cdot A_p}}{2\lambda} \quad (5.32)$$

Then the height of the plate could be calculated out:

$$H_t = \frac{D_p + \sqrt{D_p^2 + 4\lambda \cdot A_p}}{2} \quad (5.33)$$

What's more, in order to achieve good flow distribution, a plate height/width ratio is usually designed from 2 to 3, as presented in equation (5.34) [42]:

$$2 \leq \lambda \leq 3 \quad (5.34)$$

The length of the pack of plates could be expressed as the number of plates multiplied by the pitch of adjacent plates.

$$L_t = N_{tp} \cdot P_{PHE} \quad (5.35)$$

As the agreement in Section 5.2, the heat transfer plates are selected as the core in the dimension prediction model. Therefore, the length of the core in plate heat exchanger is the length of the pack of heat transfer plates ( $L_t$ ) and the width and height of core are the width ( $W_t$ ) and height ( $H_t$ ) of heat transfer plates respectively. Ultimately, the final expression of core dimension of plate heat exchanger is:

$$\begin{aligned} L_{\text{core,PHE}} &= L_t \\ W_{\text{core,PHE}} &= W_t \\ H_{\text{core,PHE}} &= H_t \end{aligned} \quad (5.36)$$

## 5.4. Sizing the whole plate heat exchanger

After finishing dimension prediction of the core in a plate heat exchanger, the next task for us is sizing the whole dimension of the machine. Figure 5.5 shows the core construction of a plate heat exchanger. From Figure 5.5, the schematic implies that the height and width of two fixed plate are actually counted as the whole dimension of the machine based on the constructional feature of a plate heat exchanger. Figure 5.6 is the overall configuration of a plate heat exchanger which is from a manufacturer brochure. Based on Figure 5.5 and Figure 5.6, the shape of plate heat exchanger actually is similar with the shape of its core (pack of heat transfer plates) which are both in rectangular shape. As we can see in Figure 5.6, the dimension disturbance mainly exists at the length evaluation of the whole machine. The carrying bar and support column in a plate heat exchanger add the extra length of the machine. In order to build up the relationship between core construction and the whole machine, regression analysis of these two dimensions need to be done.

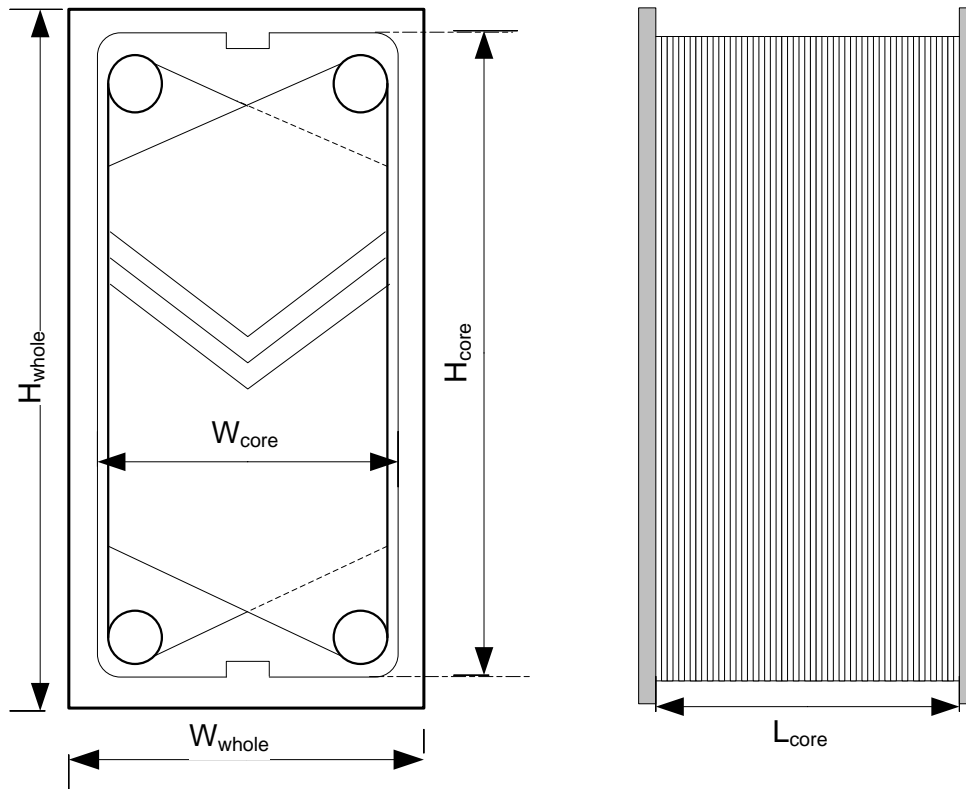


**Figure 5.5 Core construction of plate heat exchanger**

As same as the previous method employing in a shell and tube heat exchanger, the dimension relationship between the core and the whole machine uses linear relationship:

$$\begin{aligned}
 L_{\text{PHE}} &= A_1 \bullet L_{\text{core,PHE}} \\
 W_{\text{PHE}} &= B_1 \bullet W_{\text{core,PHE}} \\
 H_{\text{PHE}} &= C_1 \bullet H_{\text{core,PHE}}
 \end{aligned}
 \tag{5.37}$$

Based on the linear relationship, the ‘first principle’ model of the plate heat exchanger will be implemented in the Excel based on manufacturer data in the next section. The relationship between the core dimension and the whole dimension of plate heat exchangers, as well as the range of main parameters, will be discussed as well.

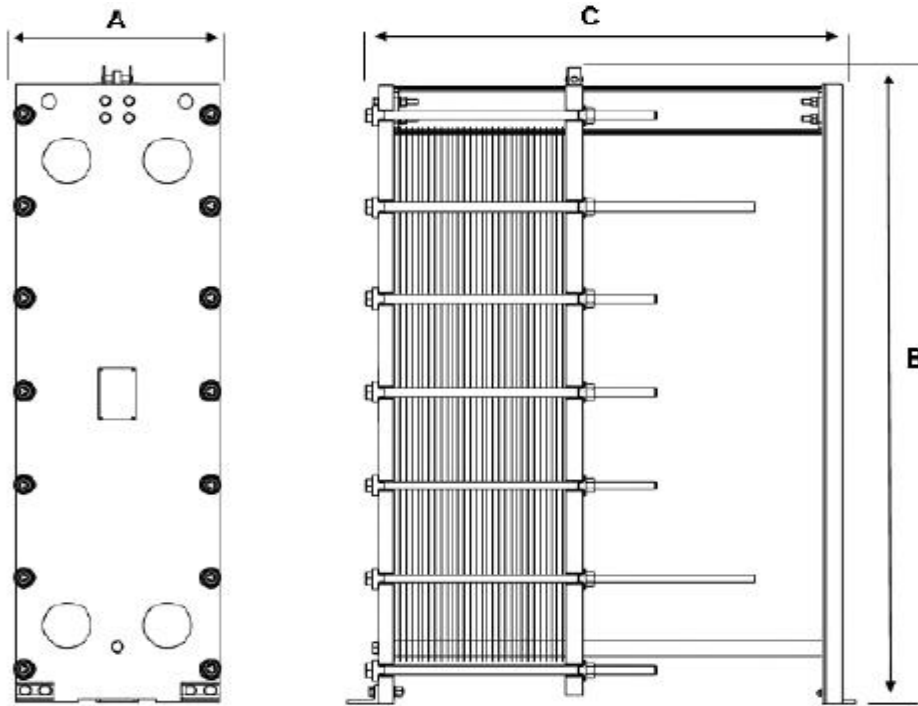


**Figure 5.6 Typical construction of plate heat exchanger. Source: online Grundfos MFT gasketed plate heat exchanger**

## 5.5. Model implementation and results discussion of plate heat exchanger

The implementation process of the plate heat exchanger model is similar with the shell and tube heat exchanger. Since the establishment of the model is based on three basic equations (5.1), (5.2) and (5.3) which are as same as that of shell and tube heat exchanger model, there are also 165 cases could be raised from different parameters combination. The implemented manufacturer data is collected from FUNKE which is a heat exchanger manufacturer company. As we can see in the figures below, the useful manufacturer data is scarce compared with that of shell and tube heat exchangers. However it is still enough to imply the dimension correlation between the core and the whole plate heat exchanger.

Before implementation the manufacturer data, some presumptions need to be made in advance. The function of the plate heat exchanger in the marine systems are diverse, here the author chooses cooling lubrication oil for investigation. As shown in Table 5-2, the hot fluid is lube oil and cold fluid is seawater. For the design purpose, the lube oil is designed to be cooled from 60°C to 49°C and temperature of cooling seawater increases from 29.5°C to 35°C.

**Table 5-2 Designed temperature change of fluids in plate heat exchangers**

<u>Plate heat exchangers</u>		
	°C	K
<b>Hot fluid: <i>Lube oil</i></b>		
Inlet temperature	60	333,15
Outlet temperature	49	322,15
<b>Cold fluid: <i>Seawater</i></b>		
Inlet temperature	29,5	302,65
Outlet temperature	35	308,15

The results of the model implementation are shown in figures below. And we can see the scatter for gasketed plate heat exchanger in Figure 5.7, 5.8 and 5.9, the dimensional correlations distribute linearly. Therefore, the linear distribution implies the efficiency of the applied linear relationship again.

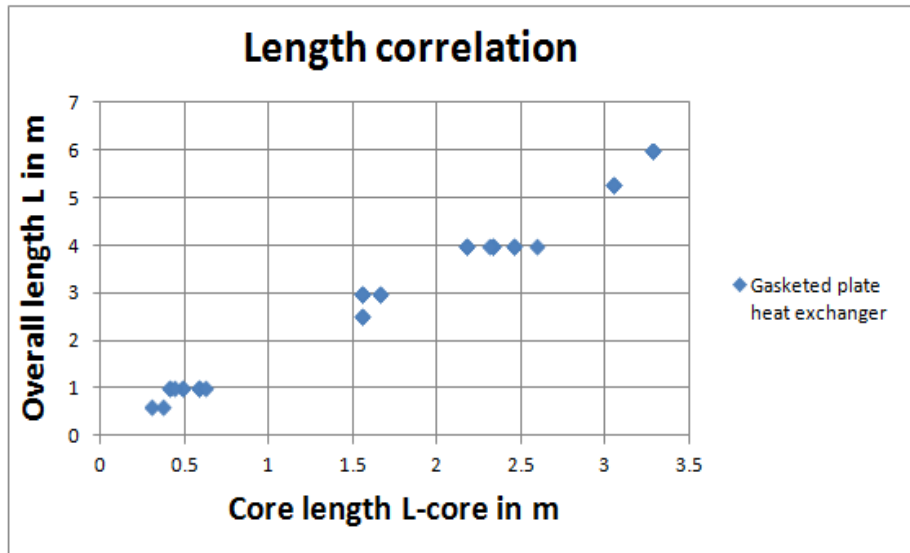


Figure 5.7a Correlation of actual length with theoretical core length for plate heat exchangers

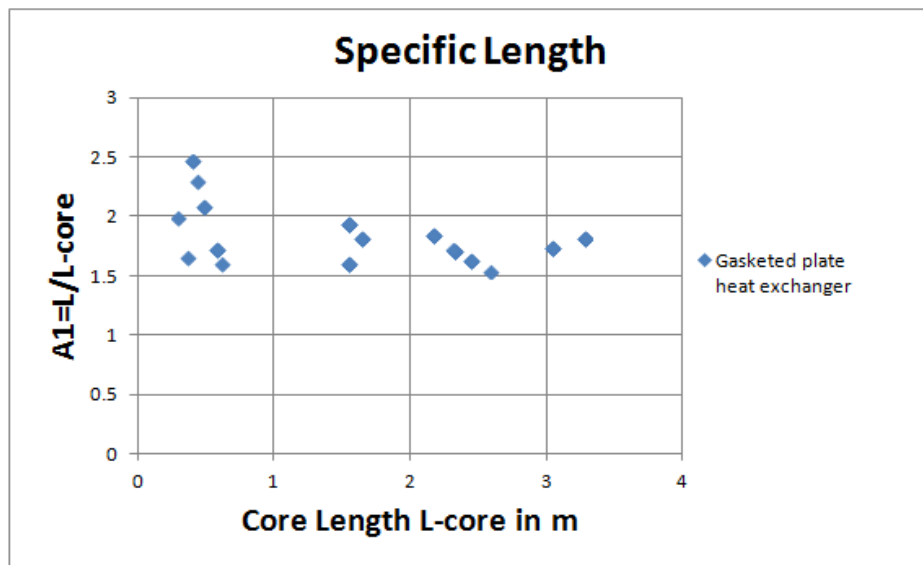


Figure 5.7b Correlation of specific length with theoretical core length for plate heat exchangers

The length of plate heat exchangers correlates not that well compared with that of width and height. The disturbance of the length correlation is mainly due to the carrying bar mounted on the top of the machine. The heat transfer plates are hung on the carrying bar so that it is easy for plates adding or removing. Also from Figure 5.6 can be seen that, there is still some space between the fixed plate and the end of the carrying bar. Therefore, it is rational shown in Figure 5.7a that the same overall length could match different core length of the core element, and whose length basically changed by adding or removing heat transfer plates. Observed from the Figure 5.7b, it can be concluded that the constant value 'A<sub>1</sub>' (in equation (5.37)) of the length correlation is in the range of 1.5-2.5.

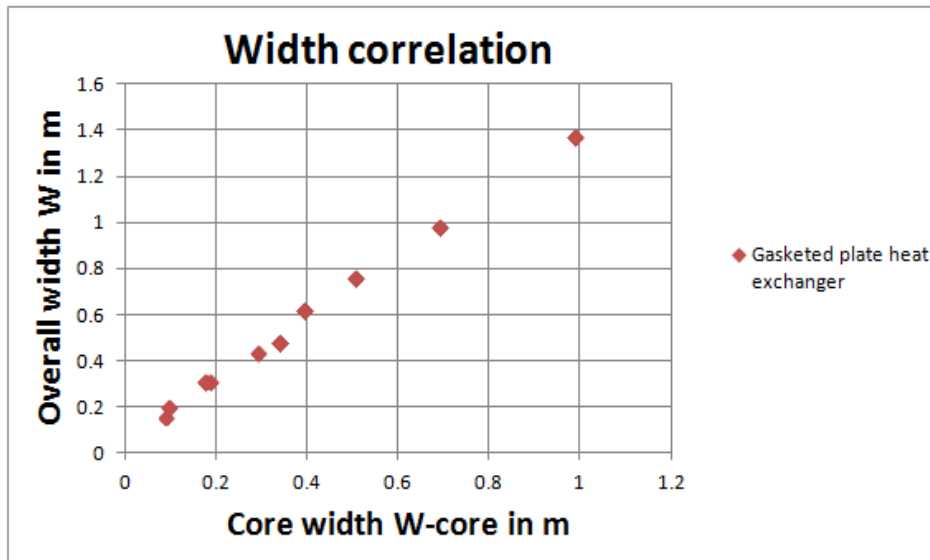
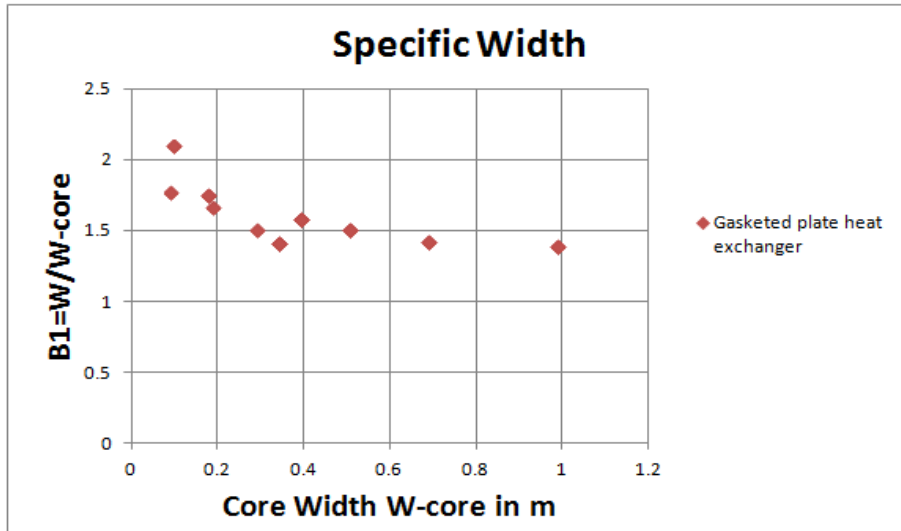
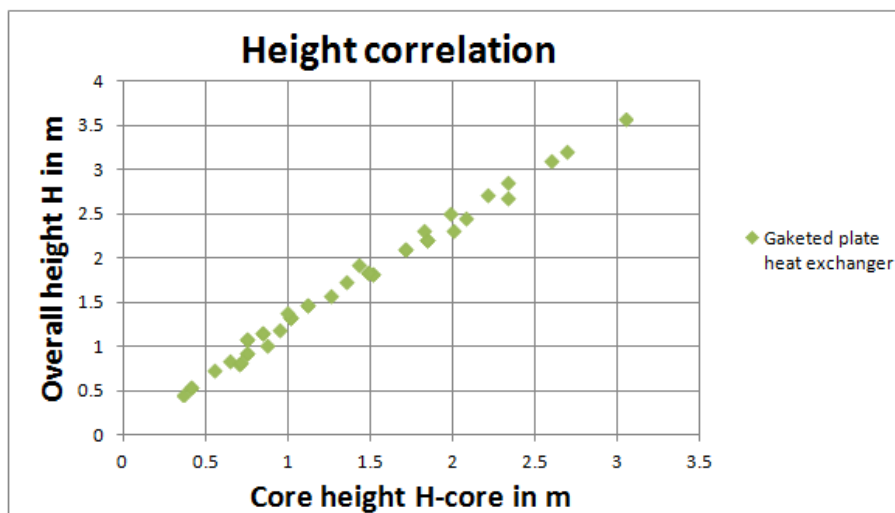


Figure 5.8a Correlation of actual width with theoretical core width for plate heat exchangers



**Figure 5.8b Correlation of specific width with theoretical core width for plate heat exchangers**

The width correlations of plate heat exchangers shown in Figure 5.8a are almost linear. The overall width of the machine actually is the width of the fixed plate which is just a little wider than the heat transfer plates (core element). The ratio between the overall width and the core width of plate heat exchanger as shown in Figure 5.8b is approximately in the range of 1.4-2.1.



**Figure 5.9a Correlation of actual height with theoretical core height for plate heat exchangers**

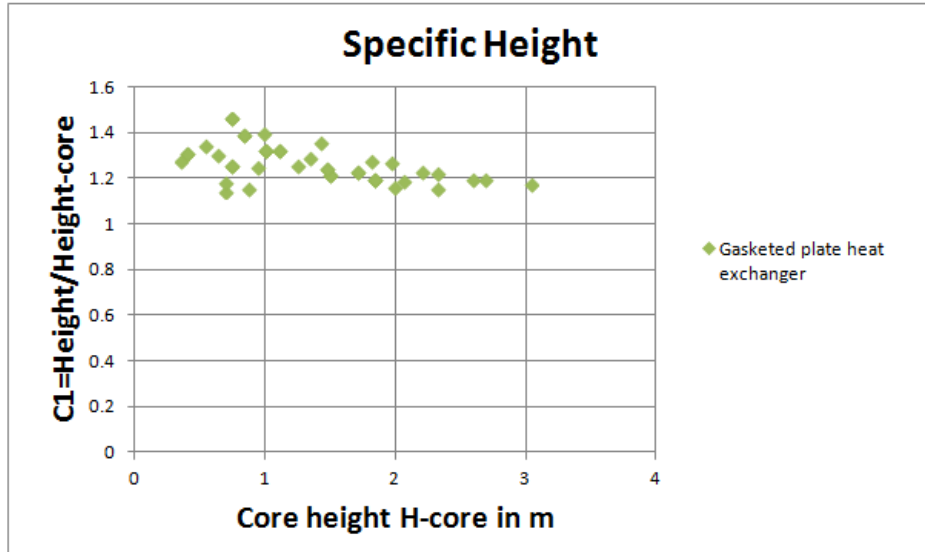


Figure 5.9b Correlation of specific height with theoretical core height for plate heat exchangers

As shown in Figure 5.9a, the situation of the height correlation is similar with that of the width, an approximately linear relation happens between the overall height and the core height of the plate heat exchanger. And the range of ratio 'C<sub>1</sub>' is narrow compared with 'A<sub>1</sub>' and 'B<sub>1</sub>'. From Figure 5.9b can be concluded that the linear fitting factor of the height correlation 'C<sub>1</sub>' is in the range of 1.15-1.45.

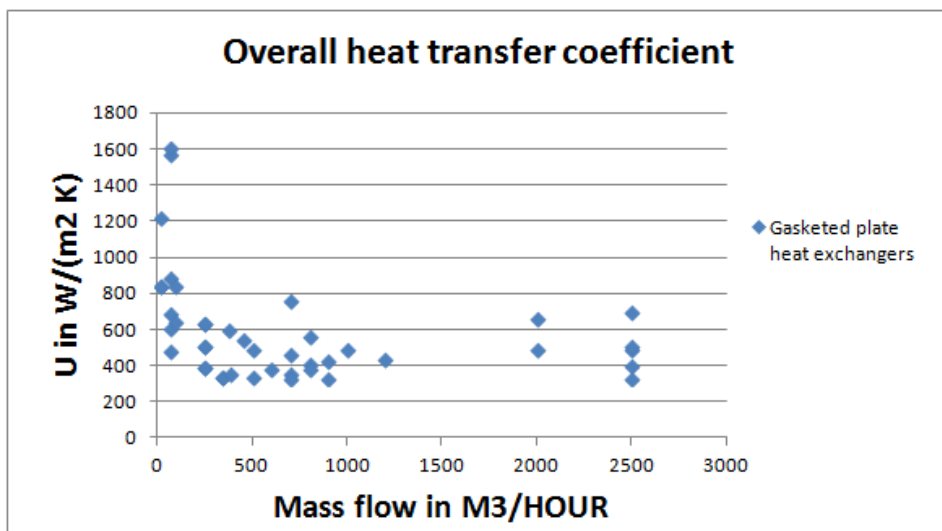
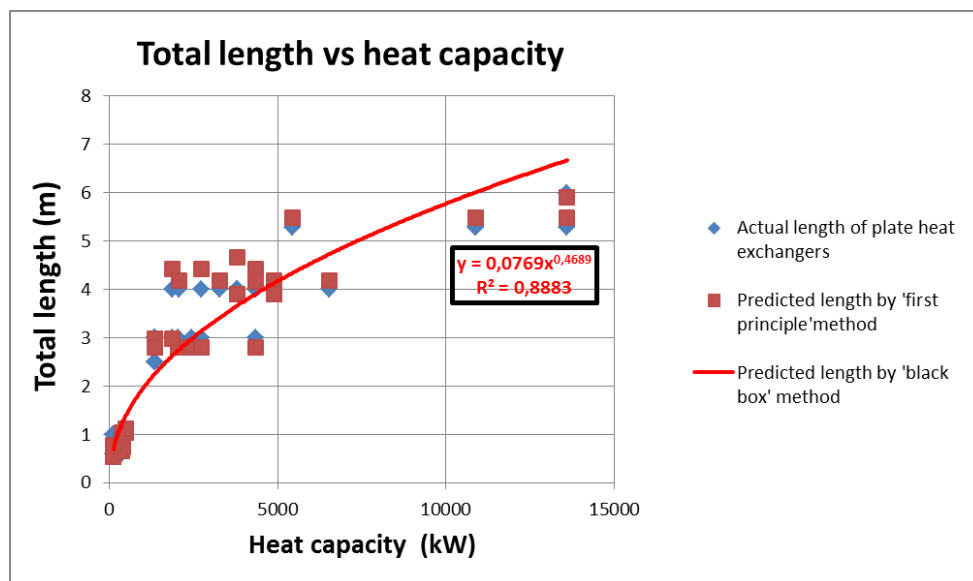


Figure 5.10 Range of overall heat transfer coefficient for plate heat exchangers

The Figure 5.10 shows the spread range of value of the ‘player in the game’ which is the overall heat transfer coefficient. As we discussed in the methodology, the range of the main parameter would have an influence on the ultimate overall dimensions of the machine. For a plate heat exchanger, the ‘main parameter’ is the overall heat transfer coefficient. It can be concluded in Figure 5.10, the overall heat transfer coefficient of the plate heat exchanger is in a wide range from around 300 W/(m<sup>2</sup> K) to 1600 W/(m<sup>2</sup> K). In the following part, the author will compare the predicted dimension by ‘first principle’ model and the ‘black box’ model separately.



**Figure 5.11 Predicted length by ‘black box’ method and ‘first principle’ method against the actual length of plate heat exchangers**

As same as what have done in Chapter 4, the heat capacity of the plate heat exchanger and some variables need to be set at first. The heat capacity of plate heat exchangers here we assume are always given which is the initial input of the model. A mean value is estimated for the overall heat transfer coefficient of 500 W/(m<sup>2</sup> K). Furthermore typical value assumed for the linear constant  $A_1$  is 1.8 according to Figure 5.7b. It can be seen in Figure 5.11, the ‘first principle’ deviations are smaller compared with the ‘black box’ deviations. The cause of the ‘first principle’ deviation is also clear which is due to the setting of variables (overall heat transfer coefficient and

linear constant). However, for the deviations generated by 'black box' method, it is difficult to explore the reason of the deviations by the simple mathematical expression.

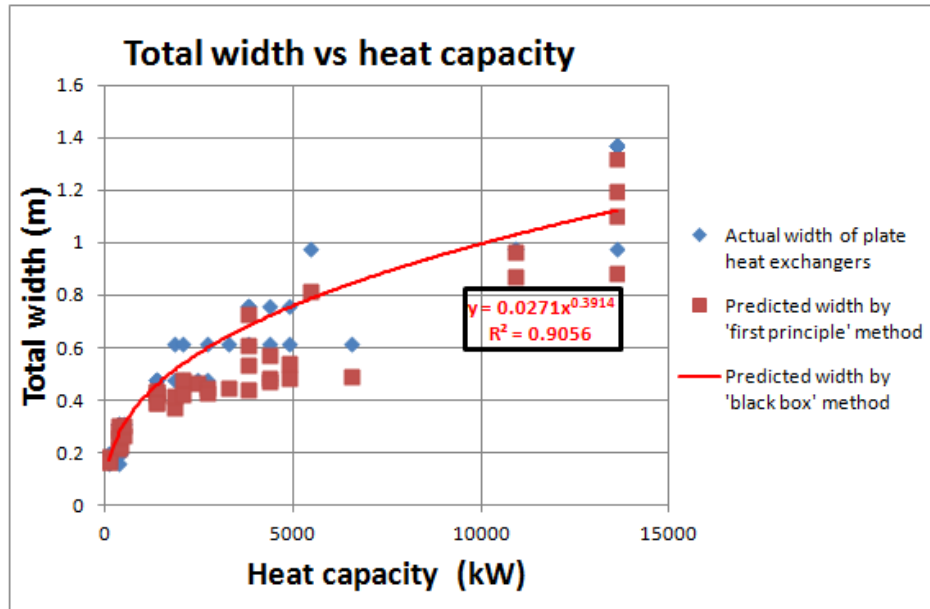


**Figure 5.12 Predicted width by 'black box' method and 'first principle' method against the actual width of plate heat exchangers**

Figure 5.12 shows the results of the predicted width of plate heat exchangers by 'first principle' model and 'black box' model separately. Before implementing the 'first principle' model, some presumptions need to be made. The overall heat transfer coefficient remains the same as that of length prediction. The linear constant  $B_1$  is set 1.4. Compared with the length, the difference is that one more variable needs to be evaluated, which is the diameter of the port ( $D_p$ ). In practice, the diameter of the port needs to be matched with the diameter of the pipe. It can be seen in Figure 5.12, the non-linear effects are reduced compared with the trend-line function generated by 'black box' model.

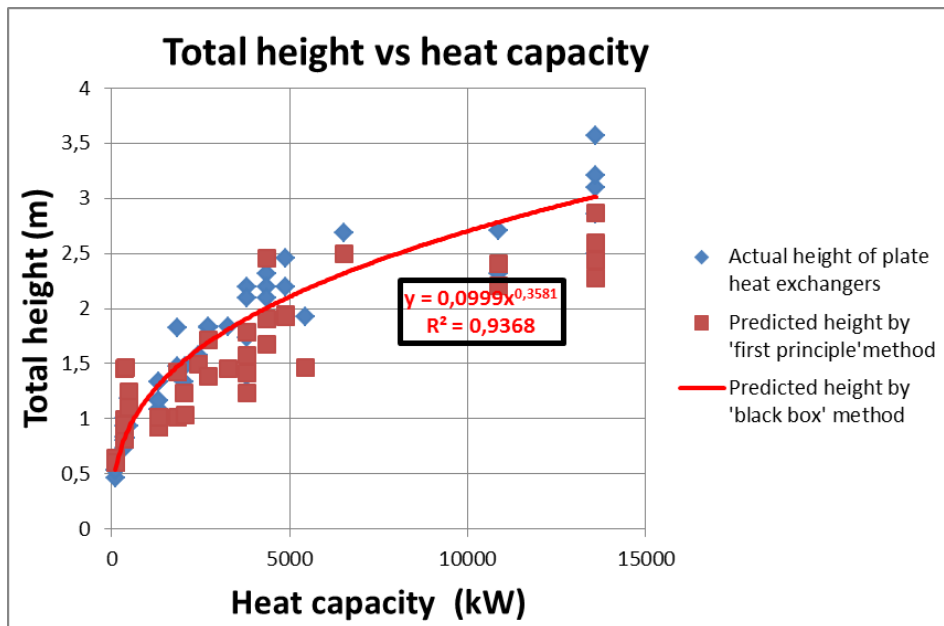


**Figure 5.13 Predicted height by ‘black box’ method and ‘first principle’ method against the actual height of plate heat exchangers**

The linear constant  $C_1$  is set 1.2 for height dimension prediction of plate heat exchangers. The deviations between the red plots and blue plots in Figure 5.13 are mainly caused by the linear constant, overall heat transfer coefficient and the evaluated diameter of the port side.

## 5.6. Summary

This chapter discussed the ‘first principle’ model applied to plate heat exchangers. First of all, based on the working principle of the plate heat exchanger, the heat energy is transferred between the adjacent heat transfer plates. Based on the given heat balance, the mathematical relationship between the dimension of the plates and heat load would be established. Then the dimension of the primary element could be determined by the load balance. Unlike other marine components (diesel engine, electric machine, etc.), whose core part consists of both primary element and secondary element. Since the pack of the heat transfer plates has already taken up the major part of the machine, there is no secondary element is needed to be

determined for a plate heat exchanger in the model. The 'main parameter' overall heat transfer coefficient in the model could also be evaluated by two approaches which are as same as that of the shell and tube heat exchangers. The first approach is more likely to be applied in preliminary ship design stage for indicating the approximate dimension of the plate heat exchangers. After establishing the model of the core part, the mathematical relationship between the core part and overall dimension of the machine are also evaluated based on the regression analysis. The linear relationships between the core dimension and the overall dimension are explored successfully.

The successful application proves the 'first principle' sizing model is a generic model again. And it also indicates not only power output (diesel engine, gearbox, etc.) but heat capacity could be employed for evaluating the dimension of the machine based on first principles. At last, the comparison between the 'first principle' model and 'black box' model is discussed. It can be concluded the 'first principle' method keeps the fidelity of the model and can be analyzed the deviation of the results with the actual dimension. That is not possible for 'black box' sizing method.

# 6. Centrifugal Pump

---

Pumps are one of the most commonly used marine components in various marine systems such as cooling system, lubrication system, fuel cleaning and supply system, etc. Among various types of pumps, centrifugal pumps are widely used in marine engineering system because of its high efficiency, simple configuration, ease of maintenance and operation. In this chapter, the author will apply the 'first principle' method to predict dimensions of centrifugal pumps. The general information, including definition, working principle, etc, will be discussed first. After that, the detailed configuration of a centrifugal pump will also be investigated which is helpful to select the primary and secondary element in the following procedure. And then the dimension prediction model of centrifugal pumps will be established, which is also the main part of this chapter. Finally, the results and discussion about the model implementation based on manufacturer data will be presented.

## 6.1. General information of centrifugal pump

A centrifugal pump is a kinetic device which adds energy to the internal liquid by increasing its velocity. Figure 6.1 and Figure 6.2 show a typical construction of a centrifugal pump and the fluid flowing in a centrifugal pump separately. As shown in Figure 6.2, a rotating impeller driven by a shaft creates a suction force on the fluid and draws the fluid flowing into the pump through the impeller eye. The fluid within the impeller is accelerated by the centrifugal force in the circumferential direction and diffused in the volute of the centrifugal pump. The volute cross-sectional area increases gradually in the flow direction, such that the high velocity of diffused fluid from impeller is reduced and converted into pressure.



**Figure 6.1 A typical centrifugal pump**

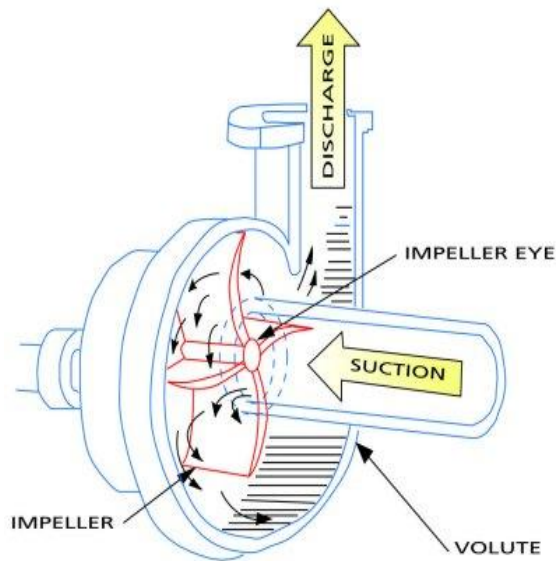


**Figure 6.2 Working principle of a centrifugal pump**

In order to get knowledge about the performance of a centrifugal pump, some key specifications, including flow rate ' $Q_{\text{impeller}}$ ', head ' $H$ ', net positive suction head ' $NPSH$ ', velocity triangle, need to be investigated in advance.

The volume flow rate ' $Q_{\text{impeller}}$ ' of the pumped liquid is an essential measurement of the performance of a centrifugal pump. The required flow rate is normally determined by the material and energy balances. The head 'H' is another important characteristic of a centrifugal pump. The head of the pumped liquid raised by the centrifugal pump is stated as meters (feet) and could be expressed by the pressure and the density of the liquid:

$$H = \frac{\Delta p}{\rho \cdot g} \quad (6.1)$$

Normally, the value of head is preferred to be used to measure a centrifugal pump's energy instead of pressure because the pressure of the pump will change if the specific gravity of the liquid changes, but the head will not. In the pumping systems, there are various head terms such as static head, velocity head, suction head, net positive suction head, discharge head, differential head, etc. Among these different head terms, the net positive suction head (NPSH) is normally regarded as an important reference characteristic during designing and selecting process.

In general, the NPSH is a measure of liquid at the suction side of the pump which is used for avoiding cavitation occurred on the impeller and other pump components during working operation. Cavitation occurs when the suction pressure of the liquid is lower than its vapor pressure which would damage the impeller and also lead to a reduction of pumping efficiency and capacity. The concept of NPSH consists of two terms:  $NPSH_{\text{req}}$  (required NPSH) and  $NPSH_{\text{avi}}$  (available NPSH). The required NPSH represents the minimum NPSH required by the centrifugal pump to prevent the inception of the cavitation. While the available NPSH is the actual working NPSH made by suction side. Thus, in order to avoid the occurrence of cavitation in a centrifugal pump, we must ensure the  $NPSH_{\text{avi}}$  is larger than the  $NPSH_{\text{req}}$ . The  $NPSH_{\text{avi}}$  can be calculated by:

$$\text{NPSH}_{\text{avi}} = H_A \pm H_Z - H_F - H_{vp} \quad (6.2)$$

Where:

$H_A$  = The absolute pressure on the surface of the liquid in the supply tank in meters

$H_Z$  = Vertical distance between the surface of the liquid and the centerline of the pump in meters

$H_F$  = Friction loss in meters

$H_{vp}$  = Vapor pressure in meters

For the fluid flow through the impeller, the velocity triangle of the fluid and impeller is another important specification and which is also used in the establishment of dimension prediction model later. By means of the velocity triangle, the performance of the centrifugal pump can be predicted in connect with the changes of e.g. impeller diameter and width.

An example of velocity triangle is shown in Figure 6.3 which depicts the velocities at the entrance and exit of the impeller separately. In Figure 6.3, 'U' represents the impeller's tangential velocity (m/s) and 'V' describes the fluid's absolute velocity compared with the surroundings (m/s). The relative velocity of the flowing fluid 'W' is a velocity compared to the rotating velocity (m/s). The angles ' $\alpha$ ' and ' $\beta$ ' describe the angles of fluid's absolute and relative velocity compared to the tangential direction (rad). The relationship between these velocities can be described in the velocity triangle (Figure 6.3b). The absolute velocity of fluid (V) is a vectorial sum of impeller's tangential velocity (U) and the fluid's relative velocity (W). For the impeller's tangential velocity (U) could also be expressed by the angular velocity of impeller ( $\omega$ ) or the rotational speed (n) that:



## 6.2. Configuration of centrifugal pump

In this section, the detailed configuration of a centrifugal pump will be introduced which is essential before selecting and sizing the dimension of the primary and secondary element. The Figure 6.4 below is an overview of a centrifugal pump's detailed construction. The name of each part of a centrifugal pump is listed below:

- A. Stuffing Box
- B. Packing
- C. Shaft
- D. Shaft Sleeve
- E. Vane
- F. Casing
- G. Eye of impeller
- H. Impeller
- I. Casing wear ring
- J. Impeller
- K. Discharge nozzle

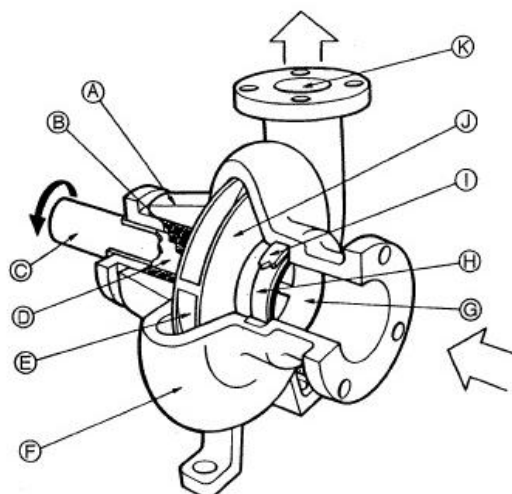


**Figure 6.4 Configuration of a centrifugal pump**

Based on the working principle of a centrifugal pump, the fluid is sucked from the eye of the impeller (G) into the channel of the rotating impeller (J). The rotating impeller (J) with vanes (E) is generated by a connected shaft (C) which is driven by a motor. The fluid within the channel of the impeller diffuses into the chamber of the casing (F). The high speed fluid within the casing (F) is decelerated and finally discharged through the discharge nozzle (K) with a high pressure. From the stated basic working principle of a centrifugal pump associated with the components within the machine, we can find the major working performance changes (velocity, pressure) happened in the channel of the impeller (G) and the chamber of the casing (F). Thus, the impeller is chosen as the primary element and the casing (volute) is the secondary element (as shown in Figure 6.5). In the following sections, the 'first principle' model of sizing the primary and secondary element will be built up.



**Figure 6.5 Construction of an impeller and a volute of a centrifugal pump**

### 6.3. Sizing the primary element of a centrifugal pump

Based on the first principle approach, the dimension of the primary element (impeller) will be sized in this section. First of all, start with the basic first principle equation:

$$P=M \cdot \omega=M \cdot 2\pi \cdot n \quad (6.4)$$

Equation (6.4) is as same as the basic equations of diesel engine, electric machine and gearbox, which relates the power output to the torque and angular speed. Where 'P' is the power output (W), 'M' is the torque (Nm), 'ω' is the angular velocity (rad/s) and 'n' is the rotational speed (rps). For a centrifugal pump, the torque is delivered by the force acting on the circumference surface of the impeller's channel. Thus, the delivered torque is given by:

$$M=HF \cdot \frac{D_2}{2} \quad (6.5)$$

In equation (6.5), the 'HF' is the hydraulic force acting on the circumferential surface of the fluid channel (N) and 'D<sub>2</sub>' is the diameter of the impeller at the exit side (m). The hydraulic force can also be expressed as the shear stress which is calculated by dividing the hydraulic force by an area. As discussed by *Stapersma* and *de Vos*, the shear stress is the characteristic stress rather than the actual shear stress, but it do have a relation with the actual shear stress and can help determine the expressions that relate power and size of the primary element [1]. The expression of hydraulic force based on shear stress is given by:

$$HF=\tau_{cp} \cdot A_2 \quad (6.6)$$

Where 'τ<sub>cp</sub>' is the shear stress (N/m<sup>2</sup>) and 'A<sub>2</sub>' is the circumferential ring area of impeller channel at the exit side (m<sup>2</sup>). From Figure 6.6, the outlet circumferential ring area 'A<sub>2</sub>' is calculated as:

$$A_2 = 2\pi \cdot r_2 \cdot b_2 = \pi \cdot D_2 \cdot b_2 \quad (6.7)$$

Where 'r<sub>2</sub>' is the radius of the impeller (m) and 'b<sub>2</sub>' is the width of the channel (m). Then based on equations (6.3), (6.4), (6.5), (6.6) and (6.7), the relationship between the power output and dimension of impeller channel can be concluded that:

$$P = \tau_{cp} \cdot \pi^2 \cdot D_2^2 \cdot b_2 \cdot n \quad (6.8)$$

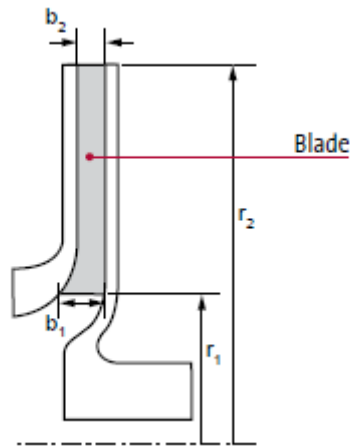


**Figure 6.6 Schematic diagram of the primary element of a centrifugal pump**

Also, a designer may want to vary the shape factor  $\lambda = b_2/D_2$ . Therefore, the equation (6.8) could be rewritten as:

$$P = \tau_{cp} \cdot \pi^2 \cdot D_2^3 \cdot n \cdot \lambda \quad (6.9)$$

Theoretically, according to the Newton's second law, torque 'M' equals the change of angular momentum. Therefore, in the case of the centrifugal pump, the torque 'M' to drive the impeller equals the changes of momentum of fluid:

$$M = \dot{m} \cdot \left( V_{u,2} \cdot \frac{D_2}{2} - V_{u,1} \cdot \frac{D_1}{2} \right) \quad (6.10)$$

Where ' $\dot{m}$ ' is the fluid mass flow (kg/s), ' $V_u$ ' is the fluid speed at tangential direction at impeller's entry and exit respectively (m/s) and ' $D_1$ ' and ' $D_2$ ' are the diameter of the impeller's entry and exist (m). As discussed before, the flow at impeller entry is normally non-rotational. Therefore, according to the velocity triangle in Figure 6.3, the angle ' $\alpha_1$ ' is  $90^\circ$  which also means the fluid's velocity at tangential direction ( $V_{u1}$ ) is 0. Then equation (6.10) could be changed to:

$$M = \dot{m} \cdot V_{u,2} \cdot \frac{D_2}{2} \quad (6.11)$$

Combine equations (6.3) (6.4) and (6.11), the hydraulic power output is calculated as:

$$P = M \cdot \omega = \dot{m} \cdot V_{u,2} \cdot \frac{D_2}{2} \cdot \omega = \dot{m} \cdot V_{u,2} \cdot U_2 = Q_{\text{impeller}} \cdot \rho \cdot V_{u,2} \cdot U_2 \quad (6.12)$$

The mass flow rate in equation (6.12) is described by the volumetric flow rate ' $Q_{\text{impeller}}$ ' ( $\text{m}^3/\text{s}$ ) and density of the fluid ' $\rho$ ' ( $\text{kg}/\text{m}^3$ ). According to the equation (6.12), the hydraulic power could also be expressed by the increase in pressure ' $\Delta p$ ' and the volumetric flow rate through the impeller ' $Q_{\text{impeller}}$ ':

$$P = \Delta p \cdot Q_{\text{impeller}} \quad (6.13)$$

The increase of the pressure could also be expressed by the increase of head:

$$\Delta p = \Delta H \cdot \rho \cdot g \quad (6.14)$$

Combine equations (6.12) and (6.14) the increase of head could be denoted by the velocities (' $V_{u,2}$ ' and ' $U_2$ '):

$$\Delta H = \frac{V_{u,2} \cdot U_2}{g} \quad (6.15)$$

Based on the velocity triangle in Figure 6.3b, the fluid speed at tangential direction at impeller's exit '  $V_{u2}$  ' can be calculated as:

$$V_{u,2} = U_2 - \frac{V_{m,2}}{\tan\beta_2} \quad (6.16)$$

As the entire flow must be diffused through the ring area at the exit of the impeller ( $A_2$ ) and the velocity of fluid flowing through the ring area is the meridional velocity '  $V_{m,2}$  '. Thus the 'meridional velocity' ( $V_{m,2}$ ) could be calculated by the volumetric flow rate ( $Q_{\text{impeller}}$ ) at the ring area at the exit of impeller ( $A_2$ ):

$$V_{m,2} = \frac{Q_{\text{impeller}}}{A_2} \quad (6.17)$$

Finally, based on equations (6.7) (6.15) (6.16) and (6.17), the increase of head could be calculated as:

$$\Delta H = \frac{(\pi \cdot n \cdot D_2)^2}{g} - \frac{n}{g \cdot b_2 \cdot \tan(\beta_2)} \cdot Q_{\text{impeller}} \quad (6.18)$$

Compared with equation (6.8) which builds up the relation between the power output and the dimension of impeller, equation (6.18) actually associates the dimension of the impeller with the head increase ( $\Delta H$ ) and volumetric flow ( $Q_{\text{impeller}}$ ) of the centrifugal pump which are also essential parameters interested by designers. Also, introduce the shape factor '  $\lambda$  ' into equation (6.18), we can get:

$$\Delta H = \frac{(\pi \cdot n \cdot D_2)^2}{g} - \frac{n}{g \cdot D_2 \cdot \lambda \cdot \tan(\beta_2)} \cdot Q_{\text{impeller}} \quad (6.19)$$

Equation (6.19) set up the relationship between the dimension of the impeller ( $D_2$  and  $b_2$ ) with increase head and flow rate. This relationship is mainly based on the design

of the impeller.

Furthermore, based on the expressions of power output of centrifugal pump in equations (6.8) and (6.9), the dimension of the primary element could also be defined as:

$$D_2 = \sqrt[3]{\frac{P}{\tau_{cp} \cdot \pi^2 \cdot n \cdot \lambda}} \quad (6.20)$$

$$b_2 = \sqrt[3]{\frac{P \cdot \lambda^2}{\tau_{cp} \cdot \pi^2 \cdot n}} \quad (6.21)$$

In equations (6.20) and (6.21) the dimension of the primary element is determined not only by the power output (P) but also the shear stress ( $\tau_{cp}$ ), shape factor ( $\lambda$ ) and rotational speed (n).

The 'effort' and 'flow' within a centrifugal pump is the torque 'M' and the rotational speed 'n' respectively. The expressions of these two variables are shown in equations (6.22) and (6.23). From the equations below, it can be found that the dimension of impeller really has an effect on the torque and the rotational speed.

$$M = \tau_{cp} \cdot \pi \cdot b_2 \cdot \frac{D_2^2}{2} \quad (6.22)$$

$$n = \frac{U_2}{\pi \cdot D_2} \quad (6.23)$$

The larger dimension of the impeller will lead larger torque and lower rotational speed. That also corroborates the fact that the machines with higher rotational speed are usually smaller.

Finally, equations (6.19), (6.20) and (6.21) are employed in the 'first principle' model

for sizing the primary element.

## **6.4. Sizing the secondary element and core of centrifugal pump**

As discussed in Section 6.2, the volute casing of the centrifugal pump is selected as the secondary element in the dimension prediction model of centrifugal pumps. The main function of the volute casing is theoretically decreasing the velocity of fluid diffused from the rotating impeller and leading the pressure increase of the fluid before leaving the nozzle of the centrifugal pump. In this section, the dimension of centrifugal pump's secondary element and the core (combination of the primary element and secondary element) will be estimated.

The schematic of centrifugal pump core construction is shown in Figure 6.7, it is clear that the primary element (impeller) is completely within the chamber of the secondary element (volute). Therefore, the dimension of the core of centrifugal pump, combination of the primary element and secondary element, is actually the dimension of the volute in the centrifugal pump. However, since the function of volute casing is basically decreasing the velocity of diffused fluid, the cross sections of the volute are designed not identical. As can be seen in Figure 6.7, the largest cross section of volute casing is at the discharge part of the volute casing.

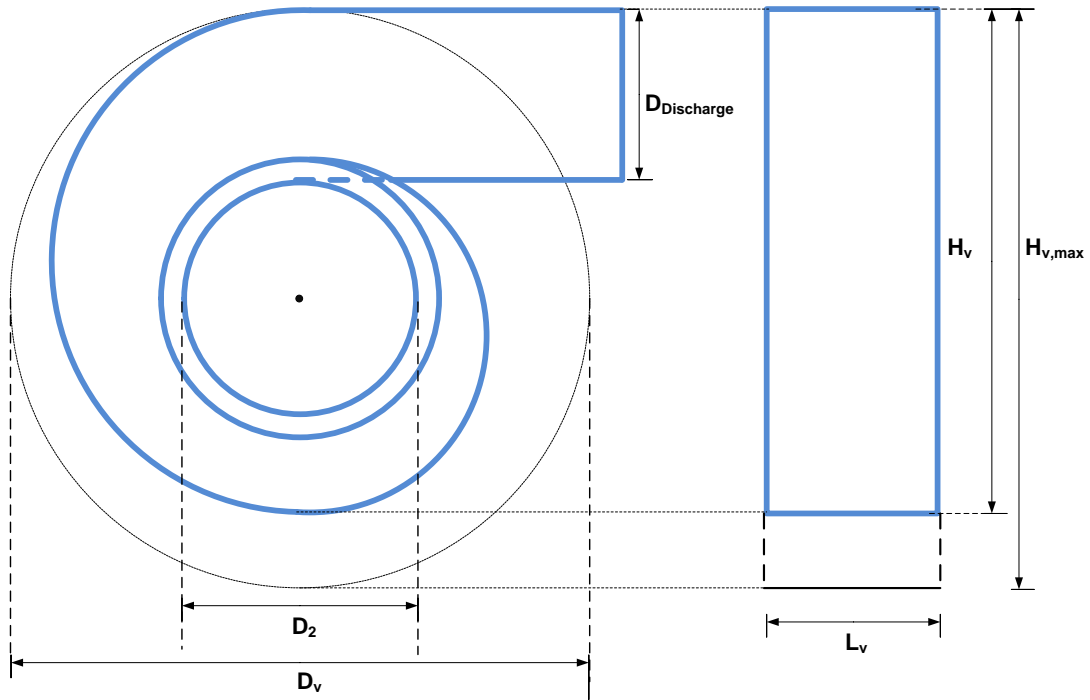


**Figure 6.7 Schematic of centrifugal pump core dimension**

The diameter of the cross-sectional area at the discharge part can be calculated by the volumetric flow rate of impeller and discharge velocity of the fluid, that is:

$$D_{\text{discharge}} = \sqrt{\frac{4 \cdot Q_{\text{impeller}}}{\pi \cdot V_{\text{discharge}}}} \quad (6.24)$$

Based on the largest diameter of cross-sectional area of the volute casing, the maximum value of the length width and height of volute casing would be calculated based on the geometrical relationship. Here need to be clear that our final target of the dimension model is sizing the overall dimension of the machine and the method of evaluating the whole dimension of the machine is using linear relationship. Therefore, using the maximum dimension value of the volute casing to estimate the overall dimension of the machine will not influence the accuracy of the estimation, which would only decrease the fitting factor ( $A_1$ ,  $B_1$ ,  $C_1$ ) of the linear relationship. Therefore, based on the geometrical relationship between the primary element and secondary

element shown in Figure 6.7, the core dimension of the centrifugal pump is calculated as:

$$\begin{aligned}L_{\text{core,CP}} &= D_{\text{discharger}} \\ W_{\text{core,CP}} &= D_2 + 2 \bullet D_{\text{discharger}} \\ H_{\text{core,CP}} &= D_2 + 2 \bullet D_{\text{discharger}}\end{aligned}\tag{6.25}$$

And the diameter of the impeller at the existing side is already evaluated by equation (6.20) in the primary sizing model.

## 6.5. Sizing the whole centrifugal pump

After establishment the model of sizing the core of centrifugal pump, the final task is building up the relationship with respect to the dimension between the core construction and the overall machine. Figure 6.8 is a typical drawing of the centrifugal pump of the manufacturer, it can be concluded that the height and width of the core have already taken over most part of the actually overall dimension of a centrifugal pump. However, the length of the core element is only in the small part of the whole machine. The reason of the length disturbance is because of the shaft and the motor which are connected to the impeller of the centrifugal pump. Even though the hydraulic working environment is inside the volute casing, the centrifugal pump can not work without the electric motor and shaft.

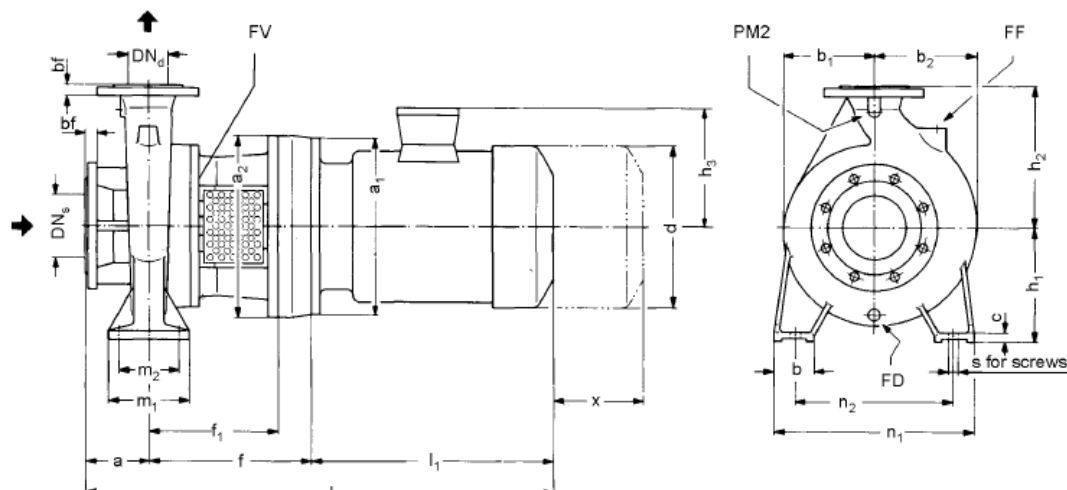


**Figure 6.8 Typical construction of a centrifugal pump. Source online ALLWEILER series NB volute casing centrifugal pump**

Now we need a mathematical relation between the core construction and the whole machine to fit the model to the actual manufacturer data. As discussed before, the linear relationship is used:

$$\begin{aligned}
L_{CP} &= A_1 \cdot L_{core,CP} \\
W_{CP} &= B_1 \cdot W_{core,CP} \\
H_{CP} &= C_1 \cdot H_{core,CP}
\end{aligned}
\tag{6.26}$$

In the next section, the range of the fitting factors in equation (6.26) will be determined based on the manufacturer data. Furthermore, the comparison between ‘first principle’ method and ‘black box’ method of sizing centrifugal pumps will be discussed.

## **6.6. Model implementation and results discussion of centrifugal pump**

The model implementation of the centrifugal pumps is done in the Excel as well. The input manufacturer data of centrifugal pumps mainly collected from KSB and Carver these two manufacturers. The flowing capacity of the collected centrifugal pump is ranging from 3 m<sup>3</sup>/hour to 3500 m<sup>3</sup>/hour. For the data input, the flowing fluid within the centrifugal pump we set in advance is the fresh water with the 1000 kg/m<sup>3</sup> density.

The results of the model implementation are shown below including the dimension correlation between the core element dimension and the overall dimension of the machine, the spread range of the main parameter of the centrifugal pumps etc.

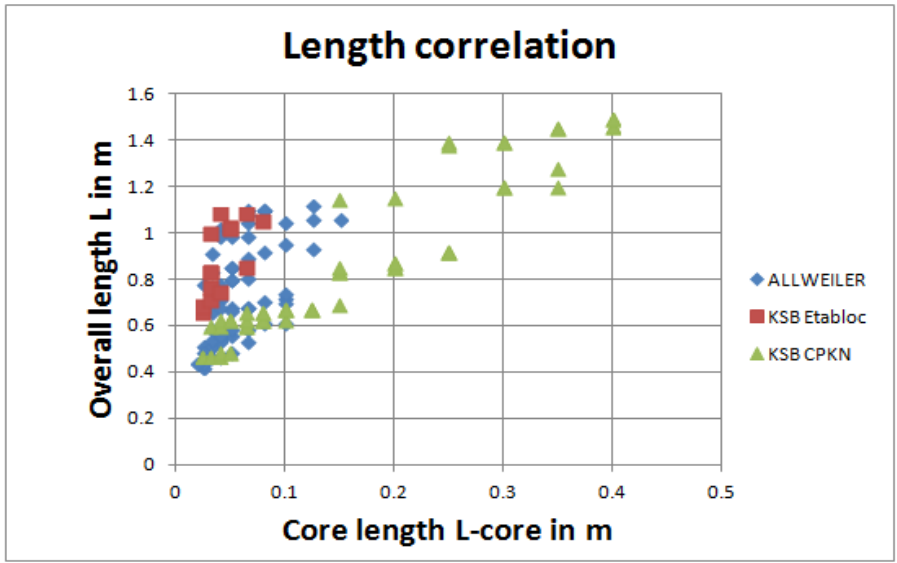


Figure 6.9a Correlation of actual length with theoretical core length for centrifugal pumps

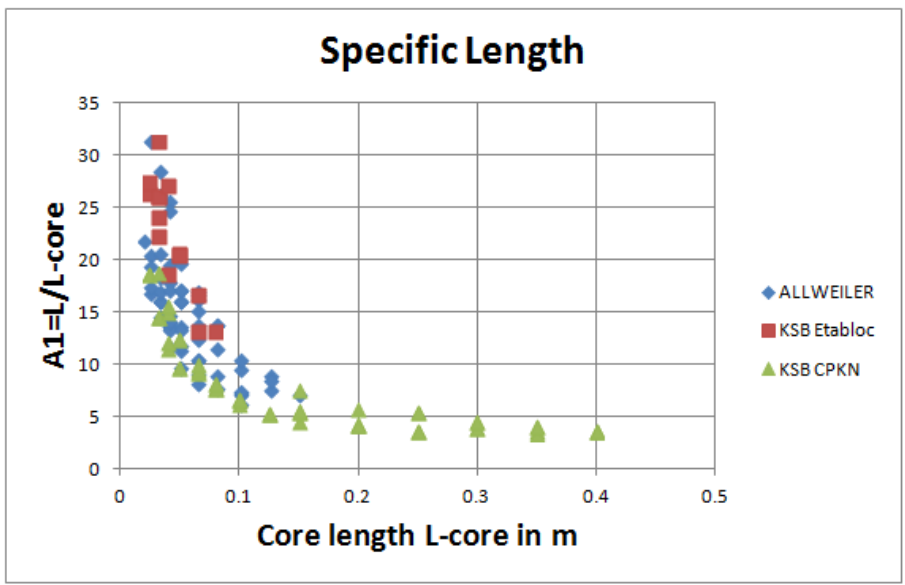


Figure 6.9b Correlation of specific length with theoretical core length for centrifugal pumps

The length correlation between the core element and overall length is shown in Figure 6.9 above. From the figure we find the length correlation is not quite clear compared with the nearly linear length correlation of heat exchangers in previous chapters. The reason of the non-linear length correlation is due to the construction of the centrifugal

pumps. As can be seen the typical construction drawing of a centrifugal pump in Figure 6.8, a centrifugal pump graphically is composed by a casing and a motor. The length of the motor takes up the main part of the overall length of a centrifugal pump and that is also a big disturbance of the length correlation between the core length and the overall length of the machine. Besides that, the dimension of the electric motor is also influenced by the power out as we discussed in Chapter 2. Therefore, the increasing power out of a centrifugal pump would lead to the increasing length of both casing and the motor. The range of the linear constant value  $A_1$  shown in Figure 6.9b is approximately from 3 to 31. From these high values it can be concluded that the calculated core length data do not cover a significant part of the machine, which was the case for the heat exchanger dimensions and will also be the case for width and height of the pump as well. But in fact, the core length is probably a lot closer to the overall length of the centrifugal pump. Then the high values for specific length imply as the reference length is not the length of the actual centrifugal pump but the length of the pump and electric machine combination.

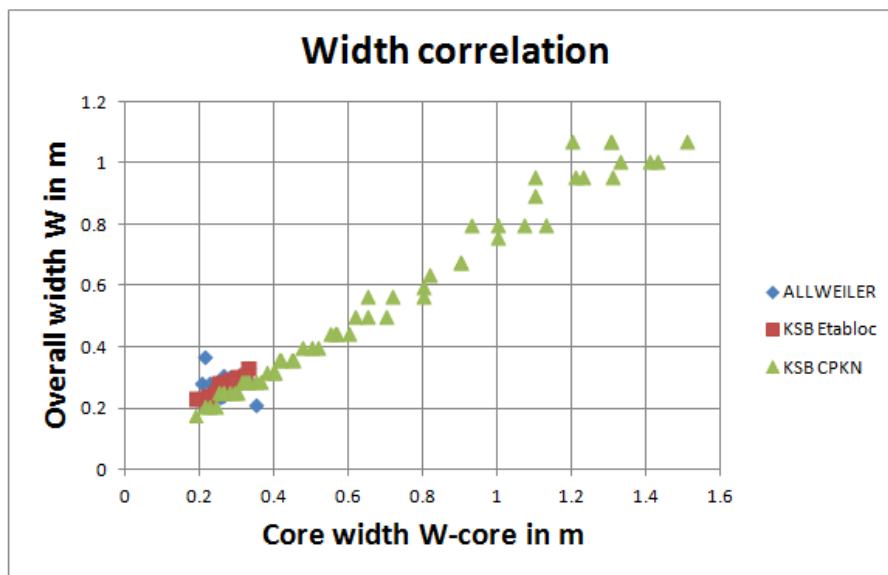
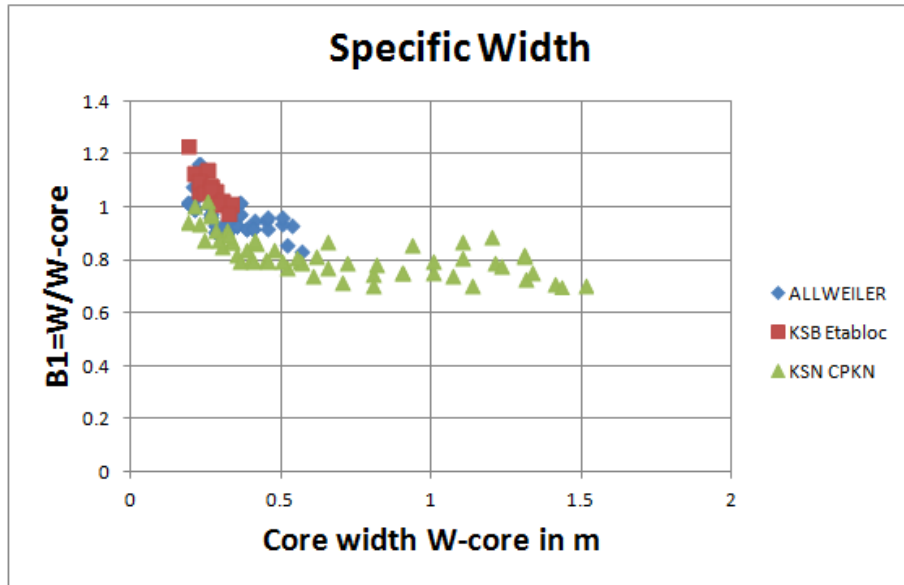


Figure 6.10a Correlation of actual width with theoretical core width for centrifugal pumps



**Figure 6.10b Correlation of specific width with theoretical core width for centrifugal pumps**

The width correlation shown in Figure 6.10a is much clearer with the nearly linear relationship between the core width and overall width of the machine. As discussed in Section 6.4, the author utilized the diameter of the discharge part of the volute casing to calculate the total width and height of the core element. The diameter at the discharge part is the maximum diameter of the volute channel. Accordingly, the evaluated diameter of the core element in some cases is larger than the overall dimension. It is also reflected in the results shown in Figure 6.10b, the range of the specific width ratio is around 0.7-1.2.

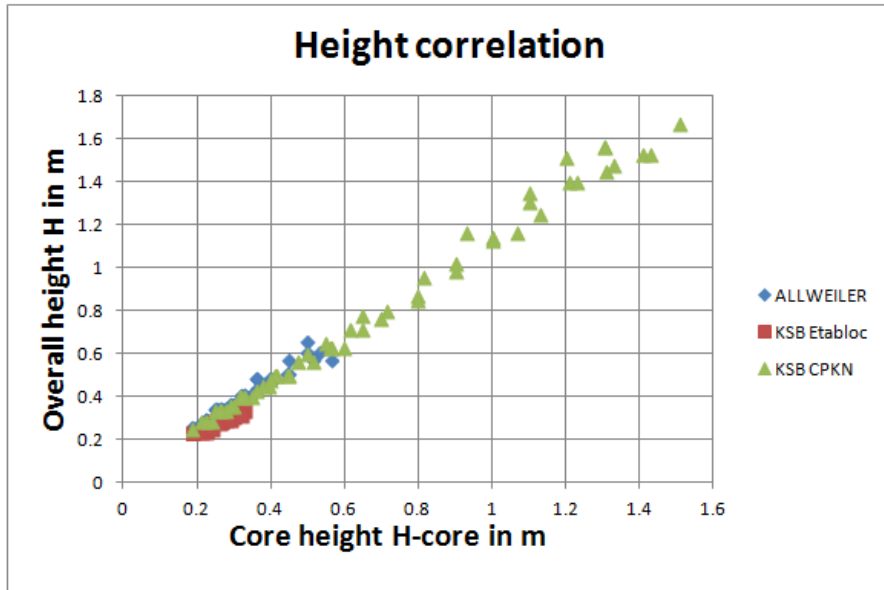


Figure 6.11a Correlation of actual height with theoretical core width for centrifugal pumps

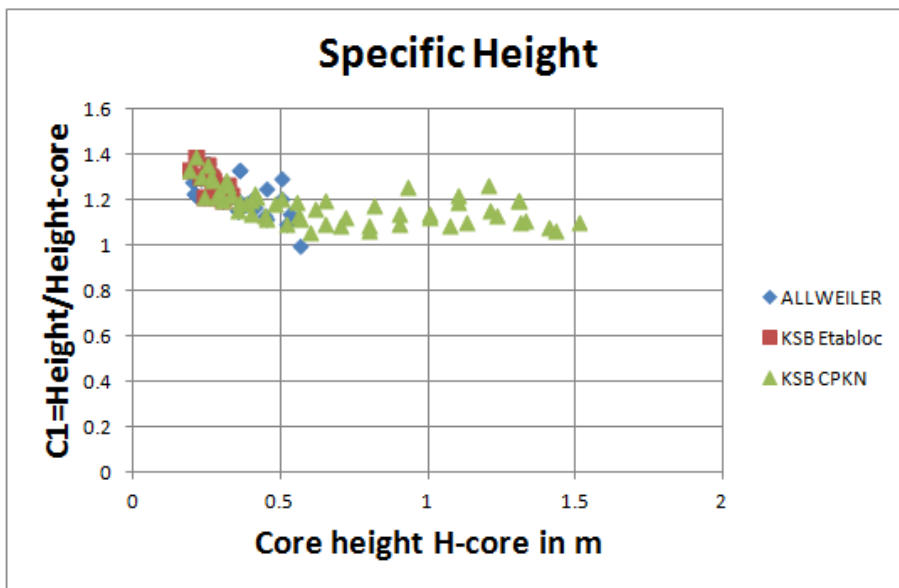


Figure 6.11b Correlation of specific height with theoretical core width for centrifugal pumps

As shown in Figure 6.11a, height value correlates linearly as well. The range of the specific height ratio is in the range of 1-1.4 read from Figure 6.11b.

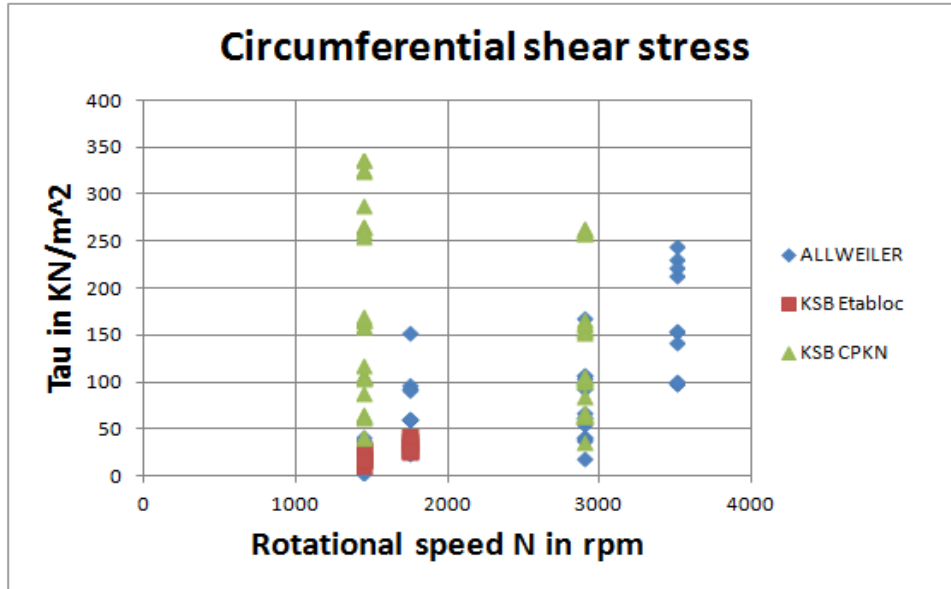
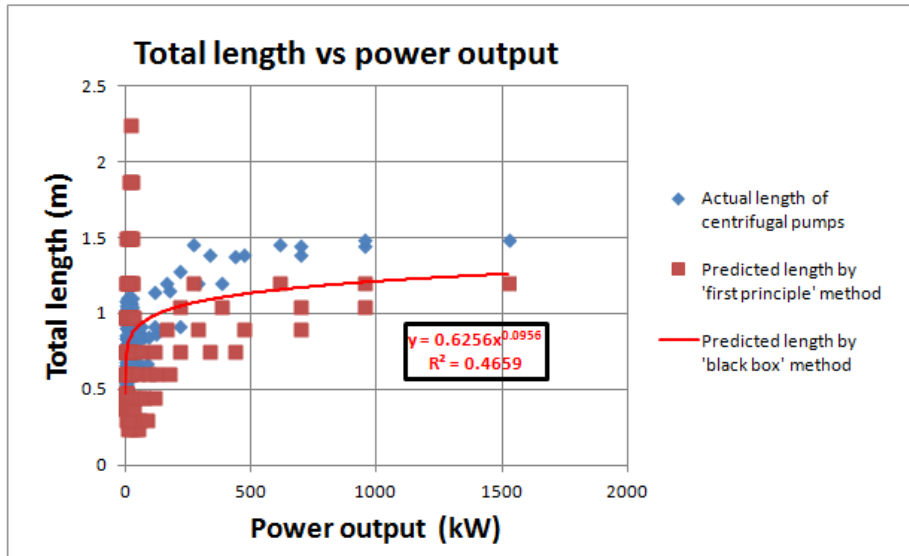


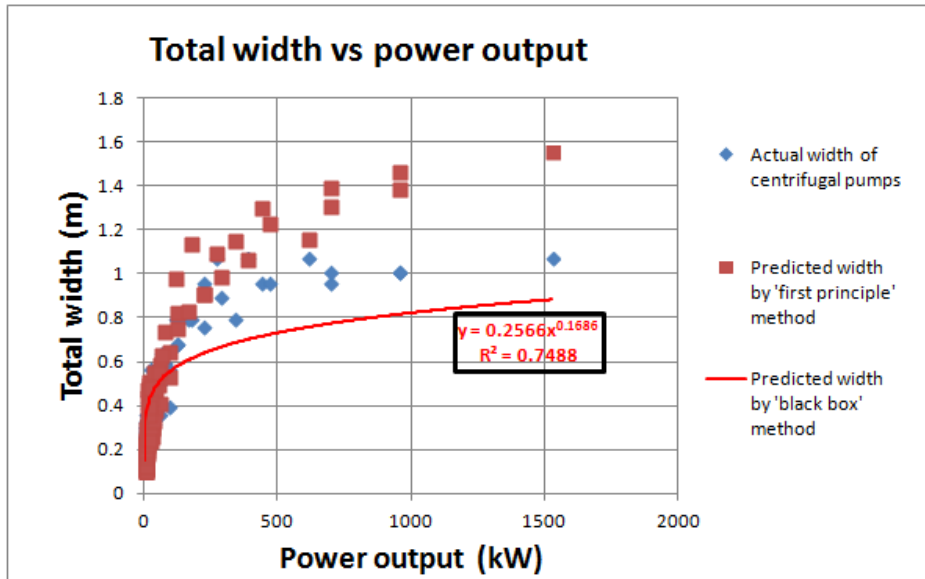
Figure 6.12 Range of the circumferential shear stress for centrifugal pumps

Figure 6.12 gives an overview of the circumferential shear stress specified by the rotational speed of the impeller in rpm. It can be seen in the figure, the value of the rotational speed of the centrifugal is specified which are 1450rpm, 1750rpm, 2900rpm and 3500rpm separately. That is due to the certain types of the installed electric motor driving the rotating impeller. Based on the given manufacturer data, the range of this 'main parameter' is from 0.5 kN/m<sup>2</sup> to about 350 kN/m<sup>2</sup>.



**Figure 6.13 Predicted length by ‘black box’ method and ‘first principle’ method against the actual length of centrifugal pumps**

The Figure 6.13 shows the predicted length of centrifugal pumps produced by ‘first principle’ model (red plots) and ‘black box’ model (red trend-line) separately. For ‘first principle’ model the variables are the circumferential shear stress, linear constant  $A_1$  and the discharge velocity of the fluid ( $V_{\text{discharge}}$ ). The value of these variables is set in advance which are  $80 \text{ kN/m}^2$ , 20 and 5m/s separately. The rule of the variable setting is according to the range of the parameter and the available data in the built database. It can be seen in the figure, the deviations between blue plots and red plots still exist which are mainly caused by the deviation of the variable settings compared with the actually variable values. Again, the deviations between the red trend-line and the blue plots are difficult to be clear.



**Figure 6.14 Predicted width by 'black box' method and 'first principle' method against the actual width of centrifugal pumps**

According to the range of the linear constant  $B_1$  shown in Figure 6.10b, the value of  $B_1$  is set 0.8. The other two variables are the same as the length prediction. Since the predicted mean shear stress and discharge velocity are different from the actual value, the deviation appears. In our model, the variables are predicted roughly, so the deviation is large. In practice, the shear stress and discharge velocity are influenced by power output, flow rate, etc and could be evaluated according to the database in the 'first principle' model with different values.

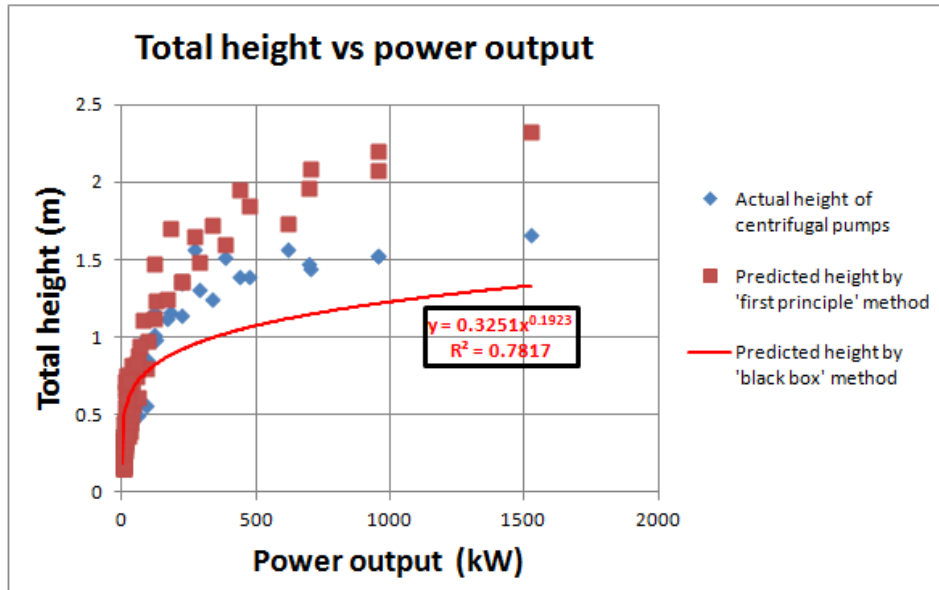


**Figure 6.15 Predicted height by 'black box' method and 'first principle' method against the actual height of centrifugal pumps**

It can be seen in Figure 6.15, the situation of the height results is similar with the predicted width dimension. The linear constant value  $C_1$  is chosen a typical value 1.2 and other variables are the same with that of length and width.

## 6.7. Summary

In this chapter, the 'first principle' model successfully applied to centrifugal pumps. In the model, the impeller and volute are selected as the primary and secondary element separately. The model of sizing impeller, the author proposed two methods to express the dimension of the impeller. The first method is based on the design of the impeller as shown in equation (6.19), using the increased head and flow rate to indicate the dimension of the impeller. The other method of evaluating the impeller's dimension is a common way, depending on the power output and main parameter as stated in equations (6.20) and (6.21). The performance of head, flow rate and power output are all essential to be considered when marine engineers select or size the centrifugal pumps. Therefore, the author combined these two methods together into the model

for sizing the primary element. Then the dimension of secondary element (volute) was evaluated through geometrical analysis base on the dimension of the primary element. After that, the results of the manufacturer data implementation showed the linear relationship between core dimension and overall dimension of the machine. Since the electric machine is mounted on the back of the volute which influences the results of the length correlation, the future work would probably combine the 'electric model' into the model to eliminate the length disturbance. Ultimately, the comparison between the 'first principle' model and 'black box' model of centrifugal pumps are made. From the generated results by both methods it can be concluded that compared with 'black box' method, the 'first principle' model is more flexible and have a higher degree of fidelity. The deviation between the predicted dimension and actual dimension could be analyzed and even reduced by manipulating the value of specific variables in the model.

# 7. Case Study

---

In the previous chapters, the 'first principle' sizing model has been applied to shell and tube heat exchangers, plate heat exchangers and centrifugal pumps. With the model of diesel engines, electric machines and gearboxes built by *Stapersma* and *de Vos*, this dimension prediction model based on first principles approach has already been applied to six primary marine equipment on board. In this chapter, author will check whether these models would be utilized in real cases for dimension prediction. The case study is only about verifying the applicability of the new approach in marine industry practice. There is no comparison between the 'black box' method and 'first principle' method (that has been discussed in Section 4.6, 5.5 and 6.6). The selected vessels for case study are a tug vessel and an FPSO vessel. In the following part, the dimension prediction model would apply to the propulsion system for the TUG vessel and the auxiliary system for the FPSO vessel separately.

## 7.1. Propulsion system of the 'BERNARDUS' tug vessel

The "BERNARDUS" vessel is a harbor tug vessel built by Damen shipyard. The drawing of the vessel is shown in Figure 7.1. In this case study, the author will apply the dimension prediction model to the propulsion system of this vessel. The relevant information of the propulsion system is provided in Table 7-1. More detailed information and general arrangement drawing of the tug vessel is given in Appendix D.



Figure 7.1 Damen ASD Tug Vessel “BERNARDUS” Source: online Damen ASD Tug

Table 7-1 Technical information of the “BERNARDUS” propulsion system

<b>GENERAL</b>	
Yard Number	512319
Delivery Date	May 2014
Basic Functions	Towing, mooring and fire-fighting operations
Classification	Lloyd's Register
Flag	Dutch
Owner	Sleepdienst B.Iskes&ZN B.V.
<b>DIMENSIONS</b>	
Length O.A.	28.67 m
Beam O.A.	10.43 m
Depth At Sides	4.38 m
Draught Aft	5.15 m
Displacement(Approx)	604 ton
<b>PROPULSION SYSTEM</b>	
Main Diesel Engines	2*MTU 16V4000M63R
Total Diesel Power	3680bkw(4935bhp)at 1600rpm
Propulsion Gen Set	1*MTU 12V 2000M41B, 800kVA,440V-60Hz
Exhaust Gas Treatment	DOC+DPF+SCR system, IMO Tier compliant
Battery Packs	2* 120 kWh
Main Electric Engines	2* ABB M3LP450/2* 230 bkW
Azimuth Thrusters	2* Rolls Royce US 205
Propeller Diameter	2400 mm
Forced Ventilation	55.00 m3/hr

From Table 7-1, we got the main engine and the propulsion generation set are both diesel engines. The target equipment needs to be studied for dimension prediction in this case are two main diesel engines, one diesel engine for propulsion generation and two main electric machines. The actual dimension of the equipment could be evaluated from the arrangement drawings (in Appendix D) or from the website of the machinery supplier. It should be emphasized here again that the aim of the case study is about whether this new dimension prediction model works in early ship design stage rather than the accuracy degree of the evaluated dimension. What's more, according to the approach, the value of the fitting ratio between the core and the overall dimension and the 'main parameter' are not fixed value but in the confined range. Therefore, it is reasonable to accept some degree of the deviation between the predicted dimension by our model and the actual dimension of the machine. In other words, the tolerant range of the dimension evaluation is in meter-level but not in centimeter-level.

Based on the process of dimension prediction methodology, the input data (e.g. power output, mean pressure, the number of cylinders, etc) and the predicted dimension of the main diesel engine and propulsion generation diesel engine are provided in Table 7-2 and Table 7-3. Since the range of the main parameter mean pressure is in range of 20-30 bar, in this case study we select 23 bar for evaluation. And the results of the predicted dimension and actual dimension of these two diesel engines are compared in Table 7-4.

**Table 7-2 Result of the predicted dimension of the main engine**

<b>Main Engine</b>		
<b>MTU 16VA400M63R</b>		
Construction type	V type	-
Power output	1840	kW
Mean pressure	23	bar
Mean piston speed	9,5	m/s
Number of cylinders	16	-
Shape factor	1,25	-
Diameter of the cylinder	0,16	m
Length of the core element	1,31	m
Width of the core element	0,45	m
Height of the core element	0,41	m
Fitting factor of length	2,4	-
Fitting factor of width	3,5	-
Fitting factor of height	5	-
Predicted overall length	3,1	m
Predicted overall width	1,6	m
Predicted overall height	2,0	m

**Table 7-3 Result of the predicted dimension of propulsion generation engine**

<b>Propulsion Generation Set DE</b>		
<b>MTU 12V 2000 M41B</b>		
Construction type	V type	-
Power output	695	kW
Mean pressure	23	bar
Mean piston speed	12	m/s
Number of cylinders	12	-
Shape factor	2,35	-
Diameter of the cylinder	0,10	m
Length of the core element	0,62	m
Width of the core element	0,44	m
Height of the core element	0,45	m
Fitting factor of length	2,4	-
Fitting factor of width	3,5	-
Fitting factor of height	5	-
Predicted overall length	1,5	m
Predicted overall width	1,6	m
Predicted overall height	2,2	m

**Table 7-4 Comparison between the predicted dimension and real dimension of diesel engine**

<b>MTU 16VA400M64R</b>	Length (m)	Width (m)	Height (m)
Predicted dimension	3,1	1,6	2
Real dimension	3	1,8	2,1
<b>MTU 12V 2000 M41B</b>	Length (m)	Width (m)	Height (m)
Predicted dimension	1,5	1,5	2,2
Real dimension	1,4	1,6	2

After implementation the data of the diesel engine, the results are shown in Table 7-4. From Table 7-4, it can be seen that the deviations between the predicted dimension and the actual dimension of the diesel engine are in meter-level which are acceptable. The results also prove the dimension prediction model of the diesel engine is effective in practice at the preliminary design stage.

The dimension results of the ABB electric machine is shown as well in Table 7-5 and 7-6 below:

**Table 7-5 Result of the predicted dimension of ABB electric machine**

<b>Electric machine</b>		
<b>ABB M3LP450</b>		
Power output	230	kW
Mean stress force	35	kN/m <sup>2</sup>
Rotational speed	1000	rpm
Shape factor	2,6	-
Diameter of the rotor	0,249	m
Length of the core element	1,94	m
Width of the core element	0,452	m
Heith of the core element	0,452	m
Fitting factor of length	3	-
Fitting factor of width	1,5	-
Fitting factor of height	1,6	-
Predicted overall length	1,94	m
Predicted overall width	0,7	m
Predicted overall height	0,72	m

**Table 7-6 Comparison between the predicted dimension and real dimension of ABB  
electric machine**

<u>ABB M3LP451</u>	Length (m)	Width (m)	Height (m)
Predicted dimension	1,9	0,7	0,7
Real dimension	2,1	1	1

From the results of the predicted dimension of the electric machine using the ‘first principle’ model, it can be seen that the deviation of the predicted result is also in the tolerant range. In other words, it is rational to apply the model in the preliminary ship design stage.

In this case study, the author successfully applied the dimension prediction model based on first principles to the equipment (diesel engine, electric machine) in the propulsion system of Damen ASD Tug vessel. In the next section, the dimension prediction model will be checked about whether it could be utilized for sizing the equipment (shell and tube heat exchanger, plate heat exchanger and centrifugal pump) in the auxiliary marine system of a vessel.

## **7.2. Auxiliary system of the ‘PETROJARL 1’ FPSO vessel**

TEEKAY Petrojarl Production AS is proposing its FPSO Petrojarl 1 to Queiroz Galvao in Brazil for a lease term of 5 years on the Atlanta Field. Before mobilization to the Atlanta Field, the FPSO Petrojarl 1 (Figure 7.2) must undergo various works to make it suitable for the intended operation. The modification work of the vessel is conducted in both Damen shipyard and Iv Groep marine company.

The heating devices utilized for cargo oil heating are six shell and tube heat exchangers for each cargo tank. The capacity of the current deck heat exchanger is influenced by the physical property of the Atlanta crude oil. Due to the increased viscosity, in comparison with the oil at the Glitne Field, the flow pattern of the oil through the deck heater is different than for which they were designed. The Reynolds number is much lower and indicates a laminar flow. This has a negative effect on the heat transfer. Also the flow rate through the heat exchanger, at equal pressure difference over the heater, will be reduced. Both effects reduce the capacity of the current deck heaters when used to heat up the Atlanta crude oil. See the Table 7-7 below:

**Table 7-7 Heating capacity of the shell and tube heat exchangers at Glitne Field and Atlanta Field**

Cargo Tank Heater	Capacity old situation (Glitne Field) [kW]	Cargo oil flow through the deck heater [m <sup>3</sup> /hr]	Heating area [m <sup>2</sup> ]	Capacity new situation ( Atlanta Field ) [kW]	Cargo oil through the deck heater [m <sup>3</sup> /hr]
1	617,2	115	63	380	69,7
2	664,2	115	68	410	75,2
3	797	115	80	482	88,5
4	783,1	115	79	476	87,4
5	779,6	115	80	482	88,5
6	607,9	115	62	373	68,5



**Figure 7.2 FPSO 'Petrojarl 1' owned by Teekay company**

The hot fluid for heating crude oil within the shell and tube heat exchanger is steam generated by two boilers with constant 158°C temperature. The crude oil within the cargo tank should be heated to 65°C. Based on the heat capacity and flow rate of the crude oil of the old situation in Table 7-7, the dimensions of the six shell and tube heat

exchangers could be evaluated by the dimension prediction model. Some presumptions are made in advance. The scenario is set by the author is in early ship design stage, a 'meter-level' evaluation is efficient for dimension prediction. Therefore, the 'main parameter' overall heat transfer is evaluated by the 'Approach 1' input with the typical value in a confined range. Since the range of the overall heat transfer coefficient is still wide, as shown in Appendix B, the evaluated value should also be integrated the value of the mass flow and other factors when selecting the typical value. Furthermore, the author also investigated the database as a reference. The value of the 'main parameter' overall heat transfer coefficient is set  $97 \text{ W/m}^2\text{°C}$  in this case. Besides that, the linear constant  $A_1$ ,  $B_1$  and  $C_1$  are set 1.3, 1.3 and 1.4 separately which are set according to the evaluated range discussed in Chapter 4. After implementation with the model, the results of the predicted dimension of the shell and tube heat exchangers and the actual dimension of the heat exchanger supplied by the Iv Nevesbu company is shown in Table 7-8 below. The detailed calculation data and the technical drawing of six shell and tube heat exchangers are provided in Appendix C and Appendix D.

**Table 7-8 Comparison between the predicted dimension and real dimension of shell and tube heat exchangers**

<b>Shell and tube heat exchanger</b>			
<b>No.1</b>	Length (m)	Width (m)	Height (m)
Predicted dimension	2,6	0,8	0,9
Real dimension	3,1	0,9	0,9
<b>No.2</b>	Length (m)	Width (m)	Height (m)
Predicted dimension	3,2	0,8	0,9
Real dimension	3,3	0,9	0,9
<b>No.3</b>	Length (m)	Width (m)	Height (m)
Predicted dimension	3,5	0,8	0,9
Real dimension	3,7	0,9	0,9
<b>No.4</b>	Length (m)	Width (m)	Height (m)
Predicted dimension	3,4	0,8	0,9
Real dimension	3,6	0,9	0,9
<b>No.5</b>	Length (m)	Width (m)	Height (m)
Predicted dimension	3,6	0,8	0,9
Real dimension	3,7	0,9	0,9
<b>No.6</b>	Length (m)	Width (m)	Height (m)
Predicted dimension	2,7	0,8	0,9
Real dimension	3	0,9	0,9

The results shown in Table 7-8 prove the applicability of the dimension prediction model based on the first principles again. The deviation basically caused by the selected fitting factor and the evaluated overall heat transfer coefficient which are both evaluated in a certain range but not a certain value.

The pumps delivering the crude oil up to the deck shell and tube heat exchangers are six identical centrifugal pumps. The available data of the centrifugal pumps are like

power output, flow rate, head etc which usually required by ship owners or designed by marine engineers. Also there are some evaluated data (shear stress, tangential velocity of the impeller, linear constant value). Here the 'main parameter' shear stress is evaluated from the researched range. Since the range is still wide, the author relates this to the database and search a typical value which also match the given power output and flow rate etc. At last, the value of the shear stress is set 31 kN/m<sup>2</sup>. Finally, the predicted dimension of the centrifugal pump based on the first principle is given below:

**Table 7-9 Result of the predicted dimension of the centrifugal pump**

<b>Centrifugal pump</b>		
Fluid	<i>Cargo oil</i>	
Power output	4	kW
Flow rate	115	m <sup>3</sup> /hr
Height	13,5	m
Rotational speed	1450	rpm
Tangential velocity of the impeller	22	m/s
Mean stress force	31	kN/m <sup>2</sup>
Diameter of impeller	0,29	m
Thickness of volute	0,049	m
Diameter of Volute	0,388	m
Length of the core element	0,05	m
Width of the core element	0,39	m
Height of the core element	0,39	m
Fitting factor of length	15	-
Fitting factor of width	0,9	-
Fitting factor of height	1,2	-
Predicted overall length	0,74	m
Predicted overall width	0,35	m
Predicted overall height	0,47	m

Due to the information of the 'Petrojarl' FPSO is limited in hand, the actual dimension of the centrifugal pump is not available. However, it can be seen from the table above, the predicted dimension of the centrifugal pump could be regarded locating in the 'safe zone' according to the database from manufacturer collected by the author.

As illustrated before, the heat capacity of the deck shell and tube heat exchangers reduces due to the changing of the crude oil property from Glitne Field to Atlanta Field. At the new situation, the deck shell and tube heat exchangers are not able to maintain the temperature of the crude oil at 65°C within the cargo tank. In order to increase the heat capacity of the cargo oil heating system, one of the solutions is generated that replacing the six shell and tube heat exchangers by six plate heat exchangers with high heat capacity. In order to be capable for future different working condition, the designed heat capacity of the plate heat exchanger is set twice of shell and tube heat exchangers at old situation shown in Table 7-7. The overall heat transfer coefficient is also evaluated by 'Approach 1' which is 120 W/m<sup>2</sup>°C. Then the shape factor 'λ' is set 2.5 which is in the range of 2-3. After implementing the designed data (heat capacity, overall heat transfer coefficient, shape factor, etc) into the model, the dimension of the plate heat exchangers could be calculated. The detailed evaluated form of these six plate heat exchangers are provided in Appendix C. The final results of the dimensions are shown below:

**Table 7-10 Results of the predicted dimension of the plate heat exchangers**

<b><u>Plate heat exchanger</u></b>			
<b>No.1</b>	Length (m)	Width (m)	Height (m)
Predicted dimension	1,2	0,8	1,6
<b>No.2</b>	Length (m)	Width (m)	Height (m)
Predicted dimension	1,2	0,9	1,8
<b>No.3</b>	Length (m)	Width (m)	Height (m)
Predicted dimension	1,4	0,9	1,8
<b>No.4</b>	Length (m)	Width (m)	Height (m)
Predicted dimension	1,4	0,9	1,8
<b>No.5</b>	Length (m)	Width (m)	Height (m)
Predicted dimension	1,4	0,9	1,7
<b>No.6</b>	Length (m)	Width (m)	Height (m)
Predicted dimension	1,4	0,8	1,5

As we can see from the table above, the predicted dimension of the plate heat exchangers is all in normal size. If this solution is adopted, the engineer could easily order the plate heat exchangers from suppliers based on the predicted dimension.

### **7.3. Conclusion**

In this chapter, the author successfully applied the ‘first principle’ dimension prediction model to real cases and the deviation is in meter-level which is acceptable in preliminary ship design stage. It is, therefore, reasonable thought the ‘first principle’ method is generally applicable. Since the approach of the model is based on the physical principle of the machine, that would be beneficial for engineers to design and predict the dimension of the marine components according to the power output or heat capacity.

# 8. Conclusion and Recommendation

---

## 8.1. Conclusions

This section considers whether the raised questions and research objectives in Chapter 1 are actually met. In the introduction of this thesis, there are two questions were raised. The first one is:

*What exactly are the differences between the 'black box' method and the 'first principle' method and is this 'first principle' method an improvement?*

In Chapter 2, the literature review concludes weaknesses of the 'black box' method. The 'black box' method, as its name implies, is like a 'black box': the generated mathematical relationship by regression analysis is hard, if not impossible, to understand from a physical perspective. This fact in itself may not be a problem as long as the implied risks are accepted. The implied risks as concluded in Chapter 3 are that reasons for low accuracy may not be understood and, perhaps more importantly, the fact that a certain fit-function has a low accuracy may be lost when the function is adopted by someone else.

Compared with that, the 'first principle' method is a physical-based method which demands engineers that use it to understand the basic working principles of machines. The mathematical expressions of the model relate to the working principle of the machine, thereby mitigating the risks for not understanding low accuracy of the dimension prediction models when this occurs. As the comparison made in Chapters 4, 5, 6, it is difficult to explain the dimension deviation between the predicted dimension and actual dimension by 'black box' method. However, the reason of the dimension deviation through 'first principle' method is clear, that is caused by the variables (e.g. main parameters, constant value of the linear relationship, etc) in the

model. Thus, with the 'first principle' method low accuracy may still be an issue, but the fact that variables that have physical meaning have to be estimated means one can have more confidence in the estimates and/or can know whether the estimate is reasonable. Furthermore, by manipulating the value of variables could also reduce the dimension deviation. Therefore, compared with 'black box' method, the 'first principle' method offers a higher degree of fidelity and flexibility. From that point of view, one could argue that the 'first principle' method is an improvement to the 'black box' method.

The second question: *Is it also possible to apply this 'first principle' method to other marine components?*

As stated before, this new sizing method, proposed by *Stapersma* and *de Vos*, has already applied to diesel engines, electric machines and gearboxes. One of the main objectives of this thesis is "*Apply the method to making dimension prediction model for new components: shell and tube heat exchangers, plate heat exchangers and centrifugal pumps*". The results of Chapter 4, 5 and 6 do prove the applicability of the sizing model to these three target marine components. Plus the previous three applied marine components (diesel engines, electric machines and gearboxes), there are already six primary equipment's dimensions have been predicted using this first-principle sizing model. That could say this new sizing method is generally applicable as it seems to be now.

## **8.2. Recommendations for future work**

The future work could be summarized into two parts. The first one is continuing to apply the 'first principle' sizing method to more ship system components (gas turbine, steam turbine, battery, compressor, etc) to assess whether it is even more generally applicable.

The second part is improving the built 'first principle' model. Gathering more manufacturer information of electric machines, diesel engines, gearboxes, heat exchangers and centrifugal pumps is still necessary. For instance, in the second case study, the actual dimension data of the centrifugal pump is unavailable for now. That could be collected to check the applicability of the model in the future. Through expanding the database of the model could gain more accurate range of main parameters and regression constant which both have the influence on the overall predicted machine dimension. Besides that, combining 'first principle' models into one model is also needs to be done which could increase the accuracy of the results. For example, the centrifugal pump actually is combined by a pump and an electric motor, some type of electric machine usually is mounted a heat exchanger above, a diesel engine is usually added a turbo charger. The added machines for now are still regarded as the disturbances of the model which reflect in the linear constant value. The future work would combine the 'first principle' models together and that would probably increase the accuracy of the final predicted dimension of the machines. Or at the very least inherently show the reasons for low accuracy if it persists.

# References

---

1. Stapersma , D. and P. de Vos. *Dimension prediction models of ship system components based on first principles*. in *International Marine Design Conference (IMDC)*. 2015. Tokyo.
2. Woud, H.K. and D. Stapersma, *Design of Propulsion and Electric Power Generation Systems*. 2002: IMarEST, Institute of Marine Engineering, Science and Technology.
3. van Oers, B.J., *A Packing Approach for the Early Stage Design of Service Vessels*. 2011: VSSD.
4. Andrews, D. and C. Dicks, *The building block design methodology applied to advanced naval ship design*, in *Proceedings of the 8th International Marine Design Conference*. 1997: Newcastle, United Kingdom. p. 3-19.
5. Van der Nat, C., *A Knowledge-Based Concept Exploration Model For Submarine Design*. 1999, Delft University of Technology.
6. Piperakis, A.S., D. Andrews, and R. Pawling, *An Integrated Approach to Naval Ship Survivability in Preliminary Ship Design*. 2013, University College London (University of London).
7. Andrews, D., A. Greig, and R. Pawling, *The Implications of an All Electric Ship Approach on the Configuration of a Warship*, in *I.Mar.E.S.T. 7th International Naval Engineering Conference*. 2004: Amsterdam.
8. Hyde, K.M. and D.J. Andrews, *CONDES, A preliminary warship design tool to aid customer decision making*. 1992: London.
9. Guida, G. and M. Zanella, *Knowledge-based design using the multi-modeling approach*, in *Second generation expert systems*. 1993, Springer. p. 174-208.
10. Reed, M.R., *Ship synthesis model for naval surface ship*, in *Naval Architecture and Marine Engineering*. 1976: Massachusetts Institute of Technology.
11. Harries, S., *Parametric Design and Hydrodynamic Optimization of Ship Hull Forms*. 1998: Technical University Berlin.
12. Smith, N., W. Hills, and G. Cleland, *A layout design system for complex made-to-order products*. *Journal of Engineering Design*, 1996. **7**(4): p. 363-375.
13. van Es, G.F., *Designing and evaluating propulsion concepts of surface combatants*, in *Faculty Mechanical, Maritime and Materials Engineering*. 2011, Delft University of Technology.
14. Van Dijk, e.a. *Components and Parameters*. report WP 030 and 040 1998; All Electric Ship (AES) project].
15. Frouws, J.C., *"AES Decision model"*. 2008: Delft University of Technology.
16. Stapersma , D., *Performance analysis and turbocharging*. Diesel Engines lecture notes. Vol. 1. 2010, TU Delft & NLDA.
17. Van Es, G.F. and P.d. Vos. *System design as a decisive step in engineering naval capability*. in *International Naval Engineering Conference*. 2012.

Edinburgh

18. Woud, H.K. and D. Stapersma, *Design of Auxiliary Systems, Shafting and Flexible Mounting*. To be published.
19. Thulukkanam, K., *Heat Exchanger Design Handbook*. 2000: CRC Press.
20. Serth, R.W., *Process Heat Transfer Principles and Application*. 2007, Kingsville, Texas, USA.
21. TEMA, *Standards of the Tubular Exchanger Manufacturers Association*. 2007: Tubular Exchanger Manufacturers Association.
22. Kern, D.Q., *Process Heat Transfer*. 1950: McGraw-Hill.
23. Rehman, U.U., *Heat Transfer Optimization of Shell-and-Tube Heat Exchanger through CFD Studies*, in *Department of Chemical and Biological Engineering*. 2011, Chalmers University of Technology: Goteborg, Sweden.
24. Thome, J.R., *Engineering data book III*. 2004.
25. Kakac, S., H. Liu, and A. Pramuanjaroenkij, *Heat exchangers: selection, rating, and thermal design*. 2012: CRC press.
26. Muley, A. and R. Manglik, *Experimental study of turbulent flow heat transfer and pressure drop in a plate heat exchanger with chevron plates*. *Journal of heat transfer*, 1999. **121**(1): p. 110-117.
27. Focke, W., J. Zachariades, and I. Olivier, *The effect of the corrugation inclination angle on the thermohydraulic performance of plate heat exchangers*. *International Journal of Heat and Mass Transfer*, 1985. **28**(8): p. 1469-1479.
28. Vishal R., N. and V.K. Matawala, *Experimental Investigation of single phase Chevron Type Gasket Plate Heat Exchanger*. *International Journal of Engineering and Advanced Technology*, April, 2013. **2**.
29. Shah, R.K., E.C. Subbarao, and R.A. Mashelkar, *Heat Transfer Equipment Design*. 1988: Taylor & Francis.
30. Bachus, L. and A. Custodio, *Know and understand centrifugal pumps*. 2003: Elsevier.
31. Lobanoff, V.S. and R.R. Ross, *Centrifugal Pumps: Design and Application: Design and Application*. 2013: Elsevier.
32. Wu, K.-H., B.-J. Lin, and C.-I. Hung, *Novel design of centrifugal pump impellers using generated machining method and CFD*. *Engineering Applications of Computational Fluid Mechanics*, 2008. **2**(2): p. 195-207.
33. Wen-Guang, L., *Inverse design of impeller blade of centrifugal pump with a singularity method*. *Jordan Journal of Mechanical and Industrial Engineering*, 2011. **5**: p. 119-128.
34. Westra, R.W., *Inverse-design and optimization methods for centrifugal pump impellers*. 2008: University of Twente.
35. Stepanoff, A.J., *Centrifugal and Axial Flow Pumps: Theory, Design, and Application*. 1957: Krieger Publishing Company.
36. Van den Braembussche, R., *Flow and loss mechanisms in volutes of*

- centrifugal pumps*. 2006, DTIC Document: Belguim.
37. Tiwari, N. and D. Kumar, *Analytical and Experimental Investigation of Centrifugal Pump Performance*, in *Asian International Conference on Science, Engineering & Technology*. 2015.
  38. Dick, E., et al., *Performance prediction of centrifugal pumps with CFD-tools*. *Task quarterly*, 2001. **5**: p. 579-594.
  39. Mukherjee, R., *Effectively design shell-and-tube heat exchangers*. *Chemical Engineering Progress*, 1998. **94**(2): p. 21-37.
  40. Hadidi, A., M. Hadidi, and A. Nazari, *A new design approach for shell-and-tube heat exchangers using imperialist competitive algorithm (ICA) from economic point of view*. *Energy Conversion and Management*, 2013. **67**: p. 66-74.
  41. Peters, M.S., et al., *Plant design and economics for chemical engineers*. Vol. 4. 1968: McGraw-Hill New York.
  42. Sinnott, R. and G. Towler, *Chemical engineering design: SI Edition*. 2009, Oxford: Butterworth-Heinemann.
  43. Huang, J., *Performance analysis of plate heat exchanger used as refrigerant evaporators*, in *University of the Witwatersrand*. 2010, University of the Witwatersrand: Johannesburg.
  44. Jogi Nikhil, G., *Heat Transfer Analysis of Corrugated Plate Heat Exchanger of Different Plate Geometry: A Review*. *International Journal of Emerging Technology and Advanced Engineering*, 2012.
  45. FUNKE. *Plate heat exchanger Series FP, FP-DW,FP-SW*. May of 2015]; Available from: <http://www.funke.de/>.
  46. JAMES R. , L., *Asymmetric Plate Heat Exchangers*. 2014: BATAVIA, NY.
  47. Fernandes, C.S., et al., *Friction factors of power-law fluids in chevron-type plate heat exchangers*. *Journal of Food Engineering*, 2008. **89**(4): p. 441-447.

# Nomenclature

---

A	Heat transfer area	$m^2$
$A_2$	Circumferential ring area of impeller channel at the exit side	$m^2$
$A_c$	Channel flow area of plate heat exchanger	$m^2$
$A_d$	Developed area of a plate	$m^2$
$A_p$	Projected area of a plate	$m^2$
$A_R$	Circumferential area of the rotor	$m^2$
$A_P$	Circumferential area of the pinion	$m^2$
$A_s$	Shell cross-sectional area	$m^2$
$A_t$	Total cross-sectional area of tubes of the tube sheet	$m^2$
$a_s$	Shell side cross flow area	$m^2$
B	Baffle spacing of the shell and tube heat exchanger	m
b	Mean channel spacing of a plate	m
$b_2$	Width of the channel of impeller	m
C	Spacing between tubes	m
$C_1$	Tube layout parameter	-
$C_h$	Correlation factor of overall heat transfer coefficient	-
$C_p$	Specific heat of the fluid	J/kg K
$c_m$	Translational speed of piston	m/s
D	Shell diameter	m
D	Impeller diameter	m
$D_1$	Diameter of the impeller's entry	m
$D_2$	Diameter of the impeller's exit	m
$D_{ctl}$	Centerline tube limit diameter	m
$D_{discharge}$	Diameter of the cross-sectional area at the discharge part	m
$D_e$	Equivalent diameter	m
$D_P$	Diameter of the pinion	m

$D_p$	Port diameter of a plate	m
$D_R$	Diameter of the rotor	m
$D_S$	Diameter of the stator	m
$D_W$	Diameter of the wheel	m
$d_{in}$	Inside diameter of the tube	m
$d_o$	Outside diameter of the tube	m
EMF	ElectroMotive Force	N
$F_{piston}$	Force on the piston	N
$G_s$	Mass flow rate	kg/m <sup>2</sup> s
H	Head of centrifugal pump	m
HF	Hydraulic force acting on the impeller	N
$H_A$	Absolute pressure on the surface of the liquid in the supply tank	m
$H_{core}$	Height of the core of a machine	m
HF	Friction loss in meters	m
$H_p$	The height of projected area of a plate	m
$H_s$	Total suction head or lift in centrifugal pump	m
$H_t$	Total length of a plate	m
$H_v$	Vertical distance of centre point of ports of a plate	m
$H_{vp}$	Vapor pressure in meters	m
H <sub>z</sub>	Vertical distance pressure in meters	m
$h_i$	Tube-side heat transfer coefficient	W/m <sup>2</sup> K
$h_o$	Shell-side heat transfer coefficient	W/m <sup>2</sup> K
$h_c$	Heat transfer coefficient in cold side	W/m <sup>2</sup> K
$h_h$	Heat transfer coefficient in hot side	W/m <sup>2</sup> K
i	Number of cylinders	-
$j_H$	Correction for shell-side heat transfer coefficient	-
k	Numbers of the revolutions per stroke	-
k	Thermal conductivity	W/m K

$L_{\text{shell}}$	Length of a shell	m
$L_{\text{bb}}$	Tube bundle-to-shell clearance	m
$L_{\text{c}}$	Length of the compressed plate pack	m
$L_{\text{core}}$	Length of the core of a machine	m
$L_{\text{R}}$	Length of the rotor	m
$L_{\text{S}}$	Length of the stator	m
$l_{\text{tube}}$	Length of a tube	m
$M$	Torque	N·m
$\dot{m}_{\text{hot}}$	Mass flow of hot fluid	kg/s
$\dot{m}_{\text{cold}}$	Mass flow of cold fluid	kg/s
$\dot{m}_{\text{per}}$	Mass flow per channel of a plate heat exchanger	kg/s
$N_{\text{cp}}$	Number of channel per pass of a plate heat exchanger	-
$N_{\text{ep}}$	Effective number of heat transfer plates	-
$N_{\text{t}}$	Number of tubes in the shell and tube heat exchanger	-
$N_{\text{tp}}$	Total number of heat transfer plates	-
$N_{\text{p}}$	Number of passes of a plate heat exchanger	-
$\text{NPSH}$	Net positive suction head of centrifugal pump	m
$n$	Rotational speed	rps
$P$	Power output	W
$p_{\text{me}}$	Mean pressure	N/m <sup>2</sup>
$p_{\text{PHE}}$	Plate pitch between two plates	m
$Pr$	Prandtl number	-
$P_{\text{t}}$	Tube pitch	m
$P_{\text{w}}$	Wetted surface of plate heat exchanger	m
$\Delta p$	Pressure change of liquid in centrifugal pump	Pa
$Q_{\text{impeller}}$	Volumetric flow rate centrifugal pump	m <sup>3</sup> /hour
$\dot{Q}$	Heat transfer rate of heat exchanger	KJ/s

$R_{f,o}$	Fouling factor for shell-side fluid	$m^2 K/W$
$R_{f,i}$	Fouling factor for tube-side fluid	$m^2 K/W$
Re	Reynolds number	-
$r_2$	Radius of the impeller	m
$S_{STHE}$	'Manufacturer parameter' of shell and tube heat exchanger	-
$T_{cinlet}$	Inlet temperature of cold fluid	K
$T_{hinlet}$	Inlet temperature of hot fluid	K
$T_{coutlet}$	Outlet temperature of cold fluid	K
$T_{houtlet}$	Outlet temperature of hot fluid	K
$\Delta T_m$	Mean temperature difference between hot fluid and cold fluid.	K
TF	Tooth force	N
$T_s$	Thickness of shell wall	m
U	Tangential velocity of impeller	m/s
U	Overall heat transfer coefficient	$W/m^2 K$
V	Fluid's absolute velocity within the impeller	m/s
$V_{discharge}$	Discharge velocity of the fluid in the impeller	m/s
$V_m$	Meridional velocity of fluid in impeller	m/s
$V_p$	Volume of the pinion	$m^3$
$V_R$	Volume of the rotor	$m^3$
$V_u$	Fluid speed at tangential direction of impeller	m/s
W	Relative velocity of the flowing fluid in the impeller	m/s
$W_{core}$	Width of the core of a machine	m
$W_p$	Width between gaskets of a plate	m
$W_t$	Total width of plate	m
$Z_p$	Number of teeth of the pinion	-
$\omega$	Angular velocity	rad/s
$\tau$	Mean shear stress	$N/m^2$
$\lambda$	Shape factor	-

$\mu$	Dynamic viscosity of fluid	$\text{N s/m}^2$
$\phi$	Enlargement factor of a plate	-
$\delta$	Thickness of a plate	m
$\rho$	Density of the fluid	$\text{kg/m}^3$

# Appendix A

---

In this appendix, the 'conference paper' is attached.

## **Dimension prediction models of ship system components based on first principles**

**Douwe Stapersma<sup>1</sup> and Peter de Vos<sup>2</sup>**

### **ABSTRACT**

*In this paper we describe a generic way of sizing main dimensions of primary equipment for marine applications. Contrary to a straight fit through a database the method tries to develop expressions in which, apart from the main specifications in terms of power and speed, the selection of the main machine parameters has an influence on the ultimate overall dimensions of the component. The result is a "rubber" design model that uses in an intelligent way the first principles underlying the design of machines and that can be used in preliminary design of complex maritime objects. The method will be illustrated for components as diverse as electric machines, gearboxes and diesel engines but is thought to be generally applicable.*

### **KEY WORDS**

---

<sup>1</sup> Retired professor of Marine Engineering, Delft University of Technology

<sup>2</sup> Researcher at Delft University of Technology

Dimension prediction (sizing) models; first principles; electric machines; gearboxes; diesel engines;

## INTRODUCTION

The basic idea behind first principle based dimension prediction models of ship system components (i.e. machinery or equipment like engines, motors, pumps, heat exchangers etc.) is that the dimensions of a type of machinery can be estimated by sizing the core of that machine to the required power output using first principles. The core of a machine consists of primary and secondary elements. The size of the primary elements can be determined from the required power output of the machine. The size of the secondary elements can be determined in a next step from the size of the primary elements. Together they determine the size of the core of the machine. In a final step the actual machine dimensions can be predicted from the size of the core using regression analysis.

To give an example for a diesel engine the primary element is the cylinder and indeed there is a first principle relationship between the size of the cylinder and the power output of a diesel engine. The cylinders need to be combined with a crankshaft, which is the secondary element, in order for the engine to work. The core of a diesel engine is therefore the combination of a number of primary elements (cylinders) and a secondary element (crankshaft). Together they determine the size of the core of the engine, which contributes significantly to the size of the overall machine.

In **Figure 1** the process of predicting machine dimensions using first principles based dimension prediction models is summarized in a flowchart.

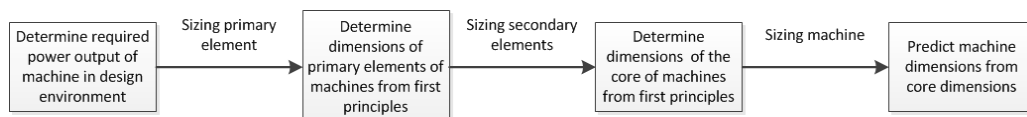


**Figure 1: Process of predicting machine dimensions based on first principles.**

The search for first principles based dimension prediction models of ship system components is part of the PhD research of the second author. The PhD project MOSES CD (Model-based Ship Energy System Conceptual Design) aims to improve the conceptual design of onboard service systems (also known as platform systems or main and auxiliary systems). It consists of three major parts: network modeling for variation of system topology (de Vos, 2014), performance modeling for prediction of system performance and dimensions modeling for prediction of component dimensions. This paper obviously is related to the latter.

This paper is divided into five sections. The first section elaborates on the general process for predicting machine dimensions from required power output using first principles as was already introduced above. The second section describes the first and second step in **Figure 1**, i.e. how the core of three different machines sizes with required power output. The third section discusses the final step of **Figure 1**, i.e. how the three different machines size with their core. The fourth section shows the correlation of the first principles based dimension prediction models with real machines, after which section five concludes the paper.

## **GENERAL PROCESS**

In a ship design environment the first step to finding dimensions of machines is determining their required power output from a load balance or similar. This required power output is usually more or less fixed by the mission and size of the ship, which are of course related. From the required power output the size of the primary elements of machines can be found using first principles (step 1). In this paper we present the direct relationships that exist between the size of the primary elements and the power output of electric machines, gearboxes and diesel engines by deriving them from first principles. This paper focuses on dimension prediction models for these machines only. It is however expected that the methodology as presented here can be used for other ship system components as well. This is however left for future papers.

For diesel engines the primary element (and secondary and core) have already been introduced in the introduction. For an electric machine the primary element is the rotor and

again there is a first principle relationship between the size of the rotor and the power output of an electric machine. The same can be stated for gearboxes for which the pinion proves to be the primary element. These first principle relationships can be applied in a design environment to size the primary elements of the machines, since in a design environment the power output of the machine is determined for maximum load conditions.

Once the size of the primary element is determined in a second step necessary additional elements can be sized as well by a geometric analysis of the construction of the machines. For the electric machine this second step means sizing the stator from the rotor dimensions. For a gearbox this means the wheel is sized from the pinion dimensions and for a diesel engine this means the crankshaft is sized from cylinder dimensions. Together the primary and secondary elements build up the core of the machines whose size is then determined. In a third and final step an estimate can be made for the dimensions of the entire machine on basis of the size of the core of the machine using regression analysis. We will hypothesize that a first order polynomial function exists between the size of the core and the size of the complete machine. This approach to dimension prediction (refer to **Figure 1**) leads to expressions for the dimensions of the machines that have more physical meaning than standard regression analysis based dimension prediction models as normally used in comparative studies; e.g. in the All Electric Ship project in the Netherlands (van Dijk, 1998) and (Frouws, 2005), and also in (van Es et al., 2012). For the diesel engine the procedure was suggested earlier (Stapersma, 1998) but not implemented until now.

Since regression analysis is still necessary on a deeper level to fit the first principle based dimension prediction models to the dimensions of actual machines (by fitting the first order polynomial functions to dimensions data in a machinery database), it is not the objective of this paper to denounce regression analysis based models, but rather to add physical meaning to them. Furthermore this paper contributes to understanding the analogies that exist between the dimensions of apparently completely different machines.

## **SIZING THE CORE OF ELECTRIC MACHINES, GEARBOXES AND DIESEL**

## ENGINES

As discussed the core of the machines consists of primary and secondary elements. In this section we will first focus on sizing primary elements from the required power output, i.e. the first step of the process. Then the second step follows: sizing secondary elements from primary element dimensions. Together they determine the size of the core of the machines.

### *Sizing primary elements*

Start with the basic equation that relates power output to torque and angular speed:

$$P = M \cdot \omega = 2\pi \cdot M \cdot n \quad [1]$$

Where P is power in W (or J/s), M is torque in Nm,  $\omega$  is angular speed in rad/s and n is rotational speed in revolutions per second (rev/s or rps). From a more generalized perspective the torque is the “effort” variable and the rotational speed is the “flow” variable; power is the product of effort and flow irrespective of the energy form that is relevant. The three machines that are discussed here all deliver or transmit rotational mechanical energy, so equation [1] is true for all three machines (electric machine, gearbox and diesel engine).

Now it can be shown that for all three machines the power depends on:

- A characteristic mean shear stress  $\tau$  or mean pressure p in  $\text{N/m}^2$ , which is determined by the manufacturer of the machine taking into account limitations due to material properties of the materials being used. The characteristic shear stress or pressure is related to the torque of the machines.
- A characteristic velocity v or c in m/s that is also determined by the manufacturer on basis of limiting inertial forces and/or wear and tear (i.e. life cycle) considerations. The characteristic velocity is related to the rotational speed of the machines.
- Characteristic dimensions of the primary elements of the machines.

The latter are of course of interest, since the objective of this section is to size the primary elements first. Applying the first two ensures that the expressions for primary element size are based on first principles. To derive these expressions note that the primary elements of the machines are all cylindrical volumes of which the characteristic dimensions are diameter D and length L (see **Figure 2**).

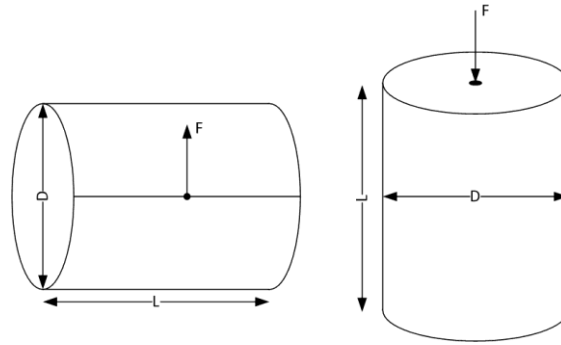


**Figure 2: Cylindrical volumes - left depicting a rotor of an electric machine or pinion/wheel of a gearbox and right depicting a diesel engine cylinder.**

For the electric machine and the gearbox the torque that is delivered or transmitted is determined by the force  $F$  that is acting at the circumference of the cylinder (as depicted at the left in **Figure 2**), i.e. at the radius  $r$  of the cylinder ( $r = D/2$ ). For the electric machine the force  $F$  is the Lorentz force or EMF (ElectroMotive Force) that acts on the current carrying conductors along the side of the rotor as a consequence of the rotating magnetic field from the stator. For the pinion (and wheel) of the gearbox the force  $F$  results from mechanical interaction (action = reaction) between the teeth of pinion and wheel. For the diesel engine the torque that is delivered is determined by the pressure in the cylinder that results in a force  $F$  acting on top of the piston (as depicted at the right in **Figure 2**).

The forces  $F$  that are present in all three machines can be expressed as a mean shear stress or mean pressure in  $\text{N/m}^2$  by dividing the force  $F$  by an area  $A$ . It should be emphasized that it is not the intention to calculate actual shear stresses or pressures present in the machines, but rather characteristic stresses or pressures that will help determine expressions that relate power and size of the machines. This means that the stresses and pressures that will be defined cannot be measured anywhere in the machine during operation even though they do have a relation with actual stresses and pressures. It also means that the area  $A$  can in principle be chosen arbitrarily, yet it is practical to choose the area rationally in order to increase the physical meaning of the model.

For the electric machine the area  $A$  that is chosen is the rotor circumferential area, which is

calculated by  $\pi \cdot D_R \cdot L_R$ , where  $D_R$  is the diameter and  $L_R$  is the length of the rotor in m. Since the rotor contains current carrying conductors all around and the Lorentz force therefore acts all around the rotor it is logical to choose the complete circumferential area. The intensity of the EMF is thus characterized by a mean shear stress that is present everywhere at the rotor side. In fact the stress as defined is sometimes referred to as working force density or average air gap shear stress; amongst others (Hodge et al. 2001) and (Rucker et al., 2005). Again it is emphasized that this is not an actual shear stress, since the latter is not equally distributed over the area, but a means to relate power and dimensions from first principles. Thus for the electric machine:

$$M = EMF \times \frac{D_R}{2} = t_R \times A_R \times \frac{D_R}{2} = \frac{\rho}{2} \times t_R \times D_R^2 \times L_R = 2 \times t_R \times V_R \quad [2]$$

This well-known expression, see a.o. (Kirtley, 2005), shows that there is indeed a first principle relation between torque of the machine and size of the primary element (the rotor) being characterized by its diameter and length. In fact it can be concluded that torque scales with volume. Also any torque can be delivered by a “short and fat” rotor (small  $L_R$ , large  $D_R$ ) or a “long and slender” rotor (large  $L_R$ , small  $D_R$ ).. The length/diameter ratio  $\lambda_R = L_R / D_R$  of the cylinder is a shape factor that characterizes slenderness of the rotor and will be used later on to relate dimensions of the primary element to power output. Clearly the intensity of the force  $F$  characterized by the mean shear stress is a parameter that is determined by the manufacturer of the machine, who will most probably try to push the limits of material properties while maintaining reasonable safety margins in order to deliver an as-compact-as-possible machine. For the gearbox the force  $F$  is a tooth force (TF) that also acts on the circumference of the cylinder, but only on a small part since the force is concentrated on one tooth pair. Therefore the circumferential area is reduced by two times the number of teeth on the pinion  $z_p$ , which means the intensity of the tooth force is characterized as a tooth shear stress that is present on a mean shear area of one tooth at the nominal contact diameter (disregarding the fact that the area at the base will be larger and that at that point there also is bending: again we are not calculating actual stresses but introducing reference stress).

$$M = TF \times \frac{D_p}{2} = t_T \times \frac{A_p}{2 \times z_p} \times \frac{D_p}{2} = \frac{\rho}{4} \times \frac{t_T}{z_p} \times D_p^2 \times L_T = \frac{t_T}{z_p} \times V_p \quad [3]$$

As before torque is a specific shear stress times the primary element volume and the similarity between expressions [2] and [3] is clear, so the gearbox manufacturer can size his primary element in a similar manner as an electric machine manufacturer. A new parameter is the number of teeth that on the pinion is limited to a certain minimum due to curvature and the risk of undercutting the tooth profile.

For diesel engines similar expressions as equations [2] and [3] have been derived in (Klein Woud et al., 2003):

$$M = \frac{1}{8} \times \frac{i}{k} \times p_{me} \times D_B^2 \times L_s = \frac{i}{2\rho \times k} \times p_{me} \times V_s \quad [4]$$

In this expression the mean shear stress as was used in equations [2] and [3] for electric machine and gearbox respectively has been replaced by the mean effective pressure  $p_{me}$  in  $N/m^2$ , which is a well-known performance parameter for marine diesel engines. The reason for this is that the force  $F$  acts on the top of the primary element (piston) instead of at the side of the primary element (rotor for the electric machine and pinion for the gearbox). The term  $i/k$  represents the number of cylinders  $i$  in the engine and the number of revolutions per power stroke ( $k=1$  for 2-stroke and  $k=2$  for 4-stroke engines). This is another difference between diesel engines and the other two machines; the fact that the torque of the machine is the result of a number of primary elements working together intermittently instead of one primary element working continuously. Still, the similarity between expressions [2], [3] and [4] is again apparent and for all three machines it can be concluded that torque scales with volume of the primary elements.

The three expressions [2], [3] and [4] for the “effort” variable torque in expression [1] have been listed in the second row of **Table 1**. In the third row the rotational speed of the machines (flow variable) has been related to a characteristic velocity; tangential velocity at circumference for electric machine and gearbox and mean piston speed for the diesel engine. These velocities are limited by inertial forces or by wear (i.e. life cycle) considerations. They are again “manufacturer” parameters and their values tend to lie in a limited range. All three expressions show that rotational speed is inversely proportional to one of the characteristic dimensions of

the primary elements. This is echoed in the well-known fact that machines with higher rotational speeds are smaller.

In the final row the expressions in the second and third row are combined using equation [1] to arrive at expressions that relate power output to machine specific parameters determined by manufacturers and size of the primary elements. Note that power always is the product of a characteristic area of the element and a “Technology Parameter” (the latter being the product of a characteristic stress or pressure and circumferential or translational speed).

**Table 1: Overview of torque, speed and power relations as function of size and machine specific parameters.**

	Electric Machine	Gearbox	Diesel Engine
Effort	$M = \frac{\pi}{2} \cdot \tau_R \cdot D_R^2 \cdot L_R$	$M_P = \frac{\pi}{4} \cdot \frac{\tau_T}{z_p} \cdot D_p^2 \cdot L_T$	$M = \frac{1}{8} \cdot \frac{i}{k} \cdot p_{me} \cdot D_B^2 \cdot L_S$
Flow	$n = \frac{v_t}{\pi \cdot D_R}$	$n_P = \frac{v_t}{\pi \cdot D_p}$	$n = \frac{c_m}{2 \times L_S}$
Power	$P = \pi \cdot \tau_R \cdot v_t \cdot D_R \cdot L_R$	$P = \frac{\pi}{2} \cdot \frac{\tau_T \cdot v_t}{z_p} \cdot D_p \cdot L_T$	$P = \frac{\rho}{8} \times \frac{i}{k} \times p_{me} \times c_m \times D_B^2$

However in a ship design environment power as function of dimensions is usually not of interest. It is the inverse that is sought after: dimensions of machines as function of power, as was already discussed before. Also a designer may want to vary rotational speed (to vary size of the machine) and shape factor  $\lambda = L / D$  (to fit the machine in a certain space). Therefore the power equations in **Table 1** are rewritten to include rotational speed and shape factors  $\lambda$ ; see second row of **Table 2**. These relations are written such that the right hand side has the parameters that are more or less fixed by technology and the manufacturer while the left hand side gives the design choices of the user of which power and speed are prime of course. For the electric motor and pinion he/she can play with the L/D ratio and for the pinion perhaps

somewhat with the number of teeth (but as said there is a minimum number, in fact around 20). For the diesel engine the choice between 2- and 4-stroke and number of cylinders is a further degree of freedom.

**Table 2: Overview of dimensioning equations for primary elements based on known power.**

Electric Machine	Gearbox	Diesel Engine
$\frac{P \cdot n^2}{\lambda_R} = \frac{1}{\pi} \cdot \tau_{EM} \cdot v_t^3$	$z_P \times \frac{P \cdot n_P^2}{l_P} = z_W \times \frac{P \cdot n_W^2}{l_W} = \frac{1}{2\rho} \times \tau_{TS} \times v_t^3$	$k \times \frac{P \cdot n^2}{i} = \frac{\rho}{32} \times \frac{p_{me} \times c_m^3}{l_s^2}$
$D_R = \sqrt{\frac{1}{\pi} \cdot \frac{1}{\tau_{EM} \cdot v_t \cdot \lambda_R} \cdot P}$	$D_P = \sqrt{\frac{2}{\pi} \cdot \frac{z_P}{\tau_{TS} \cdot v_t \cdot \lambda_P} \cdot P}$	$D_B = \sqrt{\frac{8}{\rho} \times \frac{k}{p_{me} \times c_m} \times \frac{P}{i}}$
$L_R = \sqrt{\frac{1}{\pi} \cdot \frac{\lambda_R}{\tau_{EM} \cdot v_t} \cdot P}$	$L_T = \sqrt{\frac{2}{\pi} \cdot \frac{z_P \cdot \lambda_P}{\tau_{TS} \cdot v_t} \cdot P}$	$L_S = \sqrt{\frac{8}{\rho} \times \frac{k \times l_s^2}{p_{me} \times c_m} \times \frac{P}{i}}$

Finally the equations in the second row of **Table 2** can be rewritten (using some algebra) to find expressions for the diameter and length of the primary elements as a function of power; these are, as promised in the introduction, first principle relationships between size of the primary elements and power, see row 3 and 4 of **Table 2**. Apart from power the size is determined by three main manufacturer choices: a typical stress ( $\tau$ ) or translational ( $c_m$ ) speed and a shape factor of the element ( $L/D$ ), these are the three “players in the game” of which the first two seem to be limited by material properties for all three machines. For the gearbox additionally a number of teeth on the pinion ( $z_p$ ) is required and for the diesel engine the number of cylinders ( $i$ ) and the number of revolutions per cycle ( $k$ ).

### **Sizing secondary elements and core**

Now that the primary elements have been sized the first step of the process for dimension prediction of electric machines, gearboxes and diesel engines is finished. The second step is

sizing additional elements whose size follow from the size of the primary elements.

For the electric machine this means adding an additional “manufacturer” parameter: the rotor/stator diameter ratio  $s = D_R/D_S$ . **Figure 3** shows a schematic of electric machine core construction (both in transverse and longitudinal direction) and defines important dimensional parameters.

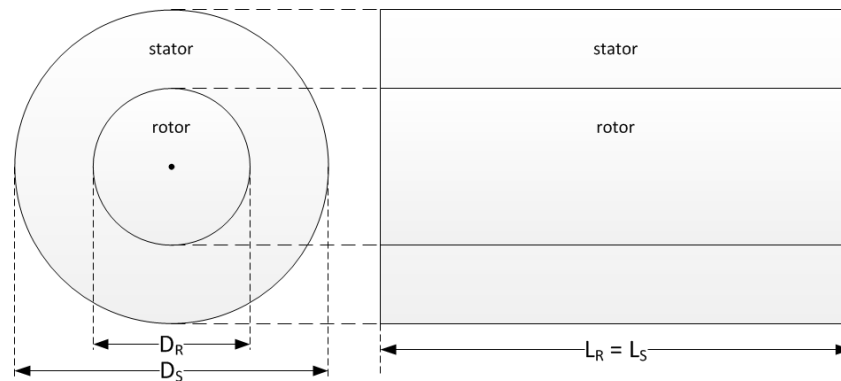


**Figure 3: Schematic of electric machine core construction.**

In contrast to the additional parameters that are needed for the gearbox and diesel engine for sizing secondary elements (which will be introduced shortly) the rotor/stator diameter ratio  $s$  regrettably is not a functional parameter that can be determined by the designer of ship systems. However typical values for  $s$  can be found in literature, e.g. (Miller, 1989); values are in the range of 0.45 – 0.55. This at least gives an idea for  $s$  which means the size of the secondary element (stator) is now found from the size of the primary element (rotor). Normally the stator length will be equal to rotor length as well. This also means the core dimensions of the electric machine are now found. In this case the primary element is completely surrounded by the secondary element, therefore:

$$\begin{aligned}
 L_{\text{core,EM}} &= L_S = L_R \\
 W_{\text{core,EM}} &= D_S = D_R / s \\
 H_{\text{core,EM}} &= D_S = D_R / s
 \end{aligned}
 \tag{5}$$

Note that for the gearbox, once the primary element (pinion) is sized and the gear ratio  $i_{\text{GB}}$  is given (or rather; chosen by the ship system designer), also the secondary element (wheel) is

sized, since:

$$i_{GB} = \frac{z_W}{z_P} = \frac{D_W}{D_P} = \frac{n_P}{n_W} = \frac{l_P}{l_W} \quad [6]$$

The last ratio (of L/D ratios) only equals  $i_{GB}$  if the length of the teeth on pinion and wheel are the same ( $L_P = L_W = L_T$ ), but this normally is the case of course. **Figure 4** shows a schematic of gearbox core construction (both in transverse and longitudinal direction) and defines important dimensional parameters. From this figure it can also be concluded that in this case the fact that the size of the secondary element can be found easily does not immediately result in the core dimensions of the machine, since the pinion can be horizontally or vertically offset with respect to the wheel (or something in between). The offset is characterized by the angle  $\alpha$ . Many single marine gearboxes (SISO = Single Input Single Output) will have a vertical offset in order to be able to place the gearbox as far back (and low) in the ship as possible, but then again for double marine gearboxes (DISO – Double Input Single Output) a (more) horizontal offset may be chosen in order to obtain sufficient space between the two driving machines. In the latter case **Figure 4** should of course be expanded to include a second pinion as well.

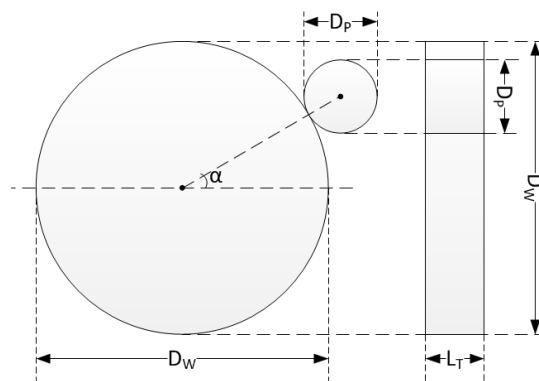


**Figure 4: Schematic of gearbox core construction.**

The core dimension of single marine gearboxes are determined by:

$$\begin{aligned}
L_{\text{core,GB}} &= L_T \\
W_{\text{core,GB}} &= \max\left(\frac{D_P + D_W}{2} + \frac{D_P + D_W}{2} \cdot \cos(\alpha); D_W\right) \\
H_{\text{core,GB}} &= \max\left(\frac{D_P + D_W}{2} + \frac{D_P + D_W}{2} \cdot \sin(\alpha); D_W\right)
\end{aligned} \tag{7}$$

For the diesel engine the secondary element is the crankshaft. The dimensions of this secondary element are just as easily found as for the gearbox if one realizes that the diameter of the crankshaft must be equal to the stroke length. The length of the crankshaft is also relatively easy and is essentially determined by the number of cylinders that are connected to the crankshaft and their diameter. For a Line-engine the core length of the crankshaft is therefore estimated as  $i \cdot D_B$ . For a Vee-engine the story is different of course; here we estimate the core length of the crankshaft to be  $i \cdot D_B / 2$ .

Determining core dimensions for the diesel engine from primary and secondary elements is however rather difficult, at least more so than for the electric machine and gearbox, because of two reasons; the engine might be a L, V or even a boxer motor (horizontal cylinders opposite of each other to the left and right of the crankshaft – in fact a very specific V-engine) and the construction type may differ because of either trunk piston type construction or crosshead type construction.

In **Figure 5** again a schematic of core construction of the machine in question is given (in both transverse and longitudinal direction), but this time for a hypothetical V-engine of crosshead type construction. These types of engines do not exist (although designs for them have been made in the past), but this figure shows best how to derive general equations for the core of diesel engines in all possible cases: L- or V-engine is characterized by angle  $\alpha$  and the difference between crosshead and trunk piston type (conceptually at least) is the extra stroke length that exists between the crankshaft outer diameter and the bottom of the cylinder. This extra stroke length does exist for crosshead engines, since the crosshead travels one  $L_S$  as well, but for trunk piston type engines this extra stroke length is zero, since for these engines the bottom of the cylinders conceptually “touches” the outer diameter of the crankshaft. To account for this the parameter “ct” (construction type) has been added; a basic assumption is

$ct = 0$  for trunk piston type engines and  $ct = 1$  for crosshead type engines. In a more refined model for  $ct$  an allowance can be made for the length of the connecting rod and the fact that the height of the piston at Bottom Dead Centre must be added to the stroke length. But information on connecting rod length and position height normally is not available so a pragmatic decision is to include both effects in the fit of the machine dimensions.

Careful analysis of **Figure 5** leads to the following expressions for the size of the core of diesel engines.

$$\begin{aligned}
 L_{\text{core,DE}} &= i \cdot D_B \quad \text{for } L \text{ engines} \\
 L_{\text{core,DE}} &= \frac{i \cdot D_B}{2} \quad \text{for } V \text{ engines} \\
 W_{\text{core,DE}} &= 2 \cdot \max \left( \left( \frac{L_S}{2} + (1+ct) \cdot L_S \right) \cdot \sin \left( \frac{\alpha}{2} \right) + \frac{D_B}{2} \cdot \cos \left( \frac{\alpha}{2} \right); \frac{L_S}{2} \right) \\
 H_{\text{core,DE}} &= \frac{L_S}{2} + \max \left( \left( \frac{L_S}{2} + (1+ct) \cdot L_S \right) \cdot \cos \left( \frac{\alpha}{2} \right) + \frac{D_B}{2} \cdot \sin \left( \frac{\alpha}{2} \right); \frac{L_S}{2} \right)
 \end{aligned} \tag{8}$$

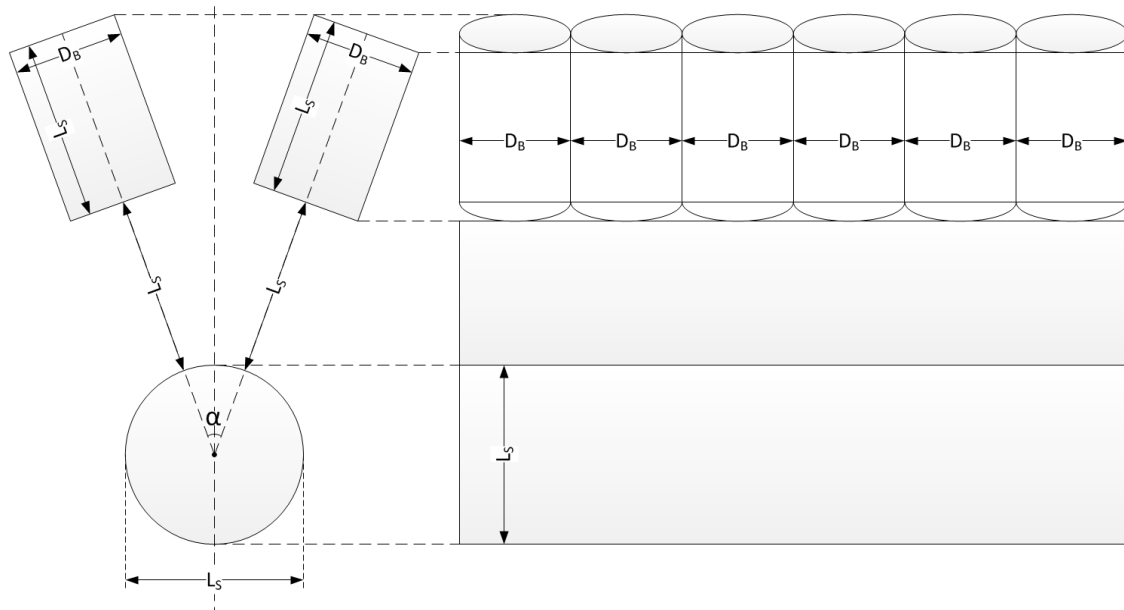


**Figure 5: Schematic of diesel engine core construction.**

## SIZING MACHINE

Now that expressions have been given that relate dimensions of primary elements to power

output of machines and core dimensions to dimensions of primary and secondary elements, the question becomes: how is size of the core related to machine size? This of course depends on the configuration of the machine that will be the topic of this section.

Start again with an electric machine. The shape of an electric machine actually resembles the shape of its core (stator + rotor) meaning the machine is also a cylindrical volume. This can also be seen from **Figure 6**, which is a drawing of an electric machine of a well-known electric machine manufacturer.

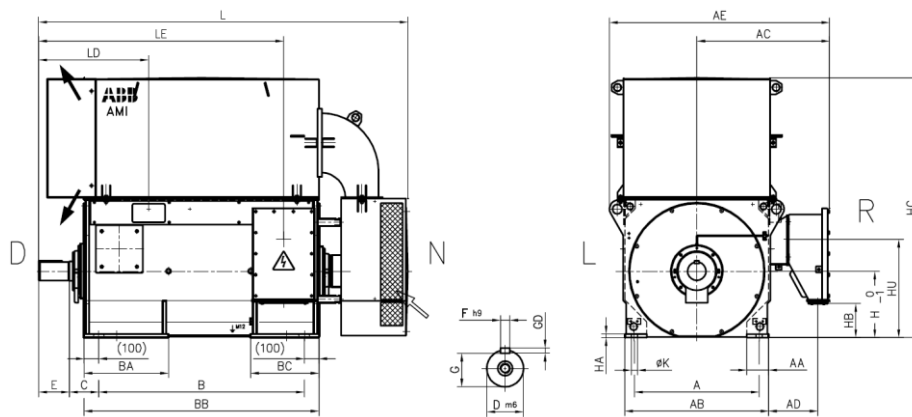


**Figure 6: Typical electric machine construction. Source: online ABB catalog of HV induction motors (see references).**

However, it also becomes clear from **Figure 6** that extra volumes are added to the machine. The main reason for this is required cooling of the machine (although the terminal box also requires quite some room). For smaller electric machines with open cooling a fan at the free end of the machine and cooling vanes around the housing will suffice for the required cooling. But for larger electric machines the heat cannot be dumped directly in the environment so they are closed and heat exchangers for cooling are required. The location of these heat exchangers represents another degree of freedom (on top or at the side or perhaps even some distance away from the electric machine). The sizing model may also be used for synchronous machines and in particular generators. Then the exciter and power electronics are further additions to the size of the electric machine.

Now a mathematical relation needs to be assumed between core dimensions and machine

dimensions in order to be able to fit the model to actual machine data. Many options exist: polynomial functions, power laws or even Fourier series, but since the idea behind the model is that the core dimensions already represent a significant part of the actual machine dimensions a rather simple, but perhaps effective, relation is assumed. It is therefore hypothesized that the electric machine dimensions are related to the core dimensions with first order polynomials:

$$\begin{aligned} L_{EM} &= A_0 + A_1 \cdot L_{core,EM} \\ W_{EM} &= B_0 + B_1 \cdot W_{core,EM} \\ H_{EM} &= C_0 + C_1 \cdot H_{core,EM} \end{aligned} \quad [9]$$

In these equations the length, width and height of the entire electric machine are given as function of the earlier derived dimensions of the core (expression [5]). The polynomial factors  $A_0$ ,  $A_1$ ,  $B_0$ ,  $B_1$ ,  $C_0$  and  $C_1$  can be used to fit the dimensions of actual machines, so here regression analysis is needed to find appropriate values for the coefficients. In order to make the coefficients dimensionless, the actual dimensions and the core dimensions could also be normalized using a typical machine as a reference. This benchmark machine must preferably be somewhere in the middle of the design space. Note that it is possible to fit dimensions of actual machines using a database containing dimensions of real machines, but it is also possible to estimate machine dimensions with this model if a database is unavailable or outdated. The only information required to do so is a reasonable estimation of the coefficients  $A_1$ ,  $B_1$  and  $C_1$  and neglecting  $A_0$ ,  $B_0$  and  $C_0$  (as will be done shortly). One could say that this approach to dimension prediction models enables “rubber” machines that are dimensioned according to a designers insight instead of manufacturer data.

The success of fitting machine dimensions using the coefficients A, B and C is determined by the degree with which the dimensions of actual machine differ from the core dimensions, or rather the variance of this degree. In the case of electric machines for instance the already discussed different cooling methods could pose quite a “disturbance” on the values of the coefficients A, B and C, if the cooling is to be included in these coefficients as well. If so, one can expect a step change in the value for C for instance when electric machines switch from open cooling to closed cooling by the “sudden” addition of a large heat exchanger on top of the

machine. Such considerations could lead to more advanced mathematical relations to fit the dimensions, but it could also be accepted as a remaining weakness of the method and a reason for anyone that uses this method to think critically on what he/she is fitting. This is true anyhow, no matter in which manner regression analysis is applied to fit data.

**Figure 7**, which is another manufacturer drawing, suggests that a similar mathematical relation between machine dimensions and core dimensions can be assumed for a gearbox as for the electric machine:

$$\begin{aligned} L_{GB} &= A_0 + A_1 \cdot L_{core,GB} \\ W_{GB} &= B_0 + B_1 \cdot W_{core,GB} \\ H_{GB} &= C_0 + C_1 \cdot H_{core,GB} \end{aligned} \quad [10]$$

Especially from the front view (right hand side of **Figure 7**) it can be seen that the dimensions of the machine should size with the core dimensions: the bottom circle in the middle of the gearbox represents the flange of the output shaft which is attached to the wheel while the relatively large circle near the top represents the aft bearing of the input shaft that contains the pinion. The smaller circle above this “pinion” circle is the flange of another output shaft: for a PTI/PTO (Power Take In / Power Take Off). Whether or not a gearbox is equipped with PTI/PTO is another example of a disturbance that can cause variance in the coefficients A, B and C. Another example of such a disturbance for gearboxes is whether or not the thrust block is integrated in the gearbox. Note that angle  $\alpha$  (refer to **Figure 4**) is in the example is  $90^\circ$ , which will often be the case for single gear units as especially width of a gearbox needs to be as small as possible to be able to place the gearbox low and far to the back in a ship; where the ship hull will be narrow.

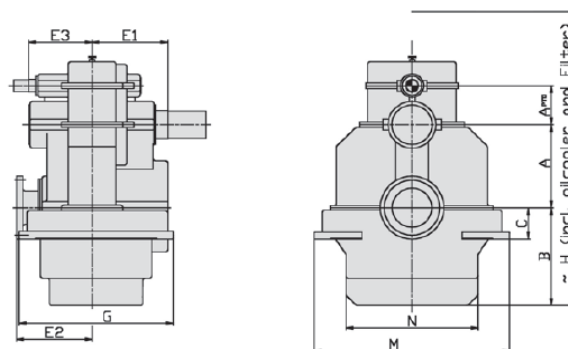


**Figure 7: Typical gearbox construction. Source: online RENK catalog of single gear units (see references).**

For the diesel engine again the same relationships are assumed between machine dimensions and core dimensions:

$$\begin{aligned} L_{DE} &= A_0 + A_1 \times L_{core,DE} \\ W_{DE} &= B_0 + B_1 \times W_{core,DE} \\ H_{DE} &= C_0 + C_1 \times H_{core,DE} \end{aligned} \quad [11]$$

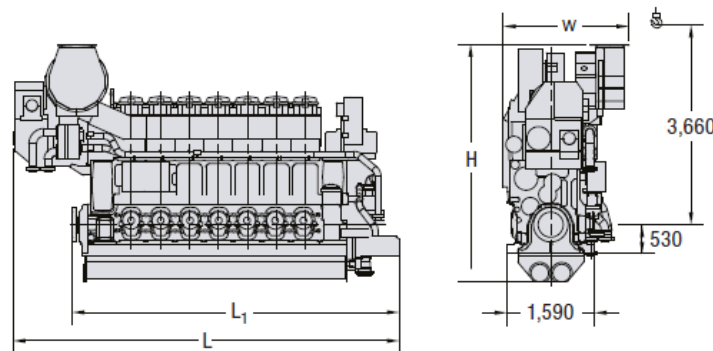


**Figure 8: Typical diesel engine construction. Source: online MAN catalog of marine diesel engines (see references).**

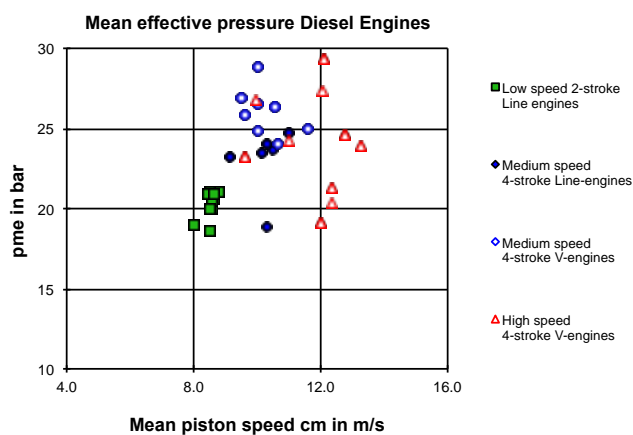
From **Figure 8** it can be seen that also for the diesel engine the core dimensions indeed represent a significant part of the machine dimensions. In this case a trunk piston type L-engine ( $ct = 0$ ,  $\alpha = 0$ ; refer to **Figure 5**) is shown and length should indeed size with  $i \cdot D_B$ , width of the machine is approximately  $L_S$  (at least at the bottom) and height should indeed be a multiple of  $2 \cdot L_S$ , refer to expression [8]. On the other hand the turbocharger with its related air and exhaust gas channels (inlet receiver, charge air cooler, outlet receiver, etc.) represent quite a disturbance factor. The same applies for cooling water and lubrication oil provisions attached to the engine. Then again, such provisions are always there (even the turbocharger, which formally is optional, is a standard piece of equipment on marine diesel engines nowadays), so perhaps the variance of coefficients A, B and C is not so large.

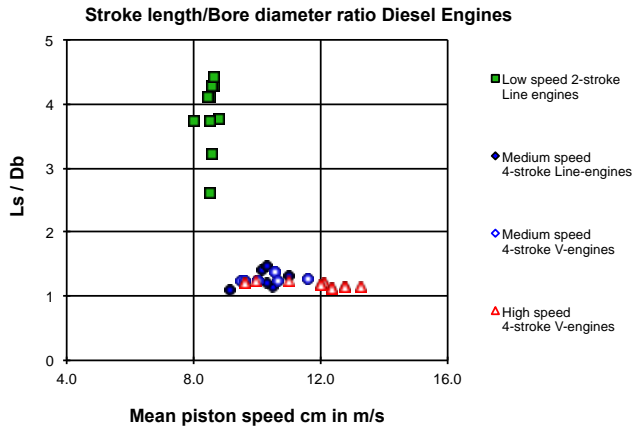
## MODEL CORRELATION

After having introduced the assumed relations between core dimensions and machine dimensions in the previous section the real question now is: what are typical values for coefficients A, B and C for the three machines and what is their variance. An equally important question is the range of the main parameters, i.e. the characteristic mean shear stress or mean effective pressure, mean circumferential or piston speed and finally the L/D ratio and whether these three “players in the game” can be easily selected.

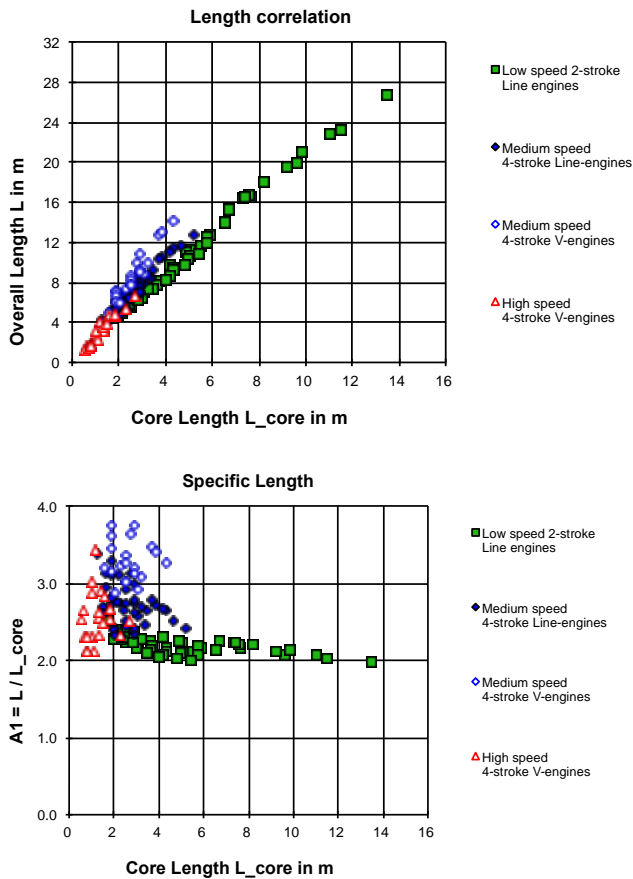
For diesel engines the manufacturers provide a lot of data; therefore we will discuss the machines in reversed order and start with the diesel engine. First of all **Figure 9** shows the “players in the game” and in particular the two parameters that, when multiplied, make up the “technology parameter”. They are in a confined space with mean effective pressure between 20 and 30 bar and mean piston speed between 8 and 13 m/s. The “shape factor” shows two distinct groups, the low speed 2-stroke diesel engines having much larger L/D values than the medium and high-speed 4-stroke engines. The relative long stroke of the slow speed engines adapts their rotational speed to the propeller such that no gearbox is required. Also the long L/D together with a low mean piston speed is beneficial for the uniflow scavenging process that is critical for these 2-stroke engines.

**Figure 10, Figure 11 and Figure 12** present at the left side the correlation between the actual length, width and height of the engines and the theoretical values as obtained from inspection of the core model.

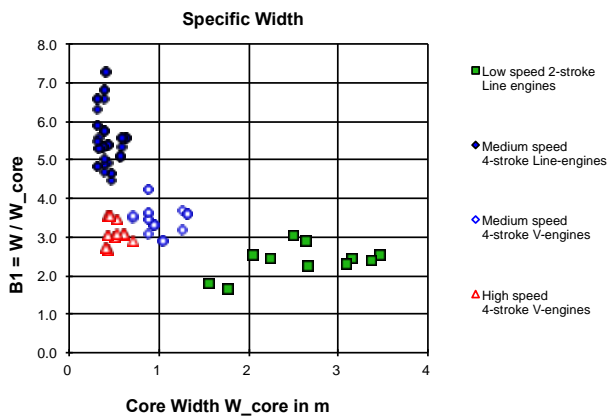
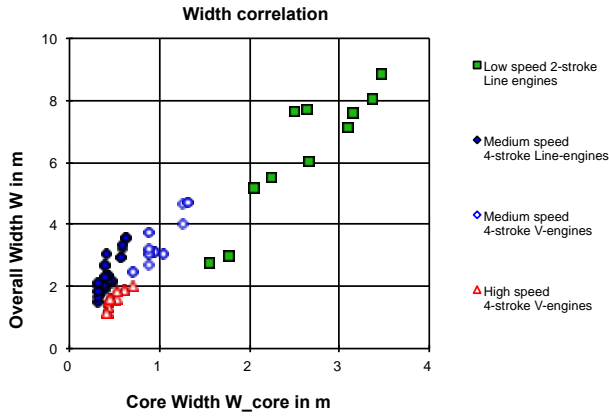




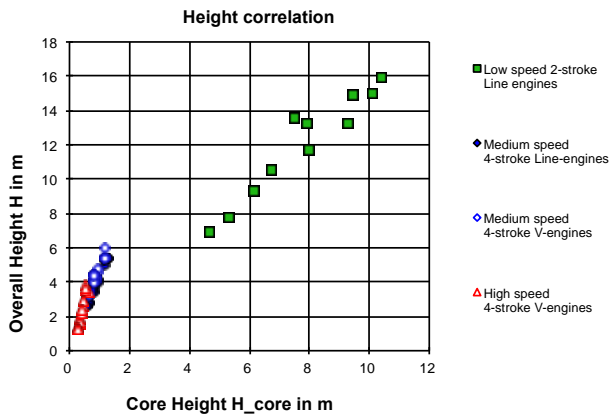
**Figure 9: Range of mean effective pressure, mean piston speed and L/D ratio for diesel engines**



**Figure 10: Correlation of actual length (left) and specific length (right) with theoretical core length for DE**



**Figure 11: Correlation of actual width (left) and specific width (right) with theoretical core width for DE**



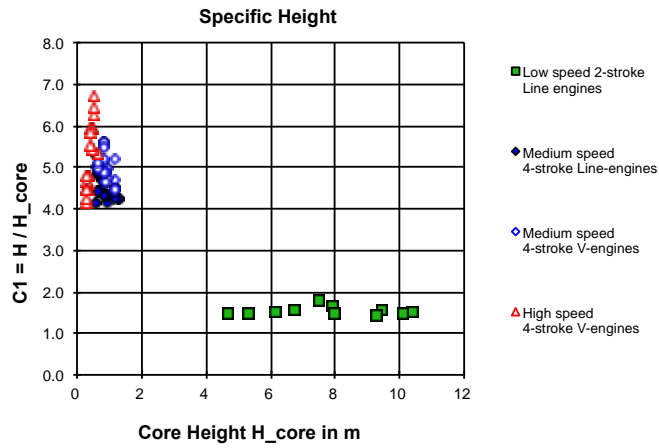


Figure 12: Correlation of actual height (left) and specific height (right) with theoretical core height for DE

All correlations show that the constants  $A_0$ ,  $B_0$  and  $C_0$  can safely be discarded leaving the inclinations  $A_1$ ,  $B_1$  and  $C_1$  to be fitted. These then effectively can be regarded as specific length, width and height that are shown at the right side of **Figure 10**, **Figure 11** and **Figure 12**.

Length correlates well, in particular for slow speed 2-stroke engines where specific length has a value of just over two times the core length. Scatter for medium and high speed engines is worse and also they seem systematically longer in terms of their specific length, in particular the medium speed V-engines. This of course is caused by the turbochargers being often mounted at the end of the engine.

Width correlates well within product groups of engines but not well across them. Low speed 2-stroke engines are between 2 and 3 times the core width. V-engines, both medium and high speed, are 3 to 4 times the core width and medium speed L-engines 5 to 7 times the core width. The latter seems surprising but the explanation must be that inlet and outlet receivers, camshaft and fuel pumps, that for these engines are attached to the sides, make them relatively wide.

Height correlates well for slow speed engines and reasonably for medium speed engines but less so for high speed engines. The reason could be that for these engines the turbocharger(s) are sometimes mounted on top, spoiling the picture. Somewhat surprising is the fact that slow speed crosshead engines are with a specific height of around 1.5, *relatively speaking* lower than medium speed engines with their specific height between 4 and 6 and certainly than high speed engines with a value between 4 and 7. Of course the extra height of the sliding bearing is in principle allowed for in the core height of the low speed crosshead engines, which is far larger than for the other engines as can also be concluded from **Figure 12**.

For gearboxes the data up to now are scarce: we have some data for eight Single Input/Single Output (SISO) gearboxes, connecting a medium speed diesel engine to a propeller and for one 2-stage locked train high speed gearbox for connection of a gas turbine to a propeller. In fact we only have number of teeth, input power and input speed, but no actual dimensions of the teeth. Therefore **Figure 13** not only gives the spread between the 9 gearboxes in the

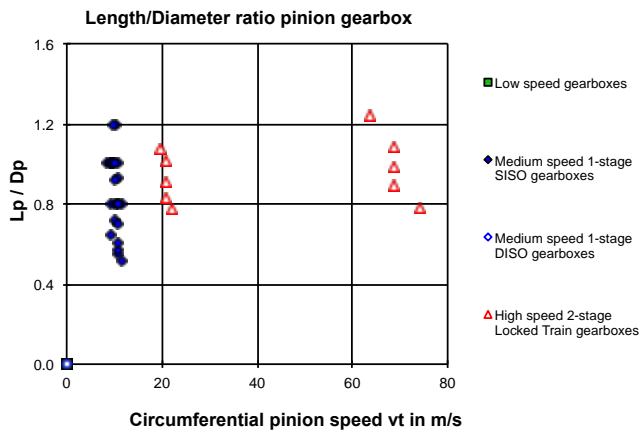
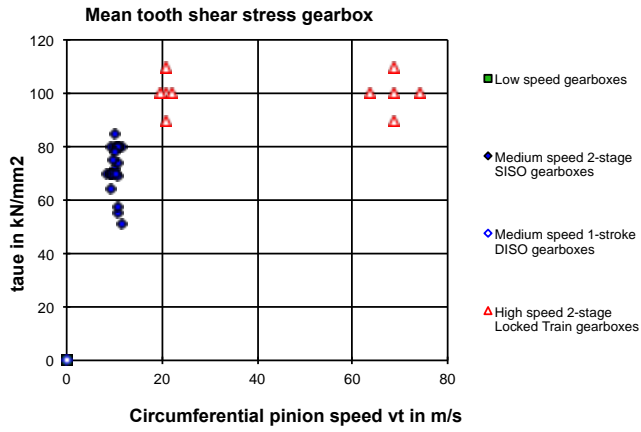
database but also a scatter in the way the mean tooth stress, circumferential speed and L/D ratio have been reconstructed.

Nevertheless by inspection of **Figure 13** spread of the range of value of the “players in the game” seems for gearboxes much wider than for diesel engines. The circumferential speed at least ranges between 10 and 80 m/s, but in super high-speed gearboxes (which are not included in the data set) they may nowadays be as high as 220 m/s. For the mean tooth shear stress as defined in this paper the knowledge really must be built up. A value of around 60 to 80 kN/mm<sup>2</sup> for medium speed gearboxes seems to be the case and a somewhat higher value for high-speed gearboxes for maritime gas turbines does not seem unreasonable.

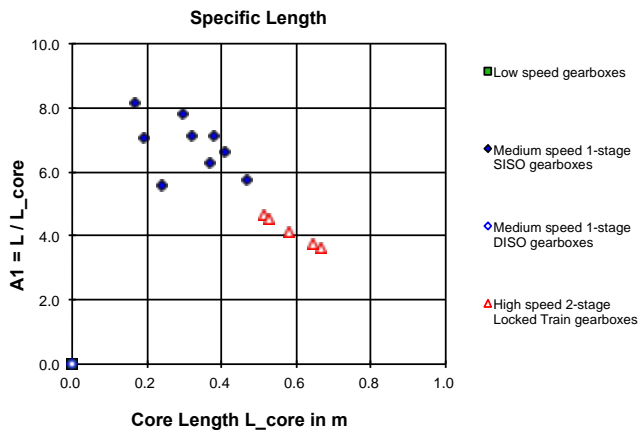
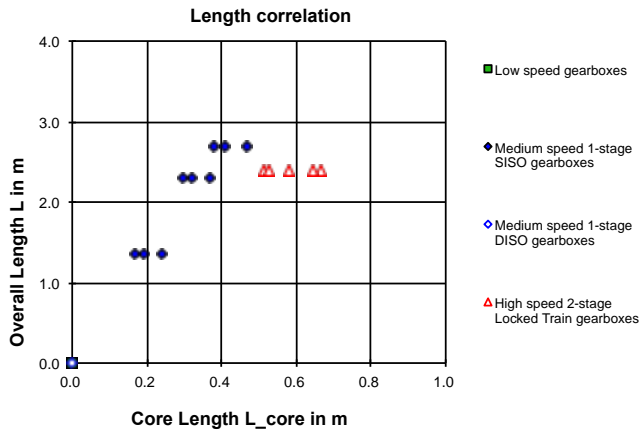
For only 3 out of the 8 medium speed gearboxes dimensional drawings are available and for the high speed locked train gearbox there is an indication of the size. So the size correlations in **Figure 14**, **Figure 15** and **Figure 16** must be regarded with some reservation. Also these figures not only show the scatter between the (only 4) gearboxes but also the scatter as a result of the uncertainty of the reverse engineering process by which the points are reconstructed. For the high speed locked train gearbox the core model was expanded, but the details will not be explained in the paper.

Nevertheless the fact that in **Figure 14** the specific length of the medium speed single stage gearbox (with a value between 6 to 10 times the core length) is relatively longer than the 2-stage gearbox (with a value around 4) seems reasonable in view of the fact that the distance between the two gear trains in the high-speed gearbox “costs” relatively not much length.

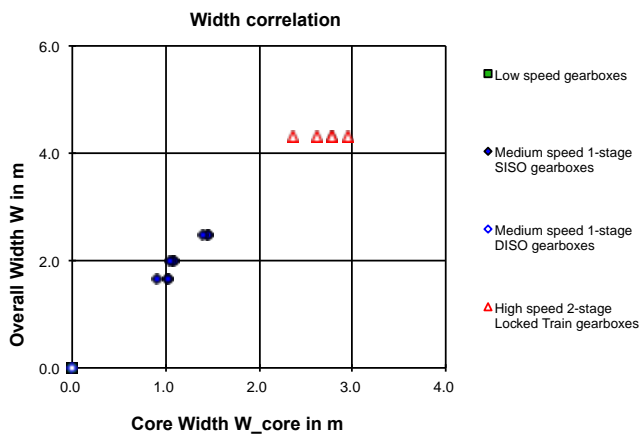
For the width and height correlations in **Figure 15** and **Figure 16** the value for the specific width and height for the medium speed single stage and high speed 2-stage gearbox seems of equal magnitude between 1.5 and 2, so here, contrary to diesel engines the conceptual model work well across product groups. This is not surprising since width and height are dominated by the size of the big wheel.



**Figure 13: Range of mean tooth shear stress, circumferential speed and L/D ratio for pinions of gearboxes**



**Figure 14: Correlation of actual length (left) and specific length (right) with theoretical core length for GB**



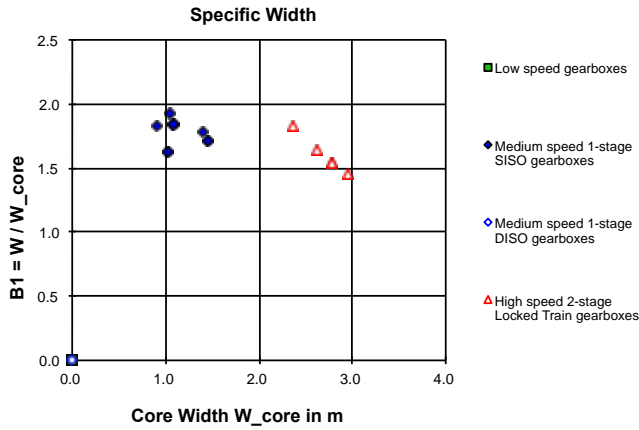


**Figure 15: Correlation of actual width (left) and specific width (right) with theoretical core width for GB**

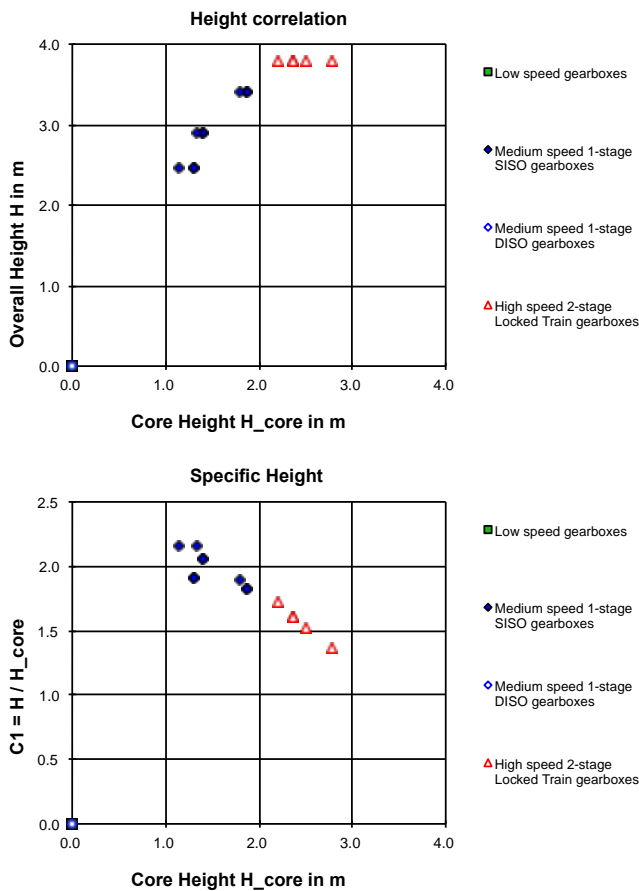


**Figure 16: Correlation of actual height (left) and specific height (right) with theoretical core height for GB**

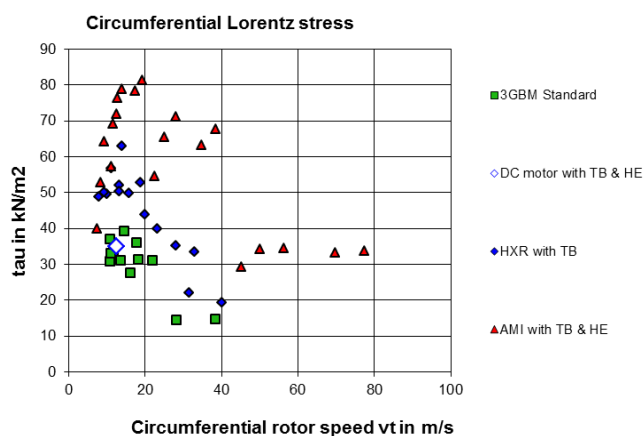
Finally for the electric machines it must be emphasized that there is also uncertainty in the data gathered (though not so much as for the gearbox). Especially rotor dimensions have been hard to find and some uncertainty exists in the values for rotor/stator diameter ratio  $s$ . Still by careful inspection of machine drawings and application of typical values for  $s$  a reasonably well filled database could be constructed that provides some confidence in the figures below.

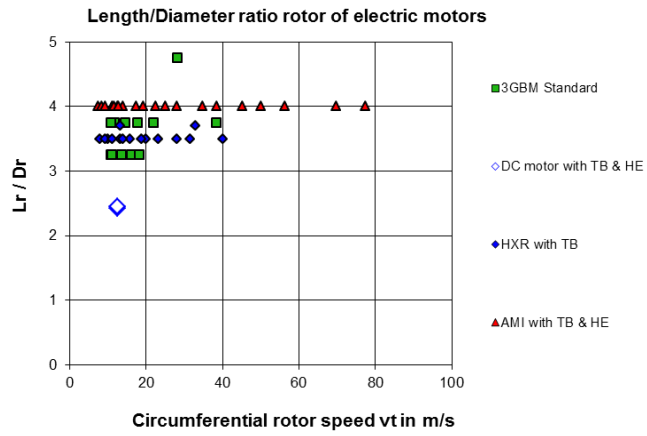
**Figure 17** shows again the spread of the range of value of the “players in the game”, which for electric machines (like for gearboxes) seems to be much wider than for diesel engines. The circumferential speed ranges between 7 and 80 m/s according to the database, but (Rucker e.a. 2005) mentions a value as high as 200 m/s for a 13000 rpm PM generator for naval applications. They also mention that such a high circumferential speed limits the attainable mean shear stress, for which they assume a value of 15 kN/mm<sup>2</sup>. From **Figure 17** it can be seen that higher values may be found, in fact the mean shear stress ranges from 15 to 80 kN/mm<sup>2</sup> in the database. The limits of mean shear stress (also referred to as force density) have been investigated by (Grauers e.a. 2004) and they conclude a maximum of 100 kN/mm<sup>2</sup> exists, but slightly higher values have already been found for special cases. Either way, both literature and the gathered values in the database suggest that the product of mean shear stress and circumferential speed, which was introduced as the “Technology Parameter”, is limited. This results in a decreasing line serving as a limit for mean shear stress and circumferential speed, which indeed can be observed in **Figure 17**. The L/D ratio for rotors was estimated on basis of machine drawings and show little spread, especially within product groups, which can be explained by the fact that product groups use similar housings. Machines with a low number of poles (2 or 4) might have somewhat higher L/D ratios for the rotor since they need more space for the salient poles of the stator. This does not change the dimensions of the housing, since the rotor/stator diameter ratio  $s$  then also changes (in the opposite direction).

Machine dimensions and core dimensions correlate well especially within each product group, like for the diesel engines, as can be seen from **Figure 18**, **Figure 19** and **Figure 20**. An exception (positively) to this rule is the length that also correlates well across all product

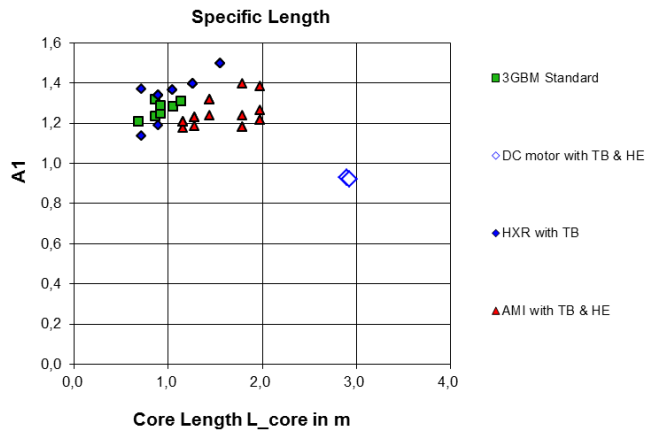
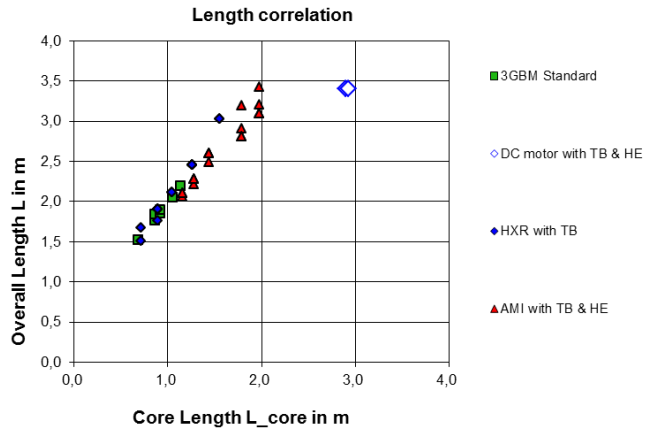
groups. The reason for width and height only correlating well within product groups can be found in the fact that terminal boxes (TB) and heat exchangers (HE) have been taken into account in machine dimensions as well and they affect only width and/or height (depending on their location). The 3GBM product group does not include a terminal box or heat exchanger; the HXR group includes only a terminal box, while the AMI group includes both. A small experiment was done by not taking into account the TB and HE for the HXR and AMI group, from which could be concluded that all dimensions correlated well; also across product groups. A designer however is interested in the overall dimensions.

From the left hand side figures in **Figure 18**, **Figure 19** and **Figure 20** it can also be observed that, contrary to the diesel engines and the gearboxes, the coefficients  $A_0$ ,  $B_0$  and  $C_0$  have a non-zero value (although a value of zero could be assumed of course; but this leads to a larger spread in coefficients  $A_1$ ,  $B_1$  and  $C_1$ ). Coefficient  $A_0$  has been estimated as 0.7,  $B_0$  as 0.4 and  $C_0$  as 0.5 by extending a linear line running through the data points. Values for  $A_1$  (right hand side of **Figure 18**) can then be found to be in a narrow range of 1.15–1.45, if one discards the DC motor: this is a relatively fat machine (small L/D as can also be seen in **Figure 17**) and also has a very low speed (200 rpm), so it has a large number of poles. Ultimately the range of values for specific width  $B_1$  and specific height  $C_1$  is larger (0.6–2.1 resp. 0.4–2.4), which is again a result of inclusion of TB and HE in machine dimensions.

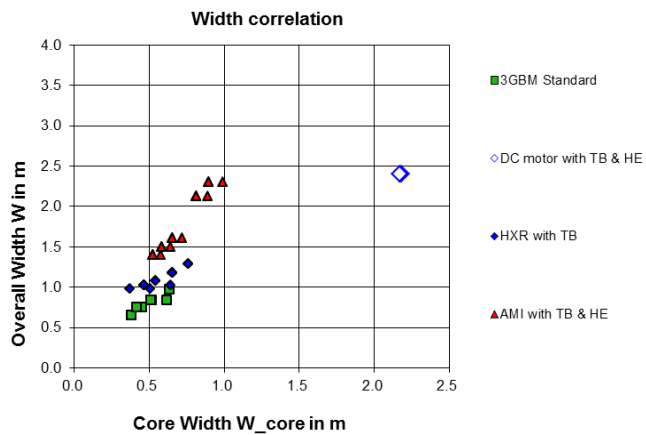




**Figure 17: Range of mean Lorentz shear stress, circumferential speed and L/D ratio for rotors of electrical machines**



**Figure 18: Correlation of actual length (left) and specific length (right) with theoretical core length for EM**



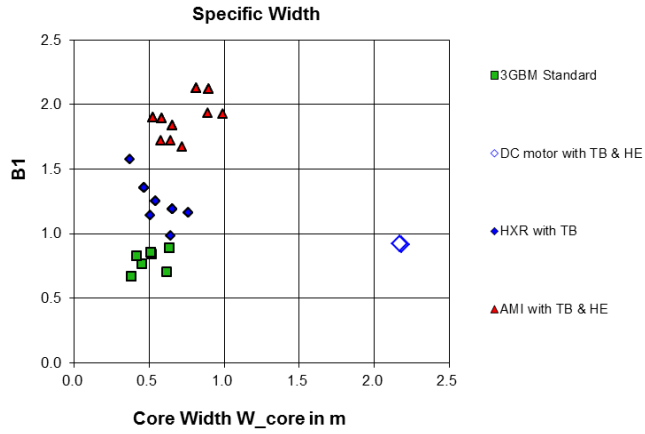


Figure 19: Correlation of actual width (left) and specific width (right) with theoretical core width for EM

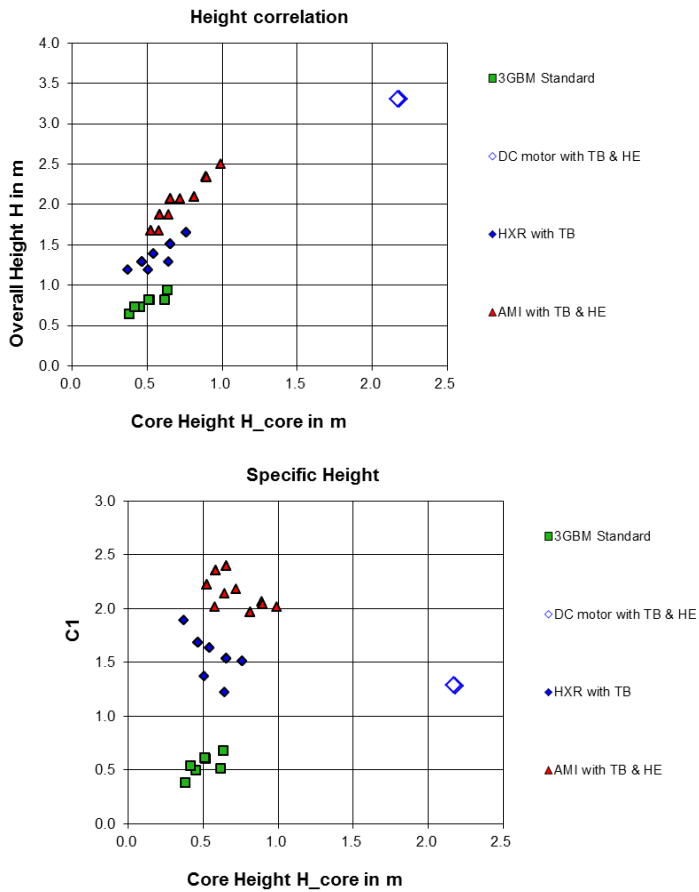


Figure 20: Correlation of actual height (left) and specific height (right) with theoretical core height for EM

## **CONCLUSIONS**

In this paper, we have presented a generic method for predicting dimensions of primary ship system components. The method has successfully been applied to diesel engines, gearboxes and electric machines and is therefore thought to be generally applicable. Similar methodologies can be found in the domains of the respective machines, but as far as the authors know no one has ever tried to use them as generic as was done in this paper.

There are two main benefits of the proposed method over direct fitting of machine dimensions data as a function of power and/or speed as is often done. First it is possible to explore the influence of (future) technology on dimensions of equipment. Second the cause of the scatter in the regression analysis can be understood better and all models can, apart from mean values for the fit constants also be provided with a standard deviation for them. That way it is possible to introduce uncertainty analysis in the design process.

In order to apply the method to realistic design questions it is necessary not only to know the constants in the regression but also the limits in the characteristic stress and speed diagrams introduced in this paper in conjunction with any limits on the shape factor  $L/D$ . In particular for gearboxes and electrical machines the author's database at the moment is too scarce to provide that insight.

Future work therefore will focus on the one hand on gathering more information on diesel engines, gearboxes and electric machines in order to expand the database, thereby increasing the knowledge about the limits of the three main machine parameters and improving the fidelity of the first principle based dimension prediction models. On the other hand the methodology will be applied to more ship system components (pumps, gas turbines, heat exchangers, batteries, etc.) to assess whether it is indeed even more generally applicable as it seems to be now.

## **REFERENCES**

Miller, T.J.E., "Brushless permanent-magnet and reluctance motor drives", Oxford Science Publications, Oxford, 1989.

Stapersma, D., Brockhoff, H.S.T., Barendregt, I.P. and Hope, G.R., "Structured Approach to Conceptual Design of Integrated electrical energy generation systems on board ships", 4th International Naval Engineering Conference, Portsmouth, March 1998 (INEC 1998)

Van Dijk et al., Components and Parameters, report WP 030 and 040, All Electric Ship (AES) project, June 1998 (in Dutch)

Hodge, C.G. and D.J Mattick, "The Electric Warship VI", Trans. IMarE, Volume 113, part 1, p 49 - 63, 2001

Klein Woud, H. and D. Stapersma, "Design of Propulsion and Electric Power Generation Systems", IMarEST, London, 2003.

Frouws, J.C., "AES Decision model", Delft University of Technology, 2008.

Grauers, A. and Kasinathan, P., "Force Density Limits in Low-Speed PM Machines Due to Temperature and Reactance", IEEE Trans. on energy conversion, Vol. 19, No. 3, 2004

Rucker, J.E., Kirtley, J.L. and McCoy, T.J., "Design and Analysis of a Permanent Magnet Generator For Naval Applications", IEEE Electric Ship Technologies Symposium, 2005.

G.F. van Es, P. de Vos, System Design as a Decisive Step in Naval Engineering Capability, 11th International Naval Engineering Conference, Edinburgh, May 2012 (INEC 2012)

P. de Vos, On the application of network theory in naval engineering: Generating network topologies, 12<sup>th</sup> International Naval Engineering Conference, Amsterdam, May 2014 (INEC 2014).

ABB, "High voltage induction motors - Technical catalog for IEC motors", PDF document from ABB website: [www.abb.com](http://www.abb.com), 2011. Download in December 2014.

RENK, "Single Marine gear Units", PDF document from RENK website: [www.renk.de](http://www.renk.de), 2014. Download in December 2014.

MAN SE, "Marine Engine Programme", PDF document from MAN website: [www.man.eu](http://www.man.eu), 2<sup>nd</sup> edition 2014. Download in December 2014.



# Appendix B

## Typical value of overall heat transfer coefficient

Shell and tube heat exchangers		
Hot Fluid	Cold Fluid	U(W/m <sup>2</sup> °C)
<i>Heat exchangers</i>		
Water	Water	800-1500
Organic solvents	Organic solvents	100-300
Light oils	Light oils	100-400
Heavy oils	Heavy oils	50-300
Gases	Gases	10-50
<i>Coolers</i>		
Organic solvents	Water	250-750
Light oils	Water	350-900
Heavy oils	Water	60-300
Gases	Water	20-300
Organic solvents	Brine	150-500
Water	Brine	600-1200
Gases	Brine	15-250
<i>Heaters</i>		
Steam	Water	1500-4000
Steam	Organic solvents	500-1000
Steam	Light oils	300-900
Steam	Heavy oils	60-450
Steam	Gases	30-300
Dowtherm	Heavy oils	50-300
Dowtherm	Gases	20-200
Flue gases	Steam	30-100
Flue	Hydrocarbon vapors	30-100
<i>Condensers</i>		
Aqueous vapors	Water	1000-1500
Organic vapors	Water	700-1000
Organics (some noncondensables)	Water	500-700
Vacuum condensers	Water	200-500
<i>Vaporizers</i>		
Steam	Aqueous solutions	1000-1500
Steam	Light organics	900-1200
Steam	Heavy organics	600-900

---

**Gasketed-plate exchangers**

---

<b>Hot Fluid</b>	<b>Cold Fluid</b>	<b>U(W/m<sup>2</sup>°C)</b>
Light organic	Light organic	2500-5000
Light organic	Viscous organic	250-500
Viscous organic	Viscous organic	100-200
Light organic	Process water	2500-3500
Viscous organic	Process water	250-500
Light organic	Cooling water	2000-4500
Viscous organic	Cooling water	250-450
Condensing steam	Light organic	2500-3500
Condensing steam	Viscous organic	250-500
Process water	Process water	5000-7500
Process water	Cooling water	5000-7000
Dilute aqueous solutions	Cooling water	5000-7000
Condensing steam	Process water	3500-4500

---

# Appendix C

In this appendix, the detailed data of predicting dimension in Chapter 6 is provided.

**Table C-1 Detailed dimension results of NO.1 STHE in FPSO vessel**

<u>Shell and Tube Heat Exchanger</u>		
<b>No.1</b>		
Hot fluid	<i>Steam</i>	
Cold fluid	<i>Cargo oil</i>	
Inlet temperature of hot fluid	55	°C
Outlet temperature of hot fluid	65	°C
Inlet temperature of cold fluid	158,1	°C
Outlet temperature of cold fluid	158,1	°C
LMTD	98	°C
Total heat load	617,2	kW
Overall heat transfer coefficient	97	W/m <sup>2</sup> °C
Heat transfer area	64,9	m <sup>2</sup>
Number of tubes	450	-
Shape factor of the tube	0,0076	-
Evaluated volume of the tube bundle	1	m <sup>3</sup>
Volume per tube	0,002	m <sup>3</sup>
Manufacture factor	2,5	-
Diameter of the tube	0,019	m
Length of the tube	2	m
Diameter of the shell	0,64	m
Length of the shell	2	m
Length of the core element	2	m
Width of the core element	0,64	m
Height of the core element	0,64	m
Fitting factor of length	1,3	-
Fitting factor of width	1,3	-
Fitting factor of height	1,4	-
Predicted overall length	2,6	m
Predicted overall width	0,83	m
Predicted overall height	0,89	m

**Table C-2 Detailed dimension results of NO.2 STHE in FPSO vessel**

<u>Shell and Tube Heat Exchanger</u>		
<b>No.2</b>		
Hot fluid	<i>Steam</i>	
Cold fluid	<i>Cargo oil</i>	
Inlet temperature of hot fluid	55	°C
Outlet temperature of hot fluid	65	°C
Inlet temperature of cold fluid	158,1	°C
Outlet temperature of cold fluid	158,1	°C
LMTD	98	°C
Total heat load	664,2	kW
Overall heat transfer coefficient	97	W/m <sup>2</sup> °C
Heat transfer area	69,9	m <sup>2</sup>
Number of tubes	450	-
Shape factor of the tube	0,0076	-
Evaluated volume of the tube bundle	1	m <sup>3</sup>
Volume per tube	0,002	m <sup>3</sup>
Manufacture factor	2,5	-
Diameter of the tube	0,019	m
Length of the tube	2,2	m
Diameter of the shell	0,64	m
Length of the shell	2,4	m
Length of the core element	2,4	m
Width of the core element	0,64	m
Height of the core element	0,64	m
Fitting factor of length	1,3	-
Fitting factor of width	1,3	-
Fitting factor of height	1,4	-
Predicted overall length	3,12	m
Predicted overall width	0,83	m
Predicted overall height	0,89	m

**Table C-3 Detailed dimension results of NO.3 STHE in FPSO vessel**

<u>Shell and Tube Heat Exchanger</u>		
<b>No.3</b>		
Hot fluid	<i>Steam</i>	
Cold fluid	<i>Cargo oil</i>	
Inlet temperature of hot fluid	55	°C
Outlet temperature of hot fluid	65	°C
Inlet temperature of cold fluid	158,1	°C
Outlet temperature of cold fluid	158,1	°C
LMTD	98	°C
Total heat load	797	kW
Overall heat transfer coefficient	97	W/m <sup>2</sup> °C
Heat transfer area	83,8	m <sup>2</sup>
Number of tubes	450	-
Shape factor of the tube	0,0076	-
Evaluated volume of the tube bundle	1	m <sup>3</sup>
Volume per tube	0,002	m <sup>3</sup>
Manufacture factor	2,5	-
Diameter of the tube	0,019	m
Length of the tube	2,7	m
Diameter of the shell	0,64	m
Length of the shell	2,7	m
Length of the core element	2,7	m
Width of the core element	0,64	m
Height of the core element	0,64	m
Fitting factor of length	1,3	-
Fitting factor of width	1,3	-
Fitting factor of height	1,4	-
Predicted overall length	3,51	m
Predicted overall width	0,83	m
Predicted overall height	0,90	m

**Table C-4 Detailed dimension results of NO.4 STHE in FPSO vessel**

<u>Shell and Tube Heat Exchanger</u>		
<b>No.4</b>		
Hot fluid	<i>Steam</i>	
Cold fluid	<i>Cargo oil</i>	
Inlet temperature of hot fluid	55	°C
Outlet temperature of hot fluid	65	°C
Inlet temperature of cold fluid	158,1	°C
Outlet temperature of cold fluid	158,1	°C
LMTD	98	°C
Total heat load	783	kW
Overall heat transfer coefficient	97	W/m <sup>2</sup> °C
Heat transfer area	82,37	m <sup>2</sup>
Number of tubes	450	-
Shape factor of the tube	0,0076	-
Evaluated volume of the tube bundle	1	m <sup>3</sup>
Volume per tube	0,002	m <sup>3</sup>
Manufacture factor	2,5	-
Diameter of the tube	0,019	m
Length of the tube	2,65	m
Diameter of the shell	0,64	m
Length of the shell	2,65	m
Length of the core element	2,65	m
Width of the core element	0,64	m
Height of the core element	0,64	m
Fitting factor of length	1,3	-
Fitting factor of width	1,3	-
Fitting factor of height	1,4	-
Predicted overall length	3,45	m
Predicted overall width	0,83	m
Predicted overall height	0,90	m

**Table C-5 Detailed dimension results of NO.5 STHE in FPSO vessel**

<u>Shell and Tube Heat Exchanger</u>		
<b>No.5</b>		
Hot fluid	<i>Steam</i>	
Cold fluid	<i>Cargo oil</i>	
Inlet temperature of hot fluid	55	°C
Outlet temperature of hot fluid	65	°C
Inlet temperature of cold fluid	158,1	°C
Outlet temperature of cold fluid	158,1	°C
LMTD	98	°C
Total heat load	779	kW
Overall heat transfer coefficient	97	W/m <sup>2</sup> °C
Heat transfer area	83,8	m <sup>2</sup>
Number of tubes	450	-
Shape factor of the tube	0,0076	-
Evaluated volume of the tube bundle	1	m <sup>3</sup>
Volume per tube	0,002	m <sup>3</sup>
Manufacture factor	2,5	-
Diameter of the tube	0,019	m
Length of the tube	2,75	m
Diameter of the shell	0,64	m
Length of the shell	2,7	m
Length of the core element	2,75	m
Width of the core element	0,64	m
Height of the core element	0,64	m
Fitting factor of length	1,3	-
Fitting factor of width	1,3	-
Fitting factor of height	1,4	-
Predicted overall length	3,58	m
Predicted overall width	0,83	m
Predicted overall height	0,90	m

**Table C-6 Detailed dimension results of NO.6 STHE in FPSO vessel**

<u>Shell and Tube Heat Exchanger</u>		
<b>No.6</b>		
Hot fluid	<i>Steam</i>	
Cold fluid	<i>Cargo oil</i>	
Inlet temperature of hot fluid	55	°C
Outlet temperature of hot fluid	65	°C
Inlet temperature of cold fluid	158,1	°C
Outlet temperature of cold fluid	158,1	°C
LMTD	98	°C
Total heat load	607	kW
Overall heat transfer coefficient	97	W/m <sup>2</sup> °C
Heat transfer area	63,9	m <sup>2</sup>
Number of tubes	450	-
Shape factor of the tube	0,0076	-
Evaluated volume of the tube bundle	1	m <sup>3</sup>
Volume per tube	0,002	m <sup>3</sup>
Manufacture factor	2,5	-
Diameter of the tube	0,019	m
Length of the tube	2,1	m
Diameter of the shell	0,64	m
Length of the shell	2,1	m
Length of the core element	2,1	m
Width of the core element	0,64	m
Height of the core element	0,64	m
Fitting factor of length	1,3	-
Fitting factor of width	1,3	-
Fitting factor of height	1,4	-
Predicted overall length	2,73	m
Predicted overall width	0,83	m
Predicted overall height	0,90	m

**Table C-7 Detailed dimension results of NO.1 plate heat exchanger in FPSO vessel**

<b>Plate heat exchanger</b>		
<b>No.1</b>		
Hot fluid	<i>Steam</i>	
Cold fluid	<i>Cargo oil</i>	
Inlet temperature of hot fluid	55	°C
Outlet temperature of hot fluid	65	°C
Inlet temperature of cold fluid	158,1	°C
Outlet temperature of cold fluid	158,1	°C
LMTD	98	°C
Total heat load	1234,4	kW
Overall heat transfer coefficient	120	W/m <sup>2</sup> °C
Heat transfer area	104,97	m <sup>2</sup>
Number of plates	150	-
Enlarge factor of the corrugated plat	1,17	-
Projected heat transfer area	0,61	m <sup>2</sup>
Shape Factor	2,5	-
Evaluated port diameter	0,05	m
Plate pitch between two plates	0,0041	m
Width of the heat transfer plate	0,50	m
Height of the heat transfer plate	1,26	m
Length of the core element	0,62	m
Width of the core element	0,50	m
Height of the core element	1,26	m
Fitting factor of length	2	-
Fitting factor of width	1,6	-
Fitting factor of height	1,3	-
Predicted overall length	1,23	m
Predicted overall width	0,80	m
Predicted overall height	1,63	m

**Table C-8 Detailed dimension results of NO.2 plate heat exchanger in FPSO vessel**

<b>Plate heat exchanger</b>		
<b>No.2</b>		
Hot fluid	<i>Steam</i>	
Cold fluid	<i>Cargo oil</i>	
Inlet temperature of hot fluid	55	°C
Outlet temperature of hot fluid	65	°C
Inlet temperature of cold fluid	158,1	°C
Outlet temperature of cold fluid	158,1	°C
LMTD	98	°C
Total heat load	1328,4	kW
Overall heat transfer coefficient	120	W/m <sup>2</sup> °C
Heat transfer area	112,96	m <sup>2</sup>
Number of plates	140	-
Enlarge factor of the corrugated plate	1,17	-
Projected heat transfer area	0,7	m <sup>2</sup>
Shape Factor	2,5	-
Evaluated port diameter	0,05	m
Plate pitch between two plates	0,0041	m
Width of the heat transfer plate	0,54	m
Height of the heat transfer plate	1,35	m
Length of the core element	0,57	m
Width of the core element	0,54	m
Height of the core element	1,35	m
Fitting factor of length	2	-
Fitting factor of width	1,6	-
Fitting factor of height	1,3	-
Predicted overall length	1,15	m
Predicted overall width	0,86	m
Predicted overall height	1,75	m

**Table C-9 Detailed dimension results of NO.3 plate heat exchanger in FPSO vessel**

<b>Plate heat exchanger</b>		
<b>No.3</b>		
Hot fluid	<i>Steam</i>	
Cold fluid	<i>Cargo oil</i>	
Inlet temperature of hot fluid	55	°C
Outlet temperature of hot fluid	65	°C
Inlet temperature of cold fluid	158,1	°C
Outlet temperature of cold fluid	158,1	°C
LMTD	98	°C
Total heat load	1594	kW
Overall heat transfer coefficient	120	W/m <sup>2</sup> °C
Heat transfer area	135,54	m <sup>2</sup>
Number of plates	165	-
Enlarge factor of the corrugated plate	1,17	-
Projected heat transfer area	0,7	m <sup>2</sup>
Shape Factor	2,5	-
Evaluated port diameter	0,05	m
Plate pitch between two plates	0,0041	m
Width of the heat transfer plate	0,54	m
Height of the heat transfer plate	1,36	m
Length of the core element	0,68	m
Width of the core element	0,54	m
Height of the core element	1,36	m
Fitting factor of length	2	-
Fitting factor of width	1,6	-
Fitting factor of height	1,3	-
Predicted overall length	1,35	m
Predicted overall width	0,87	m
Predicted overall height	1,77	m

**Table C-10 Detailed dimension results of NO.4 plate heat exchanger in FPSO vessel**

<b>Plate heat exchanger</b>		
<b>No.4</b>		
Hot fluid	<i>Steam</i>	
Cold fluid	<i>Cargo oil</i>	
Inlet temperature of hot fluid	55	°C
Outlet temperature of hot fluid	65	°C
Inlet temperature of cold fluid	158,1	°C
Outlet temperature of cold fluid	158,1	°C
LMTD	98	°C
Total heat load	1566,2	kW
Overall heat transfer coefficient	120	W/m <sup>2</sup> °C
Heat transfer area	133,18	m <sup>2</sup>
Number of plates	165	-
Enlarge factor of the corrugated plate	1,17	-
Projected heat transfer area	0,7	m <sup>2</sup>
Shape Factor	2,5	-
Evaluated port diameter	0,05	m
Plate pitch between two plates	0,0041	m
Width of the heat transfer plate	0,54	m
Height of the heat transfer plate	1,35	m
Length of the core element	0,68	m
Width of the core element	0,54	m
Height of the core element	1,35	m
Fitting factor of length	2	-
Fitting factor of width	1,6	-
Fitting factor of height	1,3	-
Predicted overall length	1,35	m
Predicted overall width	0,86	m
Predicted overall height	1,75	m

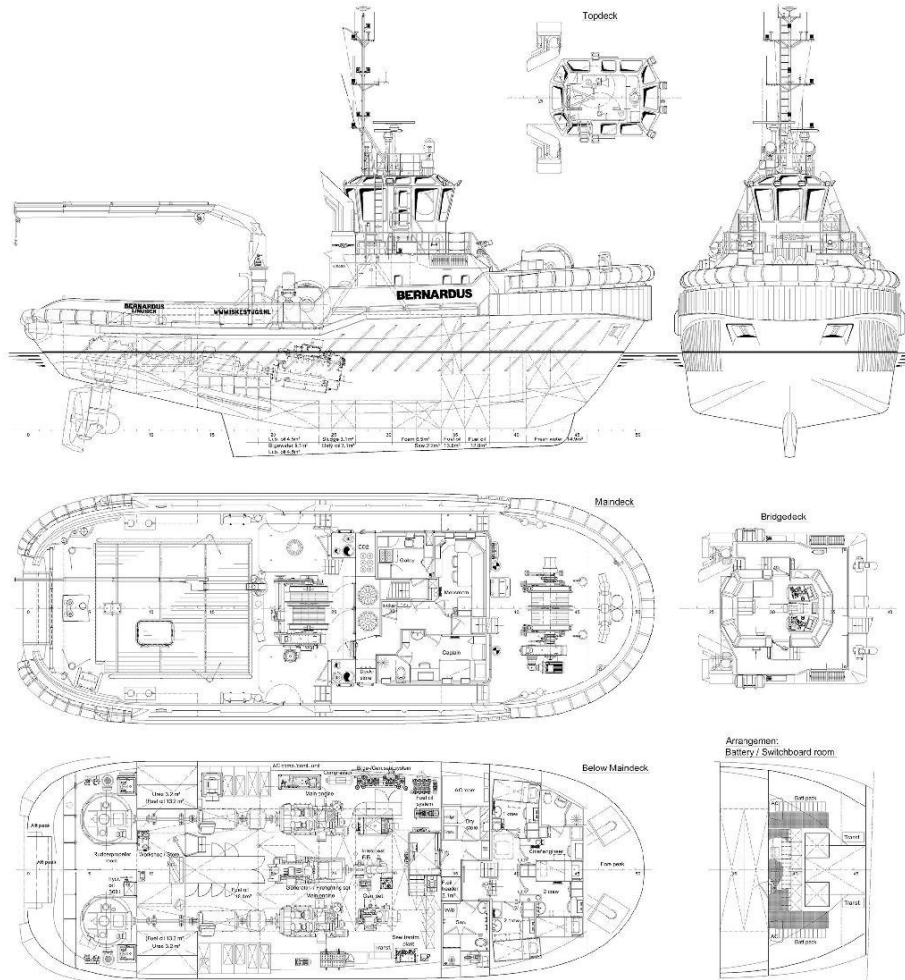
**Table C-11 Detailed dimension results of NO.5 plate heat exchanger in FPSO vessel**

<b>Plate heat exchanger</b>		
<b>No.5</b>		
Hot fluid	<i>Steam</i>	
Cold fluid	<i>Cargo oil</i>	
Inlet temperature of hot fluid	55	°C
Outlet temperature of hot fluid	65	°C
Inlet temperature of cold fluid	158,1	°C
Outlet temperature of cold fluid	158,1	°C
LMTD	98	°C
Total heat load	1559,2	kW
Overall heat transfer coefficient	120	W/m <sup>2</sup> °C
Heat transfer area	132,59	m <sup>2</sup>
Number of plates	170	-
Enlarge factor of the corrugated plate	1,17	-
Projected heat transfer area	0,7	m <sup>2</sup>
Shape Factor	2,5	-
Evaluated port diameter	0,05	m
Plate pitch between two plates	0,0041	m
Width of the heat transfer plate	0,53	m
Height of the heat transfer plate	1,32	m
Length of the core element	0,70	m
Width of the core element	0,53	m
Height of the core element	1,32	m
Fitting factor of length	2	-
Fitting factor of width	1,6	-
Fitting factor of height	1,3	-
Predicted overall length	1,39	m
Predicted overall width	0,85	m
Predicted overall height	1,72	m

**Table C-12 Detailed dimension results of NO.6 plate heat exchanger in FPSO vessel**

<b>Plate heat exchanger</b>		
<b>No.6</b>		
Hot fluid	<i>Steam</i>	
Cold fluid	<i>Cargo oil</i>	
Inlet temperature of hot fluid	55	°C
Outlet temperature of hot fluid	65	°C
Inlet temperature of cold fluid	158,1	°C
Outlet temperature of cold fluid	158,1	°C
LMTD	98	°C
Total heat load	1215,8	kW
Overall heat transfer coefficient	120	W/m <sup>2</sup> °C
Heat transfer area	103,38	m <sup>2</sup>
Number of plates	170	-
Enlarge factor of the corrugated plate	1,17	-
Projected heat transfer area	0,5	m <sup>2</sup>
Shape Factor	2,5	-
Evaluated port diameter	0,05	m
Plate pitch between two plates	0,0041	m
Width of the heat transfer plate	0,47	m
Height of the heat transfer plate	1,17	m
Length of the core element	0,70	m
Width of the core element	0,47	m
Height of the core element	1,17	m
Fitting factor of length	2	-
Fitting factor of width	1,6	-
Fitting factor of height	1,3	-
Predicted overall length	1,39	m
Predicted overall width	0,75	m
Predicted overall height	1,52	m

# Appendix D



## DAMEN ASD TUG® 2810 HYBRID "BERNARDUS"

**DAMEN**

DAMEN SHIPYARDS GORINCHEM

Member of the DAMEN SHIPYARDS GROUP



Industrieterrein Avelingen West 20  
4202 MS Gorinchem

P.O. Box 1  
4200 AA Gorinchem  
The Netherlands

phone +31 (0)183 63 99 11  
fax +31 (0)183 63 21 89

info@damen.com  
www.damen.com

© No part of the leaflet may be reproduced in any form, by print, photo print, microfilm, or any other means, without written permission from Damen Shipyards Gorinchem

**Figure D.1 General arrangement drawing of DAMEN ASD TUG**

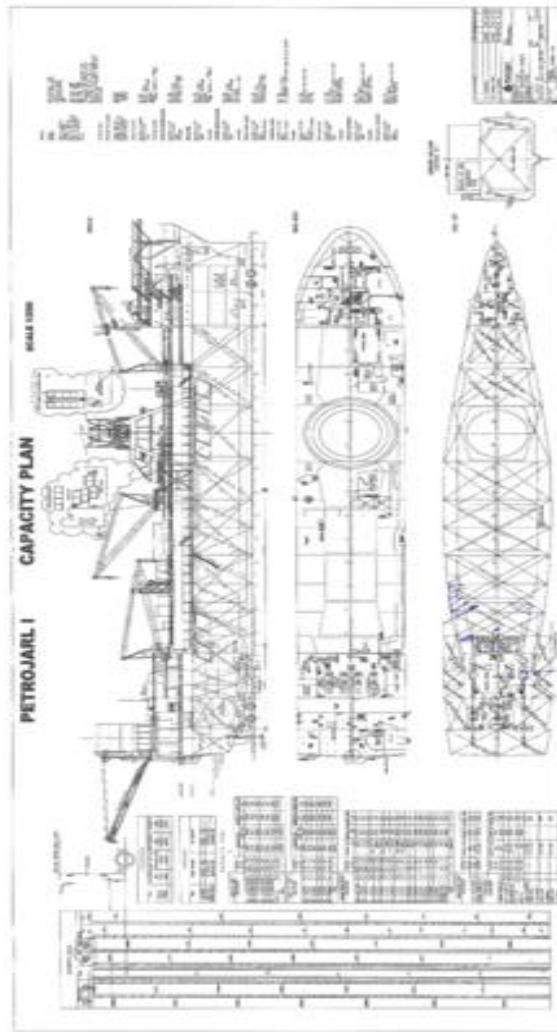


Figure D.2 General arrangement drawing of 'PETROJARL1' FPSO

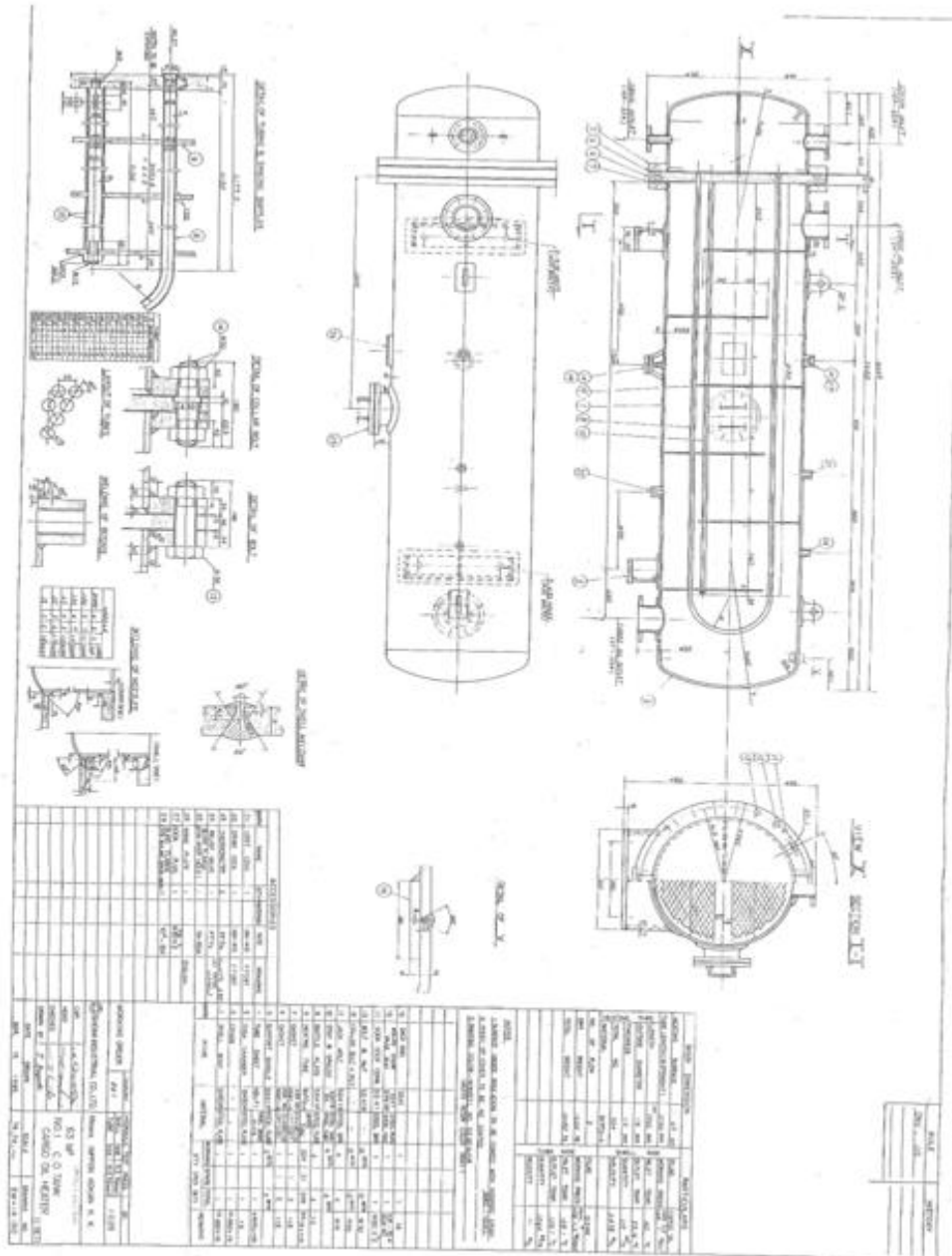


Figure D.3 Detailed drawing of NO.1 STH of 'PETROJARL1' FPSO





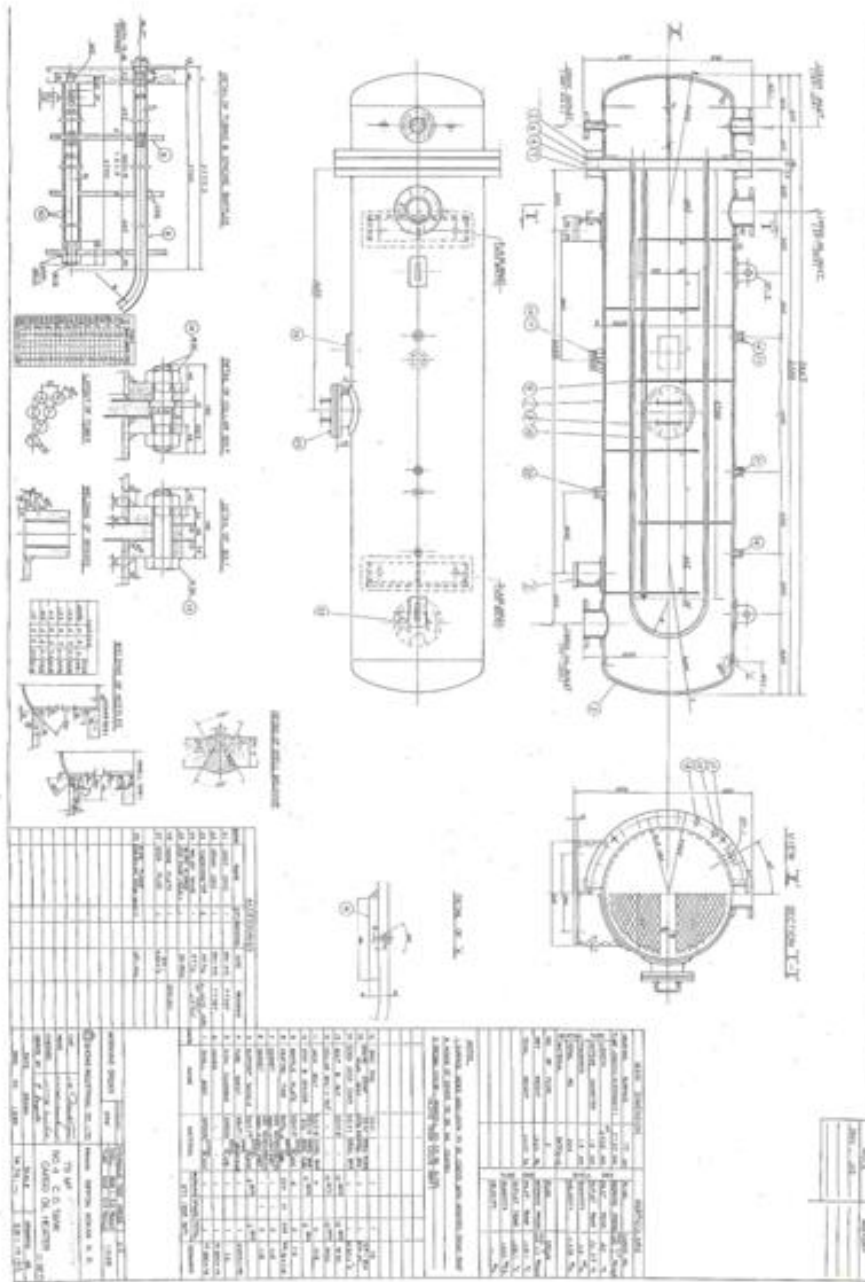


Figure D.6 Detailed drawing of NO.4 STHE of 'PETROJARL1' FPSO

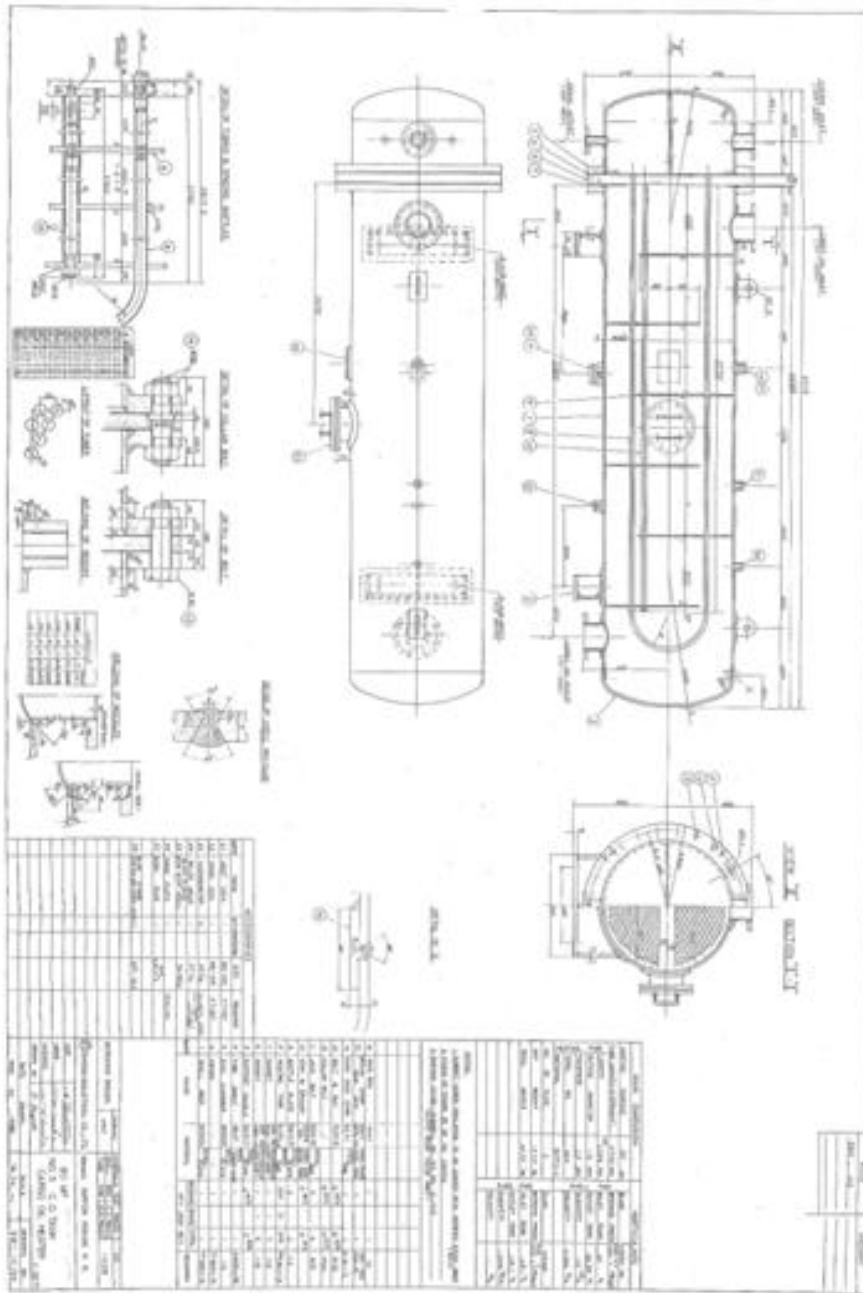


Figure D.7 Detailed drawing of NO.5 STHE of 'PETROJARL1' FPSO

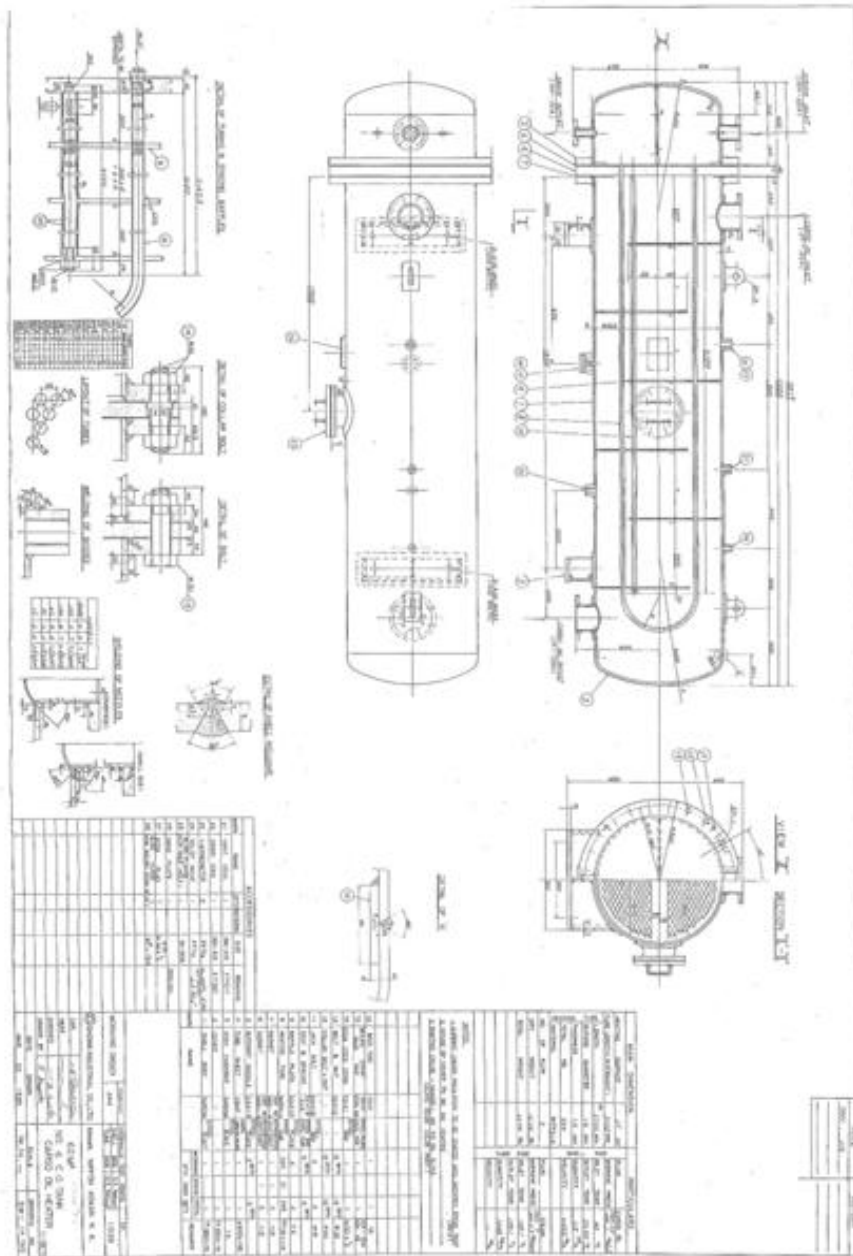


Figure D.8 Detailed drawing of NO.6 STH of 'PETROJARL1' FPSO